

Multi-Objective Optimization of Departure Trajectories at Amsterdam Schiphol Airport

Contributing to Sustainability in Air Transport by Creating
Aircraft Type Dependent Departure Trajectories Optimized
for Fuel Consumption and Noise Abatement

H. Lanwehr



Multi-Objective Optimization of Departure Trajectories at Amsterdam Schiphol Airport

Contributing to Sustainability in Air Transport by Creating
Aircraft Type Dependent Departure Trajectories Optimized
for Fuel Consumption and Noise Abatement

by

H. Lanwehr

to obtain the degree of Master of Science
at the Delft University of Technology,
to be defended publicly on Friday 27th August 2021 at 9:30 am.

Student number: 4273664
Project duration: September 2020 – August 2021
Thesis committee: Prof. dr. Ir. M. Snellen
Ir. P.C. Roling
Ir. A. Bombelli

An electronic version of this thesis is available at <http://repository.tudelft.nl/>.

Acknowledgements

It has been a tough year and I am proud of where I stand today. The corona pandemic changed the entire graduation process. Nothing about the circumstances made it any easier, but I have come this far and I couldn't have done it without my friends, family and supervisors.

Thank you, Thomas, for being there for support and encouragement literally every minute of the day. You were the one person I could discuss every aspect of my research with and you never failed to motivate and provide words of inspiration.

In the periods where lockdown was lifted and it was finally possible to sit somewhere other than at home, it was always reassuring to have Simone by my side going through the same struggles and emotions as me, always ready to motivate me to keep going. Thank you for pulling me through along with you.

A huge thank you to my supervisor Paul Roling for our bi-weekly digital meetings and his input and advice on my work. Thank you as well to Alessandro Bombelli for his valuable feedback during my milestone meetings. Thank you to Coen Vlasblom at KLM for taking the time out of his busy days to discuss my work. Our meetings were extremely valuable and your industry knowledge and insight helped tremendously to round out my thesis.

Finally, I want to thank my family. Without the moral and financial support of my parents I would not have been able to receive and complete my education. I am forever grateful to them. I wish my father could still be here to see this, I know he would be so proud of me.

Hanna Lanwehr
Delft, July 2021

Contents

List of Figures	vii
List of Abbreviations	ix
Introduction	xi
I Scientific Paper	1
II Literature Study previously graded under AE4020	35
1 Introduction	1
2 Problem Definition	3
2.1 Problem Statement	3
2.2 Research Objective	3
3 Environmental Impact of Aviation	5
3.1 Fuel and Emissions	5
3.2 Noise	5
4 Tailored Arrival and Departure Procedures	9
4.1 Tailored Arrivals.	9
4.2 Tailored Departures.	9
4.2.1 Continuous Climb Operations	9
4.2.2 Other Advanced Departure Techniques	10
4.2.3 Thesis: Tailored SID and Profile Allocation.	10
4.2.4 Conclusion.	11
5 Runway Configurations	13
5.1 Single	13
5.2 Open-V	13
5.3 Intersecting.	13
5.4 Parallel	13
5.4.1 Simultaneous parallel approaches	14
5.4.2 Simultaneous parallel departures	14
5.4.3 Segregated parallel approaches/departures	15
6 Methodology	17
6.1 Trajectory Model	17
6.1.1 Tabu Search	17
6.1.2 Simulated Annealing.	18
6.1.3 Genetic Algorithm	18
6.1.4 Multiobjective Optimization.	19
6.1.5 Integrated Noise Model	20
6.2 Allocation Model	20
7 Project Timeline	23
8 Conclusion	25

III	Supporting work	27
1	Trajectory Optimization Model	29
1.1	Maximum Thrust Calculation	29
1.2	Trajectory Parameterization	30
1.3	Optimization	31
1.4	Optimal Solutions	32
2	Case Study	33
2.1	Sensitivity Analysis	33
2.1.1	Results	33
	Bibliography	35

List of Figures

3.1	Schematic of NADP-1 [24].	6
3.2	Schematic of NADP-2 [24].	7
5.1	Independent parallel approaches [6].	14
5.2	Dependent parallel approaches [6].	14
5.3	Simultaneous parallel departures [6].	15
5.4	Segregated parallel approaches/departures [6].	15
6.1	An example of a Pareto Front [7].	19
1.1	Ground track parameterization calculation	30
1.2	Selecting a third point from the middle of the Pareto front	32
2.1	Sensitivity analysis results for the B737	34
2.2	Sensitivity analysis results for the B772	34

List of Abbreviations

$L_{A_{max}}$	Maximum A-weighted Sound Level
L_{den}	Day-Evening-Night Levels
AMS	Amsterdam Airport Schiphol
ATC	Air Traffic Control
BAS	Bewoners Aanspreekpunt Schiphol
CBS	Centraal Bureau voor de Statistiek
CCO	Continuous Climb Operation
CDA	Continuous Descent Approach
CDO	Continuous Descent Operation
CORSIA	Carbon Offsetting and Reduction Scheme for International Aviation
DARP	Dutch Airspace Redesign Project
DEA	Data Envelopment Analysis
DNL	Day-Night-Level
FAA	Federal Aviation Administration
FICAN	Federal Interagency Committee on Aviation Noise
G-MOGA	Guided Multi-Objective Genetic Algorithm
GDG	Guideline Development Group
ICAO	International Civil Aviation Organization
INM	Integrated Noise Model
IPCC	Intergovernmental Panel on Climate Change
ISA	International Standard Atmosphere
MILP	Mixed Integer Linear Programming
MOEA/D	Multi-Objective Evolutionary Algorithm based on Decomposition
multi-MADS	multi-objective Mesh Adaptive Direct Search Method
NADP	Noise Abatement Departure Procedure
NNHS	Nieuw Normen- en Handhavingstelsel Schiphol
NRM	Nederlands Rekenmodel
NSGA-2	Non-dominated Sorting Genetic Algorithm 2
RECAT	Wake Turbulence Re-categorization
RNAV	Area Navigation

SAF	Sustainable Aviation Fuels
SEL	Sound Exposure Level
SESAR	Single European Sky ATM Research
SES	Single European Sky
SID	Standard Instrument Departure
SOM	Self Organizing Map
TA	Tailored Arrival
TET	Turbine Entry Temperature
TMA	Terminal Manoeuvring Area
TNO	Nederlandse Organisatie voor Toegepast Natuurwetenschappelijk Onderzoek
TOC	Top of Climb
TOD	Top of Descent
TOW	Take Off Weight

Introduction

The air transport industry suffered greatly during the corona pandemic. In 2020, the five main airports in the Netherlands together experienced a 55% total reduction in flight movements and a 71% loss in passenger numbers. This had a great impact on airlines and airports economically. Nonetheless, flying has become an essential aspect of society nowadays and the pandemic has not lessened the public's desire to travel. Governments have also provided substantial economic support to keep the sector afloat since it is a large source of capital. For this reason, the aviation industry is expected to make a full recovery. McKinsey expects the aviation sector to return to the level it had in 2019 around 2024, after which the further growth of the industry is likely [33].

Before the pandemic, the growth of air travel was reaching its limits. In 2019, Amsterdam Airport Schiphol (AMS) was restricted to 500,000 flight movements due to environmental concerns and this amount was easily reached [40]. However, the expansion of airports and increase in flight movements to meet demand comes at the great cost of sustainability. Aircraft noise disrupting local communities and emissions leading to climate change are the two main environmental factors inhibiting growth [33]. For this reason, the overarching goal of the air transport industry is to continuously make flying more sustainable to allow for the expansion of airports and the growth of aircraft movements and passenger numbers.

In the Netherlands, this goal is currently being tackled by restructuring the airspace above the country. More direct routes to and from airports will result in fewer track-miles and thus less fuel consumption and fewer emissions. Furthermore, it will allow for fixed arrival and departure routes that limit noise annoyance near airports. This research focuses on the optimization of Standard Instrument Departures (SID) at Schiphol Airport. The objective is to contribute to making air travel more sustainable by creating new aircraft type dependent departure trajectories that are optimized for noise and fuel consumption.

Motivation & Process

The research was started in the Summer of 2020, it was an independent study that was performed at Delft University of Technology in the Air Transport & Operations department. The process started with an extensive literature study to provide a basis for many of the topics that were covered in the final thesis. The Literature Study was previously evaluated under the course: 'AE4020 - Literature Study'. This study can be viewed as a continuation of previous work by B. Ceulemans [7] where aspects of trajectory optimization modelling were covered. The current thesis evaluates the benefits of aircraft type dependent departure trajectories and allows for the analysis and comparison of optimal trajectories for many different aircraft types. Furthermore it highlights the trade-off being made between flying a fuel optimal or a noise optimal trajectory.

Research Objective

The research objective of this thesis is formulated below. The aim of this study is to:

evaluate the effect of optimal aircraft type dependent departure trajectories for a variety of aircraft types at Schiphol Airport by developing a trajectory optimization model that can calculate an aircraft type specific departure trajectory and uses multi-objective optimization to optimize them for fuel consumption and noise.

The objective can be achieved by answering the following research questions:

- What is the quantifiable benefit of tailored (aircraft type dependent) departure trajectories that are optimized for noise and fuel consumption for a variety of different aircraft types?
- What is the trade-off between noise and fuel consumption when an aircraft is flying a fuel optimal or a noise optimal departure trajectory?
- Can an aircraft fly the optimal trajectories (noise and fuel) of another aircraft?
- What is the effect on noise and fuel consumption when an aircraft flies another aircraft's optimal trajectories?

Thesis Structure

This MSc thesis is organized into three main parts. In Part I the scientific paper is presented. This paper describes the methodology, results and conclusions of the research that was conducted. Part II contains the preliminary literature study that was completed before the study was executed. Finally, in Part III supporting work is presented. This part provides supplementary information and explanations that act as support to the claims that were made in Part I of this thesis.

I

Scientific Paper

Multi-Objective Optimization of Aircraft Type Dependent Departure Trajectories at Amsterdam Schiphol Airport

Hanna Lanwehr*

Delft University of Technology, Delft, The Netherlands

Abstract

Due to the growing demand in air transport, measures need to be taken to reduce the impact of noise and emissions on local communities and the environment. The generic nature of current departure procedures leaves room for improvement in the form of aircraft type dependent departure trajectories. In this study a trajectory optimization model is implemented that uses a multi-objective evolutionary algorithm to optimize departure trajectories for fuel consumption and awakenings from noise. A parameterization technique is applied that reduces the number of optimization parameters by splitting the horizontal and vertical profiles into segments, thereby reducing the complexity of the problem. The model is used to optimize a specific departure trajectory at Schiphol Airport. A 15% reduction in fuel and a 60% decrease in number of awakenings is possible when an aircraft flies a fuel or noise optimal trajectory respectively. An intermediate trajectory provides a trade-off between the two objectives that is still superior to the reference. Medium aircraft can share an optimal trajectory without significant deterioration in performance while this does not apply for heavy aircraft. The achieved fuel savings translate to lower CO_2 emissions which contribute to reaching EU climate goals, while the reduction in number of awakenings results in fewer restrictions on the maximum number of aircraft movements. Both aspects allow the air transport industry to continue growing in a sustainable manner in the future.

1 Introduction

Air transport is an ever growing and developing industry that is greatly beneficial for economic growth [1]. However, it also has repercussions in the form of noise annoyance and emissions from fuel burn. Fuel usage directly translates to CO_2 and other pollutant emissions causing harm to the environment as well as lowering the quality of life of communities living near airports [2]. The continuous increase in air traffic demand calls for action from the industry to mitigate the adverse climate effects, therewith allowing further growth. In 2019, 81 million aircraft movements took place in civil aviation, transporting around 4.5 billion passengers across the world [3]. These numbers contribute to 2.5% of the total global CO_2 emissions and 3.5% of climate change [4]. Thus, if operations continue in the current trend without taking climate action, the air transport industry will have used up all of the allowable emissions set by the Paris Agreement between 2070 and 2100. After this, negative emissions would be necessary [5]. The Paris Agreement stipulates that greenhouse gas emissions must cease to exist around 2050 [6], however, current international measures in aviation are still not effective enough to achieve this goal [5]. The Dutch government provides guidelines ("Luchtvaartnota" [7]) for safe and sustainable aviation to help in achieving climate and noise abatement objectives. Furthermore, the Dutch Airspace Redesign Project (DARP) aims to make the airspace more efficient so that air transport can continue to grow in the future.

A continuous increase in global population causes residential areas to encroach on airports. Therefore, expanding airports to keep up with demand is met with much opposition by locals, primarily due to noise annoyances. In the Netherlands in 2016, around 48,300 people were exposed to more than 55 dB L_{den} as a direct result of air traffic from Amsterdam Schiphol Airport (AMS) [8]. Many airports are currently subject to government restrictions and regulations to limit aircraft movements [9]. These restrictions can only be alleviated if aircraft noise and emissions can be significantly reduced.

Technology is continuously developing with respect to cleaner and quieter aircraft [10]. It is the EU's goal that future aircraft result in 75% less CO_2 emissions, 90% less NO_x emissions and a reduction of the perceived noise level of 65% per passenger kilometer compared to the average aircraft that was new in 2000 [11]. While these technologies are effective, it takes time and money to develop and introduce new aircraft into an airline's fleet, therefore this is done very gradually. A more immediate solution can be to adapt the way current aircraft fly by changing operating procedures [10]. It has been shown that aircraft noise and engine emissions can be greatly

*MSc Student, Air Transport and Operations, Faculty of Aerospace Engineering, Delft University of Technology

reduced by trajectory optimization [12][13].

Currently, Schiphol Airport uses Standard Instrument Departures (SID) that are generic for all aircraft types. These SIDs provide a defined ground track and vertical procedure to be followed by every aircraft from take-off to departure fix. This provides a simple, safe departure with minimal Air Traffic Control (ATC) communication and intervention necessary. However, every aircraft type has different characteristics, such as weight and engine type, that affect its performance during departure. Therefore, the SID cannot be flown in the same way by every aircraft with the same defined thrust and speed settings. This results in sub-optimal departure trajectories. Additionally, the SIDs at Schiphol were designed when the population was smaller and less dense, and the need to slow down climate change was not as apparent and crucial as it is today [14].

The goal of this research is to evaluate the effect of noise and fuel optimal departure trajectories that are aircraft type dependent. This is achieved by creating a trajectory optimization model that can calculate the aircraft type specific ground track and vertical profile of a departure trajectory for a variety of aircraft types. A multi-objective evolutionary algorithm is used to optimize the trajectories for the two contradicting objectives: fuel consumption and total awakenings. The noise optimal and fuel optimal trajectories are compared and a third, intermediate solution is used to evaluate the trade-off that is made when optimizing for either objective. To minimize the amount of separate trajectories, the aircraft are flown on each other’s optimal routes to evaluate the effects on fuel and noise. The model is applied to a specific case scenario at Schiphol Airport.

The rest of this paper is structured as follows. The next section provides a literature review discussing current measures for aviation noise and emissions as well as previous research on tailored departure trajectories and optimization. Section 3 provides the theory and methodology for this study. The building blocks of the trajectory optimization model are discussed in detail here. Then, Section 4 describes a case study for a specific runway and departure fix combination at Schiphol Airport. This serves as the reference scenario on which the analysis of the optimized trajectories is based. Section 5 presents the results of the study and Section 6 discusses them. Finally, Section 7 gives conclusions and Section 8 provides recommendations for future work.

2 Literature Review

The environmental impact of air transport can be summed up in three groups according to the International Civil Aviation Organization (ICAO): 1) The perceived noise impact on the ground, 2) local air quality and 3) global warming [15]. Optimizing departure procedures is a large area of interest because it directly influences perceived noise level and local air quality, while indirectly affecting global warming [16]. In this section, current noise abatement and emission reduction schemes are discussed as well as previous research done on the topic of trajectory and multi-objective optimization.

2.1 Noise Abatement

There are two general ICAO measures in place at airports that aim to reduce noise levels during take-off [17]. These are referred to as Noise Abatement Departure Procedures (NADP) and their difference lies mainly in the initiation of flap retraction after take-off. NADP1 aims to reduce noise only close to the airport and NADP2 reduces the overall noise footprint. Additionally NADP2 provides significant reductions in CO_2 emissions and fuel costs [18].

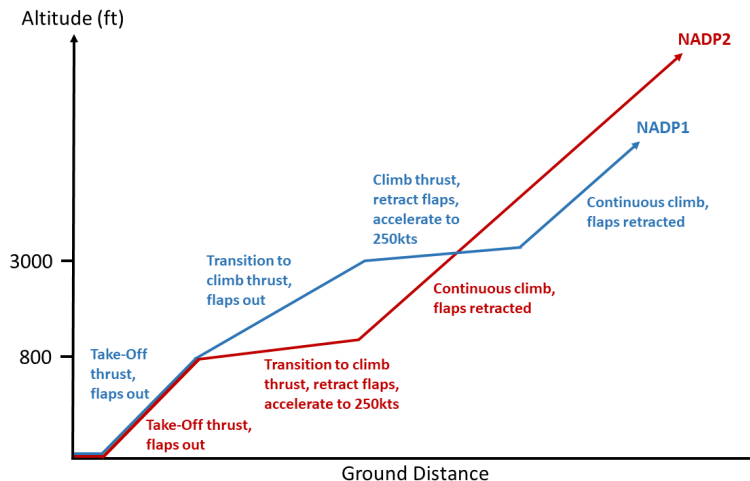


Figure 1: Vertical departure procedures

During an NADP1 departure, after initial take-off thrust a power reduction occurs at an altitude of 240 m (800 ft) while flaps and slats remain in take-off configuration. The aircraft climbs further toward 915 m (3000 ft) at which the flaps are retracted. Finally, the aircraft accelerates to en-route climb speed. Schiphol Airport is officially an NADP2 airport as this procedure ultimately provides higher noise and emission reductions than NADP1 [19]. During NADP2, flap retraction already starts at 800 ft while a power reduction occurs and the aircraft accelerates to zero flap speed. This procedure is depicted in Figure 1 alongside NADP1 [17]. ICAO regulations require the minimum acceleration altitude to be 800 ft for safety reasons. This is so that in case an engine fails during take-off, the pilot can still transition to a single-engine departure profile. NADP2 allows for a higher ground speed which shortens the noise event and has been found to decrease the number of highly annoyed people in the vicinity of the departure trajectory. The earlier thrust cutback also results in less noise and 3-4% less fuel emissions than NADP1 [18].

2.2 Fuel & Emissions

It is a well known fact that CO_2 emissions contribute greatly to global warming. As mentioned, the aviation industry accounts for around 2.5% of global CO_2 emissions resulting from human activity [4]. The majority of this stems from international aviation. To tackle this issue, the ICAO Carbon Offsetting and Reduction Scheme for International Aviation (CORSIA) compliments the goals of the Paris Agreement to significantly reduce greenhouse gases and limit global warming to a maximum of 2° Celsius [20]. This means carbon neutral growth from 2021 onwards and a 50% CO_2 reduction by 2050 [6]. On a European level, Single European Sky ATM Research (SESAR) aims to reduce fuel consumption per flight by 10%, translating directly to a 10% CO_2 reduction per flight as well [21]. An Oxford study found that the quickest way to reach this goal is better flight management by optimising horizontal and vertical flight profiles [22]. Other measures to reduce CO_2 emissions are longer-term solutions that involve the technological development of aircraft as well as the use of Sustainable Aviation Fuels (SAF). The impact that these measures will have on CO_2 emissions in aviation over time is depicted in Figure 2. Emissions are evidently destructive to the environment, which is why there are high taxes set for them. Airlines could significantly reduce their costs by limiting CO_2 emissions. One tonne of fuel by itself costs an airline about €530 [23]. Burning one tonne of fuel produces 3.16 tonnes of CO_2 [24] which in turn costs €174, and the cost of CO_2 is steadily increasing [25]. When considering the amount of aircraft movements for an airline per year, the costs add up substantially and every bit of CO_2 savings can be beneficial.

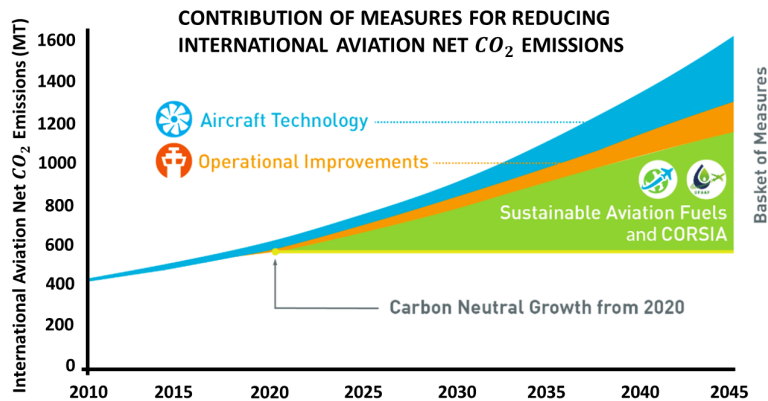


Figure 2: Contribution of basket of measures to reduce CO_2 in aviation [20]

2.3 Multi-Objective Trajectory Optimization

Optimizing flight paths and profiles can have positive impacts on fuel burn, emissions and noise exposure [22]. Using trajectory optimization, current departure paths can be improved and adapted to individual situations and aircraft types. Research has been done on this topic in the past using different methods and optimization algorithms.

Visser and Wijnen [26] combined an Integrated Noise Model, a geographic information system and a dynamic trajectory optimization algorithm into one tool to design environmentally optimal arrival and departure routes. Later on the tool was modified to optimize trajectories based on area navigation (RNAV) using gradient based optimization techniques [27]. Prats et al. [28] used numerical multi-objective optimization to mitigate the effect of noise in highly noise sensitive areas. He went on to investigate departure trajectories at Girona airport and found from numerical results that noise annoyance can be significantly reduced by using optimized trajectories [13]. Torres et al. [16] used a derivative free multi-objective mesh adaptive direct search method (multi-MADS)

to solve a trajectory optimization problem to reduce the environmental footprint of a departing aircraft. This was measured at a single measurement point. The method generates Pareto fronts by solving a number of single-objective optimization problems. Ho-Huu et al. [29] developed a multi-objective evolutionary algorithm based on decomposition (MOEA/D) to design optimal noise abatement departure trajectories. Gradient free methods such as this one have the disadvantage of a high computational cost, therefore some enhancing features were integrated to increase efficiency. Zhang et al. [12] also developed a gradient-free trajectory optimization framework, implementing a parameterization method to separate lateral and vertical flight dynamics. Finally, Ho-Huu et al. [30] formulated a newer version of MOEA/D to design optimal departure trajectories and allocate flights.

The literature shows that gradient-based and gradient-free optimization methods have both been used to solve the type of problem in question. Gradient based techniques, while efficient, can have limitations when a problem is thus complex that its objective and constraint functions are not differentiable and the variables are not continuous [12]. It is also common for solutions to be stuck in a local optimum if the problem is nonlinear and there is more than one local optimal solution. With increasing complexity of a problem, the use of gradient-based methods becomes less convenient or impossible. Furthermore, the studies mentioned use single-optimization methods. This means the multiple objectives are not being solved simultaneously within the optimization problem. Due to the mentioned limitations, it is more common to use gradient-free methods. These methods are able to deal with discontinuous problems and are able to generate a set of non-dominated optimal solutions.

This paper discusses a gradient-free approach to solving a trajectory optimization problem with two objectives; awakenings from noise and fuel consumption. A variety of different aircraft types are implemented to find optimal departure routes for each using a Non-dominated Sorting Genetic Algorithm (NSGA-2).

3 Methodology

A trajectory optimization model was developed that is able to calculate new, aircraft type dependent trajectories that are optimized for fuel consumption and noise. The model makes use of a trajectory parameterization technique. Furthermore, it has an integrated aircraft performance and fuel flow model. Finally, a replication of the Integrated Noise Model is used to output sound exposure levels (SEL). This information is then used to calculate the total number of awakenings during the entire departure based on population density data in the vicinity of the trajectory. The NSGA-2 algorithm is used for optimization. An overview of the individual blocks of the model is shown in Figure 3.

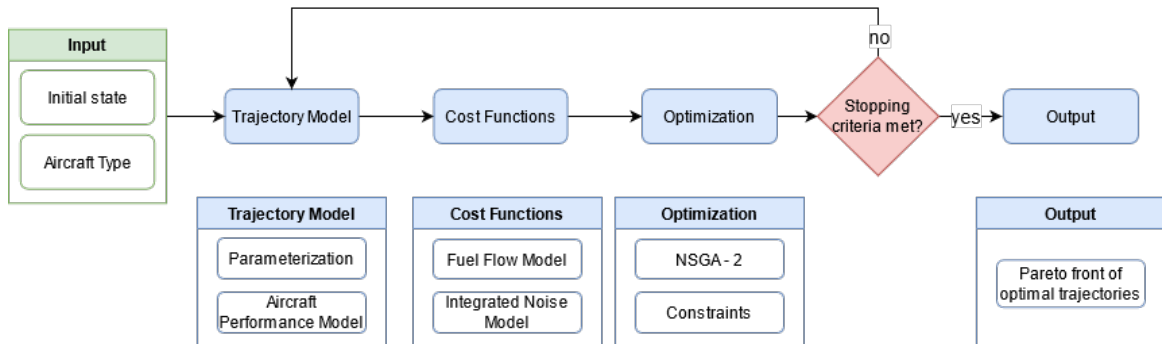


Figure 3: Block diagram of the trajectory optimization model

3.1 Assumptions & Requirements

To understand the model it is important to take note of the assumptions that were made and the requirements that need to be fulfilled. The aircraft is modelled as an intermediate point mass model with no wind present. The Earth is assumed to be flat and non-rotating. The aircraft is performing a coordinated flight. The maximum bank angle remains constant. During the entire take-off procedure it is not permitted to descend or decelerate and the weight of the aircraft is assumed to remain constant throughout. This is because the change in weight during departure is considered to be negligible compared to the take-off weight of the aircraft. The initial and final coordinates of the trajectory are fixed. Finally, an NADP2 departure trajectory is assumed.

The model is required to be capable of performing a multi-objective optimization for two opposing objectives and must be applicable to a wide variety of aircraft types. The trajectories are optimized per runway and departure fix combination. Operational and safety regulations require the minimum turn height to be 120 m (390 ft) and the bank angle in the turn segments should not exceed 25°. The trajectory should reach the final

coordinates within 50 m (160 ft) to account for rounding errors.

3.2 Aircraft Performance Model

Keeping the assumptions and requirements in mind, the equations of motion of the aircraft can be expressed as in Eq. 1 [31].

$$\dot{x} = V \cos \gamma \sin \chi \quad (1a)$$

$$\dot{y} = V \cos \gamma \cos \chi \quad (1b)$$

$$\dot{z} = V \sin \gamma \quad (1c)$$

$$\dot{\chi} = \frac{g \tan \mu}{V} \quad (1d)$$

Here x,y, and z are the position variables and χ is the azimuth of the aircraft. These equations are dependent on the following variables:

- V: the true airspeed
- γ : the flight path angle
- μ : the bank angle

The true airspeed is defined as the norm of the point mass's position derivatives:

$$V = \sqrt{\dot{x}^2 + \dot{y}^2 + \dot{z}^2} \quad (2)$$

The flight path angle, γ , can be any value between γ_{min} and γ_{max} determined using the continuous decision variable γ_n ($0 < \gamma_n \leq 1$) as shown in Eq. 3. Since descending is not permitted, $\gamma_{min} = 0^\circ$.

$$\gamma = (\gamma_{max} - \gamma_{min}) \gamma_n + \gamma_{min} \quad (3)$$

Since the turn radius and the true airspeed are determined beforehand, the bank angle μ can be calculated using Eq. 4 and is no longer seen as an input to the system of equations. This reduces the number of optimization parameters and thus computation time.

$$\mu = \tan^{-1} \left(\frac{V^2}{g_0 R} \right) \quad (4)$$

In low airspeed and low altitude, the acceleration of the aircraft can be determined by Eq. 5 [32]. This equation gives the derivative of the equivalent airspeed and is only used to determine the minimum thrust and maximum allowable flight path angle. This equation takes into account that acceleration is required when climbing to maintain a constant indicated airspeed.

$$\dot{V}_{Eq.} = \frac{1}{2\rho} \frac{\partial \rho}{\partial h} V^2 \sin \gamma + g_0 \left(\frac{T - D}{W} - \sin \gamma \right) \quad (5)$$

Using the assumption that negative acceleration may not occur, Eq. 5 can be solved when $\dot{V}_{Eq.} = 0$. This occurs in two instances: when the thrust is too low to maintain airspeed, or when the flight path angle is too large to maintain airspeed. Both instances would cause the aircraft to stall and so limitations are defined in Eq. 6 and Eq. 7 [32].

Solving for the minimum thrust needed to maintain airspeed at any given flight path angle gives:

$$T_{min} = \frac{W}{g_0} \left(g_0 \sin(\gamma) - \frac{1}{2\rho} \frac{\delta \rho}{\delta h} V^2 \sin(\gamma) \right) + D \quad (6)$$

Solving for the maximum allowable flight path angle to prevent the aircraft from stalling gives:

$$\gamma_{max} = \sin^{-1} \left(\frac{2\rho g_0 (T_{max} - D)}{W \left(\frac{\partial \rho}{\partial h} V^2 - 2\rho g_0 \right)} \right) \quad (7)$$

Here T_{max} is the maximum thrust available during take off or climb and follows from the maximum thrust model in Section 3.2.1. For situations where neither maximum nor minimum thrust are required, Eq. 8 can be used to determine the thrust.

$$T = (T_{max} - T_{min}) \eta_n + T_{min} \quad (8)$$

Here, the throttle setting η_n ($0 < \eta_n \leq 1$) can be changed to set a thrust between T_{min} and T_{max} . The variables η_n and γ_n are used to define the parameterized vertical profile as will be discussed in Section 3.4.2.

3.2.1 Maximum Thrust Model

The maximum thrust model differentiates between the maximum thrust at take-off and during climbing conditions. The maximum take-off thrust is calculated using a second degree polynomial function of speed with engine specific coefficients [33]. It is modeled as a ratio to the maximum static thrust, i.e. the maximum thrust at zero speed at sea level. The maximum take-off thrust can be adapted for airports that are not at sea level. This makes the model more flexible for varying airports.

In [33], the climb thrust is divided into three segments of different altitudes. The current study is focused on the first segment which is between 0 and 3000 *m* (10,000 *ft*). For this segment, the thrust variation with altitude is almost linear. There are two assumptions to take note of for calculating the maximum climb thrust. 1) International Standard Atmosphere (ISA) is considered for temperature variations with altitude, and 2) the Turbine Entry Temperature (TET) varies linearly with altitude.¹

3.2.2 Aerodynamic Drag Model

In a point mass model, the drag coefficient is calculated using Eq. 9 where C_{D_0} is the zero-lift drag coefficient, k is the lift-induced drag coefficient factor and C_L is the lift coefficient [34].

$$C_D = C_{D_0} + kC_L^2 \quad (9)$$

A corrected zero lift drag coefficient is applied when the aircraft is not in clean configuration. During take-off, flaps are deployed to increase drag. This increase in drag coefficient due to the flaps can be determined using Eq. 10 [34].

$$\Delta C_{D,f} = \lambda_f \left(\frac{c_f}{c} \right)^{1.38} \left(\frac{S_f}{S} \right) \sin^2 \delta_f \quad (10)$$

This equation contains various aircraft type specific variables. $\frac{c_f}{c}$ is the flap to wing chord ratio, $\frac{S_f}{S}$ is the flap to wing surface ratio, δ_f is the flap deflection angle and λ_f is dependent on the type of flaps. This value is set to 0.9 for all aircraft types examined in this study.

3.3 Fuel Flow Model

The fuel flow model uses the ICAO aircraft engine emission data-bank [35]. This databank provides fuel flow indicators for each engine type. A continuous fuel flow profile is used that is based on points from the ICAO databank. These are denoted as C_{ff3} , C_{ff2} and C_{ff1} . A linear correction factor, $C_{ff,ch}$ is also considered to take into account the change in altitude during the departure trajectory. Since $C_{ff,ch}$ is not available for all engine types, a mean value of $6.7e-7$ is used as a default for all aircraft types. The dynamic fuel flow (*kg/s*) is then computed with Eq. 11 [34]. In this equation T is the current thrust and T_0 is the maximum static thrust at sea level. h is the current altitude.

$$\begin{aligned} f_{\text{fuel}}(T, h) &= f_{\text{fuel,SL}}(T) + C_{\text{ff,ch}} \cdot T \cdot h \\ &= C_{\text{ff3}} \left(\frac{T}{T_0} \right)^3 + C_{\text{ff2}} \left(\frac{T}{T_0} \right)^2 + C_{\text{ff1}} \frac{T}{T_0} + C_{\text{ff,ch}} \cdot T \cdot h \end{aligned} \quad (11)$$

The model only calculates fuel flow and not emissions, however fuel burn is directly linked to CO_2 emissions and can be examined post optimization.

3.4 Trajectory Parameterization

The parameterization method splits the ground track and vertical profile into segments separately, allowing for the optimization of the variables that define each segment. The advantage of using a trajectory parameterization technique is that it allows for a relatively large number of optimization parameters without adding additional constraints and without compromising the computation time. This is beneficial because genetic algorithms often require significant model evaluations to find the Pareto-optimal solutions [31].

3.4.1 Ground Track

The model makes use of RNAV to parameterize the ground track. This allows aircraft to fly a specified route within a network of waypoints by using ground beacons and the Global Navigation Satellite System (GNSS). RNAV makes use of track-to-a-fix legs for straight segments and radius-to-a-fix legs for constant radius turns [17]. The same concept is implemented in the trajectory optimization model. The trajectories consist of a straight leg and a turn segment in sequence. The parameterized variables defining these segments, such as the

¹The equations used in the maximum thrust model can be found in Section 1.1 of Part III of this thesis.

length, L , for a straight segment and a radius, R , and heading change, $\Delta\chi$, for the turns, allow for flexibility in the optimization of the ground track. An example of a parameterized ground track with decision variables is given in Figure 4(a). It follows that if the first two decision variables are known (L_1 and R_2), and the final coordinates (x_f and y_f) are given, then $\Delta\chi$ and L_3 can be determined using trigonometry². This reduces the amount of optimization variables needed in the model. The number of straight and turn segments is explicitly defined in the model. A sensitivity analysis was performed beforehand with five, seven and nine ground segments to assess the optimality and duration of each³. Increasing the number of segments also increases computation time. To keep the study manageable, it was decided that five ground segments are used in the model to define the ground track. This means each trajectory has three straight segments and two turns.

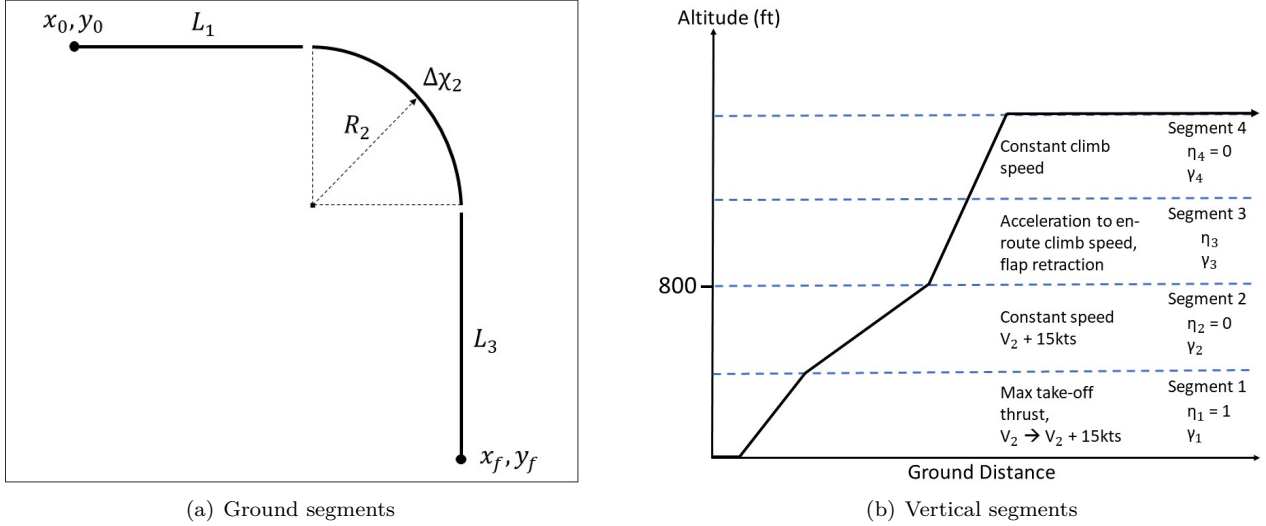


Figure 4: Trajectory segments

3.4.2 Vertical Profile

The vertical profile is determined by the departure procedure that is flown. In this case NADP2 is implemented. The profile is divided into five segments, each defined by two flight parameter settings; the flight path angle γ_n , and the throttle setting η_n . The subscript n represents the segment number. γ_n and η_n represent percentages of their respective maximum flight parameters as was defined in Eq. 3 and Eq. 8.

In the first segment the aircraft departs at maximum take-off thrust and accelerates from V_2 towards $V_2 + 15 \text{ kts}$. Here, γ is left as a decision variable and $\eta = 1$ for maximum thrust. Once this speed is reached, in the second segment the aircraft climbs at a constant airspeed towards 800 ft as defined by the NADP2 procedure. Once again, γ is left as a decision variable and now $\eta = 0$ since a constant airspeed and thus minimum thrust is required. In the third segment starting at 800 ft the acceleration segment is started to reach en-route climb speed and the flap retraction schedule is initiated. As a result, γ and η are both decision variables. In the fourth segment the aircraft climbs with constant climb speed until the final altitude is reached. γ is a decision variable and $\eta = 0$ to maintain constant airspeed. Once at the final altitude, the aircraft levels off and remains at a constant altitude until the final coordinates of the trajectory have been reached. The fifth segment occurs during the fixed-radius turns as the aircraft is assumed to climb at a constant airspeed. This means that γ is a decision variable and $\eta = 0$. These five segments result in six decision variables that define the vertical profile of the trajectory.

3.5 Noise Model

The noise originating from a single aircraft flyover can be determined using two measures. The maximum sound level ($L_{A_{max}}$) represents the peak noise level that an aircraft produces during the flyover. The Sound Exposure Level (SEL) is the level of noise produced for which, if the flyover only took 1 second, it would have the same noise energy as the entire event [36].

To assess the noise impact of the individual departure trajectories in this study, a replication of the Integrated Noise Model's (INM) in-flight noise assessment tool [37] [38] was implemented into the trajectory optimization model. This tool, called INMTM, is capable of calculating the noise impact for a single-event flyover by means of an A-weighted SEL and an A-weighted $L_{A_{max}}$ value. The A-weighting corrects the sound level to better

²The derivation for determining the last two decision variables can be found in Section 1.2 of Part III of this thesis.

³The results of the sensitivity analysis can be found in Section 2 of Part III of this thesis.

represent how people perceive noise [39]. INMTM uses Noise-Power-Distance tables to interpolate thrust levels and slant range to the observer. The tables are created under the assumption that the aircraft is flying on an infinitely long segment at a given speed, with the observer standing directly below the flight trajectory. For this reason, corrections are made in INMTM to account for non-reference conditions like different speeds or observers located ahead or behind, as well as to the left or right of the aircraft trajectory [37].

For the purpose of this study, only the SEL values are of importance since this is the metric used in the calculation of awakenings from a departure. Furthermore, the population density near the aircraft path is needed to quantify the community noise impact. The noise cost value is calculated over a predetermined area, referred to as the noise evaluation area. This area incorporates the entire departure trajectory. The noise evaluation area is made up of smaller grid points of 500x500m and is defined as an input to the noise model. The model calculates the SEL for every individual grid point. For each gridpoint the population density is also known. This data is available from the "Centraal Bureau voor de Statistiek" (CBS) [40].

When relating aircraft noise to the effect it has on the local population, a dose response relationship is commonly used. This uses the measured noise level to determine the percentage of people that are highly annoyed by an aircraft noise event. Such a relationship is usually derived from field research [36]. Eq. 12 shows the dose-response relationship determined by the Federal Interagency Committee on Aviation Noise (FICAN) based on Figure 5. This is the relationship used in this study to determine the percentage of awakenings from a single flyover. More specifically, Eq. 12 represents the "maximum percent of the exposed population expected to be behaviorally awakened" [41]. The awakenings are used as a general measure of noise annoyance in this study and also translate to day time operations.

$$\% \text{ Awakenings} = 0.0087 \cdot (SEL_{\text{indoor}} - 30)^{1.79} \quad (12)$$

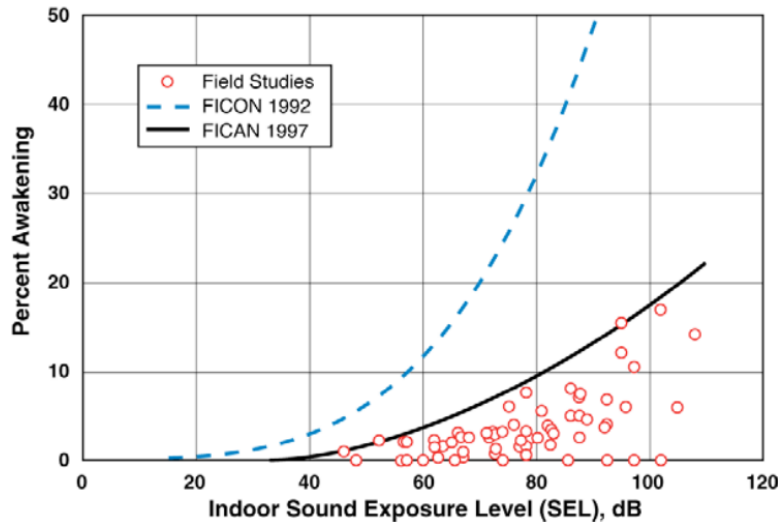


Figure 5: FICAN sleep disturbance dose-response relationship [41]

By multiplying the number of people living within a gridpoint with the expected percentage of awakenings of that particular gridpoint, one can determine the total maximum number of awakenings in that gridpoint and by addition the whole noise evaluation area. The relationship in Eq. 12 uses the indoor SEL, whereas INMTM provides the outside SEL. Therefore a correction factor of 20.5dB is applied accounting for the sound absorption of an average house [31].

3.6 Optimization

The algorithm that performs the optimization of the two objectives - fuel consumption and awakenings from noise - is the Non-Dominated Sorting Genetic Algorithm 2 (NSGA-2). This is an evolutionary algorithm that differs from the standard genetic algorithm in the way that the individual solutions are ranked. NSGA-2 starts by initializing a population and then a generational loop is repeated. This loop has two components; variation and selection [42]. An offspring population is created from the initial population by mixing the genes of better performing individuals, selected using binary tournament selection, and mutating them. This combining and mutating is done using Simulated Binary Crossover (SBX) and polynomial mutation respectively. The resulting population of parents and offspring is then twice as large as the original. In the second step, all individuals are ranked into different fronts, depending on their performance. This non-dominated sorting is purely dependent on the Pareto order. Individuals are picked from the best fronts until the size of the original population is

reached. If individuals have the same rank, they are sorted according to the crowding distance, which reflects the diversity of the solution⁴.

3.6.1 Constraints

The objective function is subject to some constraints that need to be defined explicitly. First, it is defined that the end of the calculated trajectory must be within 50 m (160 ft) of the final coordinates that are given. Furthermore, operational and safety requirements dictate that the minimum turn height is 120 m (390 ft) and the maximum bank angle in turns is 25° [17].

3.7 Output

The optimization ends once the stopping criterion is met. In this case there is a maximum number of evaluations that the optimization runs for, which is 10,000 evaluations with a population size of 100. These values were chosen based on previous work [43]. The output of the model is a Pareto set of optimal solutions for one aircraft type and one runway and departure fix combination. The Pareto front gives the fuel optimal, noise optimal, and all optimal solutions in between. These solutions represent optimal departure trajectories that are dependent on one aircraft type.

In order to analyse the results of the model, the solutions that will be used must be chosen from the Pareto optimal front. In this case the fuel optimal as well as the noise optimal solutions are of interest. These are the outermost points on the Pareto front. A third, intermediate solution is chosen to highlight the trade-off that is made between fuel and awakenings. The third point is chosen from the middle of the Pareto front. The derivatives between the points are calculated and subtracted from each other. The aim is to obtain a large positive value when the derivatives are subtracted, thereby selecting a point that can save a sufficient amount of one objective while limiting additional costs to the other objective⁵.

4 Case Study

The trajectory optimization model described in Section 3 is applied to a case scenario at Schiphol Airport. This section describes the airport and its current procedures concerning departures, noise and emissions. A reference case for the trajectory optimization for a specific runway departure fix combination is discussed as well.

4.1 Amsterdam Schiphol Airport

Schiphol Airport is one of the busiest airports in the world. With a total of around 497,000 aircraft movements, 80.5 million passengers were transported around the world in 2019 [44]. Schiphol Airport is the main airport in the Netherlands serving 104 airlines and acts as a hub for KLM Royal Dutch Airlines. The airport is located 9 km southwest of Amsterdam on an area of 27.87 km^2 , which is larger than the city of Delft [45].

4.1.1 Runway Layout & Usage

Schiphol Airport has six runways in total, five of which are used for commercial aviation. The sixth runway, the ‘Oostbaan’, is shorter and is used mainly for general aviation. Figure 6(a) [46] shows the orientation and location of the runways. Most departures from Schiphol Airport have southern or eastern destinations as depicted in Figure 6(b) [47].

At Schiphol Airport the runway usage is currently decided using a preferred sequence list. This list determines the optimal combination of runways used for take-off and landing in given weather conditions and traffic supply. The goal of this is to always find the most suitable runway that will mitigate noise nuisance to the surrounding population while guaranteeing safety. This is attained by picking runways and departure paths that avoid the most densely populated areas near the airport. Two runways are open for arrivals and one for departures during the day or vice versa. At night only one runway is used for landing and one for take-off due to lower traffic flow and noise abatement policies [47]. Preferred runways are the ‘Kaagbaan’ for arriving and the ‘Polderbaan’ for departing traffic, but this is also dependent on wind conditions. When there is wind from the east or west the ‘Buitenveldertbaan’ is used. The preference list is generic and applies the same for all aircraft types.

⁴Further information about the algorithm and optimization settings can be found in Section 1.3 of Part III of this thesis.

⁵The derivation for the selection of the intermediate point can be found in Section 1.4 of Part III of this thesis.



(a) The runway layout of AMS [46]



(b) Distribution of arriving and departing traffic for AMS in 2019 [47]

Figure 6: Runway layout and distribution of arriving and departing air traffic for Amsterdam Schiphol Airport

4.1.2 Noise

Currently, the method for calculating aviation noise exposure near airports in the Netherlands is determined by the Nederlands Rekenmodel (NRM) [48]. This model stems from the 1960s and has been adapted to the changing times. The NRM uses L_{Amax} as a metric and the noise contribution is calculated per gridpoint. L_{Amax} is not a time based metric, however it is made equivalent to the SEL in this model, resulting in inaccuracies as the duration of the noise event is not taken into account. In general, aviation standards are becoming more international rather than local, with the aims of Single European Sky (SES) in mind. For this reason, the Netherlands is starting to introduce a new noise calculation method, the ECAC Doc29. This model is more advanced, containing a larger database of aircraft performances and noise metrics, such as the SEL value that does take the duration of the noise event into account. Further aspects like topography, position of motors and calculations considering bank angles in turns are included in the new model. This allows for better representation of the true situation. Implementing a new model has consequences and takes time since it will change the norms and standards of noise contours.

With the current NRM, restrictions are in place to limit the amount of highly annoyed people within a specific noise contour around Schiphol Airport. These contours are based on the average day-evening-night levels (L_{den}). The "Nieuw Normen- en Handhavingstelsel Schiphol" (NNHS) specifies the number of highly annoyed people experiencing an average noise level of more than 48dB(A) and the number of sleep disturbed people experiencing more than 40dB(A) L_{night} . This is based on the number of flight movements, which is limited to 500,000 per year for Schiphol Airport. Table 1 shows the norms and expected disturbances for 2020 as opposed to 2015.

Indicator	Noise Exposure	Reference	Intended norms (prognosis)	
			Situation 2015	Situation for 500,000 aircraft movements 2020
Number of houses	≥ 58 dB(A) L_{den}	7,900	7,800	9,000
	≥ 48 dB(A) L_{den}	263,100	259,600	257,900
Number of highly annoyed people	≥ 58 dB(A) L_{den}	8,800	8,800	10,200
	≥ 48 dB(A) L_{den}	130,200	128,500	129,100

Table 1: Noise norms for 2020 compared to 2015 [49]

The Guideline Development Group (GDG) recommends keeping L_{den} noise levels below 45dB(A) due to negative health effects such as heart and vascular disease, sleep disorders, tinnitus and more. In the current study, single noise events are considered. Research from the "Nederlandse Organisatie voor Toegepast Natuurwetenschappelijk Onderzoek" (TNO) concluded that sleep disturbances occur upward of a 55dB(A) SEL [36]. Amsterdam Schiphol Airport, "Luchtverkeersleiding Nederland" (LVNL) and airlines all play their part in re-

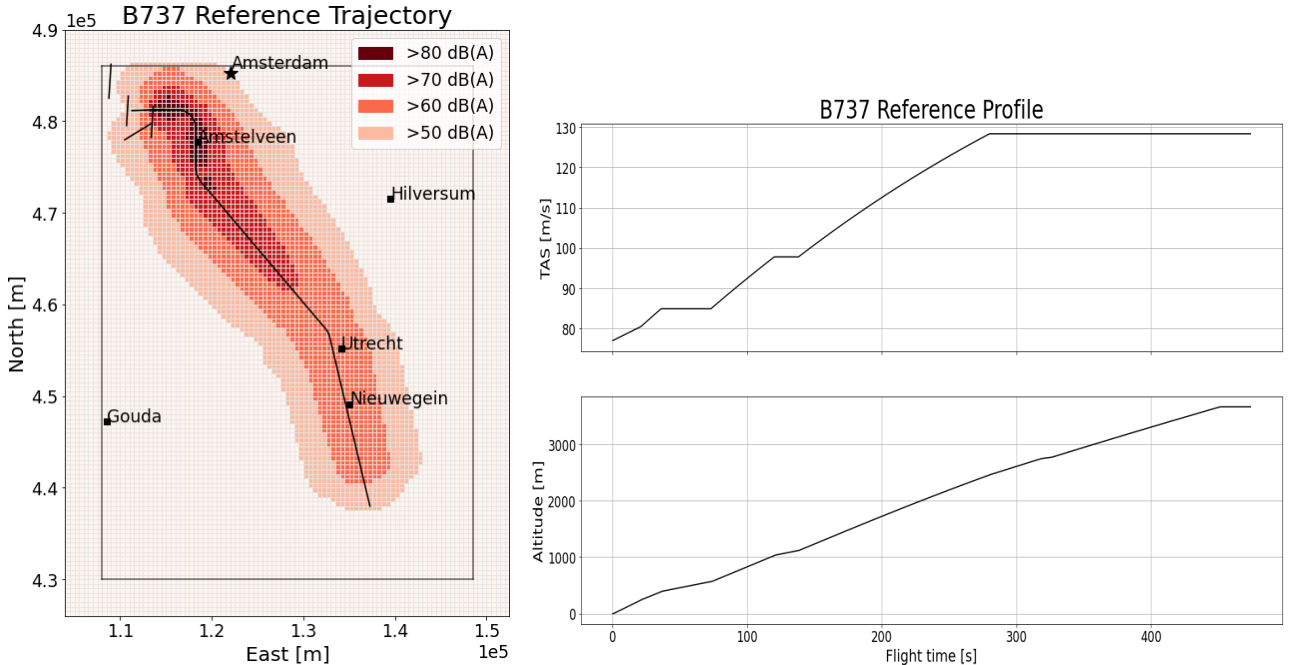
ducing noise exposure and emissions in different ways. As mentioned, the runway preference list at Schiphol Airport aims to minimize noise nuisance to the surrounding areas by choosing runway combinations that avoid densely populated areas during take off and landing. Cleaner and quieter aircraft are encouraged at Schiphol Airport by reducing airport costs for airlines that introduce new aircraft into their fleet. Flying with loud, inefficient aircraft can result in costs that are up to 180% the base rate, while the most clean and quiet aircraft can result in a 45% cost reduction [50]. In terms of procedures, Schiphol Airport uses the NADP2 as a standard departure procedure as mentioned in Section 2. Overall, this procedure generates higher noise abatement and is beneficial for fuel burn and CO_2 emissions.

4.2 Reference Scenario

For this case scenario the departure runway 09 ('Buitenveldertbaan') is chosen with the LOPIK waypoint located to the south-east of the airport as the departure fix. Although this particular runway is not used as often for departures at the moment due to military airspace restrictions, the current SID is designed to lead over a large part of Utrecht West. Furthermore, the majority of destinations from Schiphol Airport are located to the east and south-east of the Netherlands as depicted in Figure 6(b). The LOPIK SID is not available at all times because there is a large military airspace located above the south-east of the Netherlands. This area is used for military training during the week and covers a large portion of the airspace above Noord-Brabant and the southern part of Gelderland [51]. All civil aviation is restricted from flying in this airspace when it is in use and must fly around it. This results in less direct routes from and to Schiphol Airport and other Dutch airports. The longer flight times and additional track miles flown increase fuel burn and CO_2 emissions. One of the plans of the Dutch Airspace Redesign Project is to dissolve the military area in the south-east to allow for more direct arrival and departure procedures to Schiphol Airport. Once this takes effect, planned for 2023, the 09 LOPIK departure could have a much larger significance for Schiphol Airport departures.

L_1	R_2	$\Delta\chi_2$	L_3	R_4	$\Delta\chi_4$	L_5	R_6	γ_1	γ_2	γ_3	η_3	γ_4	γ_5
2800m	2000m	90°	4200m	2500m	-39°	21000m	2100m	0.9	0.5	0.8	0.99	0.7	0.4

Table 2: Decision variables for current LOPIK SID



(a) Ground track with SEL contour within noise evaluation area for reference scenario of B737

(b) Altitude and airspeed for reference scenario of B737

Figure 7: Reference scenario modeled for B737

The departure chart of the 09 runway including the LOPIK SID is shown in Figure 14 in Appendix A [52]. The trajectory consists of three turns and four straight segments. After take-off from runway 09 the path takes a sharp right turn, flying over Amstelveen to reach the EH036 waypoint. Here the path takes a left turn heading

for the OGINA waypoint located on the outskirts of Utrecht above a quite densely populated area. From there a right turn is made to line up with the final LOPIK waypoint, flying above Nieuwegein and Vianen to get there.

The reference scenario can be calculated using the trajectory optimization model. The three turns indicate that eight decision variables are needed for the ground segment. The vertical profile follows an NADP2 procedure. The decision variables of the reference case are given in Table 2 and they result in the trajectory shown in Figure 7. The decision variables are the same for all aircraft types to represent the generic current departure procedure. The reference scenario adheres to exit conditions of 3650 m (12000 ft) altitude and 128 m/s (250 kts) once the LOPIK waypoint is reached. These same conditions apply to the newly optimized trajectories. The specific trajectory in Figure 7 was modeled for the B737. The trajectory leads through a highly populated area towards the south-east. This is the city of Utrecht that has over 1.3 million inhabitants. This is more than half of the population within the entire noise evaluation area. The optimized trajectories are hypothesized to avoid this area, especially the noise optimal trajectories should find a way around the densely populated regions.

Aircraft	Weight class	Fuel [kg]	Awakenings
A319	M	509.12	4406.28
A320	M	558.81	5287.87
A321	M	749.19	9305.57
A388	H	4289.65	25963.93
B734	M	588.98	11373.65
B737	M	567.67	9796.59
B738	M	581.82	9534.32
B744	H	3263.08	65192.11
B772	H	1601.46	11683.02

Table 3: Cost values for the reference cases at MTOW

Figure 7(a) also gives an indication of the SEL contours from the current SID as modeled for the B737. Large parts of the $>50\text{dB(A)}$ and $>60\text{dB(A)}$ contours are covering Utrecht and Nieuwegein, two of the more populated areas under the trajectory. The number of awakenings and amount of fuel consumption associated with the reference scenarios are given in Table 3 for all aircraft types that were considered. These values serve as comparison material for the new, optimized trajectories. All trajectories, including the reference, were modeled with the Maximum Take-Off Weight (MTOW) of the respective aircraft. The trajectory optimization model is applied to nine different aircraft types to evaluate the noise and fuel costs individually for different aircraft characteristics. These aircraft were chosen based on the aircraft operating at Schiphol Airport. The A319, A320, A321 and B738 are part of the group of aircraft that made up more than 50% of the fleet for commercial aviation at Schiphol Airport in 2019 [47]. The B744 and A388 are among the heaviest aircraft to operate at Schiphol Airport.

4.2.1 Optimization Bounds

In order for the genetic algorithm to provide accurate results without extensive computation times, optimization bounds need to be set for the decision variables. It is important that the bounds are not set too narrow as this could mean that the true optimal solution is not within the bounds. Bounds that are too broad can result in unmanageable computation times as well as getting stuck in local minima. Table 4 provides the bounds that were used in this case study for the optimized trajectories. The γ_n and η_3 values are factors of the maximum available value for the respective parameter as was defined in Eq. 3 and Eq. 8 in Section 3.2.

	L_1	R_2	$\Delta\chi_2$	L_3	R_4	γ_1	γ_2	γ_3	η_3	γ_4	γ_5
lower bound	1000 m	1000 m	30°	1000 m	1000 m	0	0	0	0	0	0
upper bound	10000 m	8000 m	90°	40000 m	8000 m	1	1	1	1	1	1

Table 4: Lower and upper optimization bounds for the decision variables of the trajectory.

5 Results

The outcome of the trajectory optimization model is a Pareto front for each individual aircraft type. Using the method mentioned in Section 3.6, three points are selected from each front that are used in the subsequent analysis. The Pareto front for the B737 including selected solutions is shown in Figure 8. The convex nature of the curve indicates that the two objectives have an inverse relationship; when one decreases the other increases and vice versa. Furthermore, the change in fuel consumption is observed to be much smaller than the change in awakenings. The Pareto fronts for all optimized aircraft types are given in Appendix B.

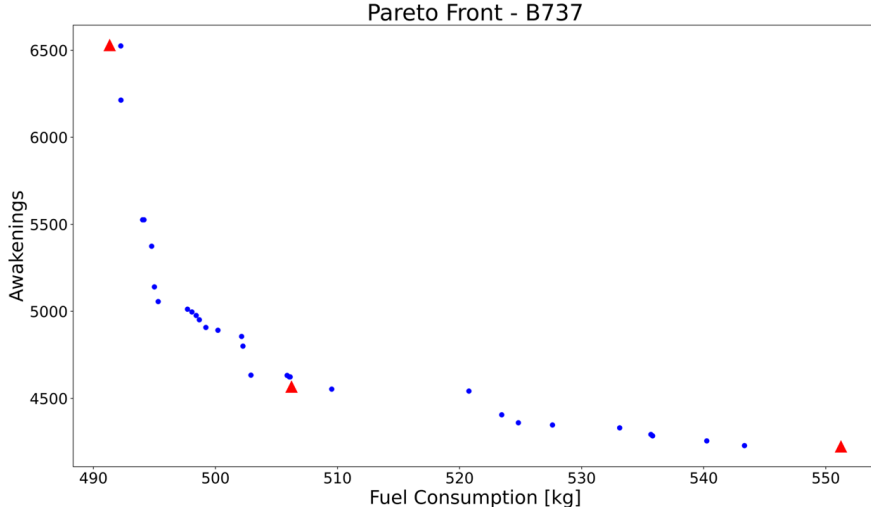


Figure 8: Pareto front of optimal solutions for the B737

5.1 Optimal vs Reference

To quantify the effect of aircraft type dependent departure routes, the optimized trajectories can be compared to their individual reference case. Overall, the altitude and speed profiles show that the optimized paths prefer to accelerate quicker and earlier, thereby remaining at lower altitudes for longer. The modeled optimal trajectories for the B737 are shown in Figure 9 along with the reference case. The optimized decision variables that define these trajectories are given in Table 5. The decision variables for the vertical profile are defined as factors of the maximum possible flight path angle or thrust as seen in Eq. 3 and Eq. 8. The ground track shows that all of the optimized trajectories avoid Utrecht more than the current SID. When optimizing for fuel, the track takes a fairly direct route towards the final way point. The noise optimal solution flies a longer distance to avoid populated areas. The optimal trajectory plots of each individual aircraft type are given in Appendix C. The SEL contours of the optimal paths are much more narrow than the reference SID, especially on the first half of the trajectory. This is especially true for the heavier aircraft. Furthermore, the SEL contours show that the trajectories try to avoid excessive noise exposure over Utrecht and Nieuwegein as much as possible. Nieuwegein is (partially) within the $>50\text{dB(A)}$ contour of most aircrafts' trajectories. The most noisy trajectory is that of the B744. This aircraft has a much larger SEL contour for all dB(A) values. For this aircraft the $>50\text{dB(A)}$ contour extends over Utrecht in its entirety and even borders on Hilversum to the north. The SEL contour plots for the noise optimal trajectories of each aircraft type are given in Appendix D.

Trajectory Type	L_1	R_2	$\Delta\chi_2$	L_3	R_4	γ_1	γ_2	γ_3	η_3	γ_4	γ_5
Fuel Optimal	1476 <i>m</i>	2222 <i>m</i>	71°	10274 <i>m</i>	5826 <i>m</i>	0.31	0.71	0.11	0.60	0.97	0.22
Intermediate	1356 <i>m</i>	2179 <i>m</i>	74°	33978 <i>m</i>	6183 <i>m</i>	0.31	0.69	0.11	0.64	0.99	0.22
Noise Optimal	5619 <i>m</i>	3869 <i>m</i>	85°	32691 <i>m</i>	4554 <i>m</i>	0.33	0.10	0.17	0.80	0.97	0.22

Table 5: Decision variables for selected B737 trajectories

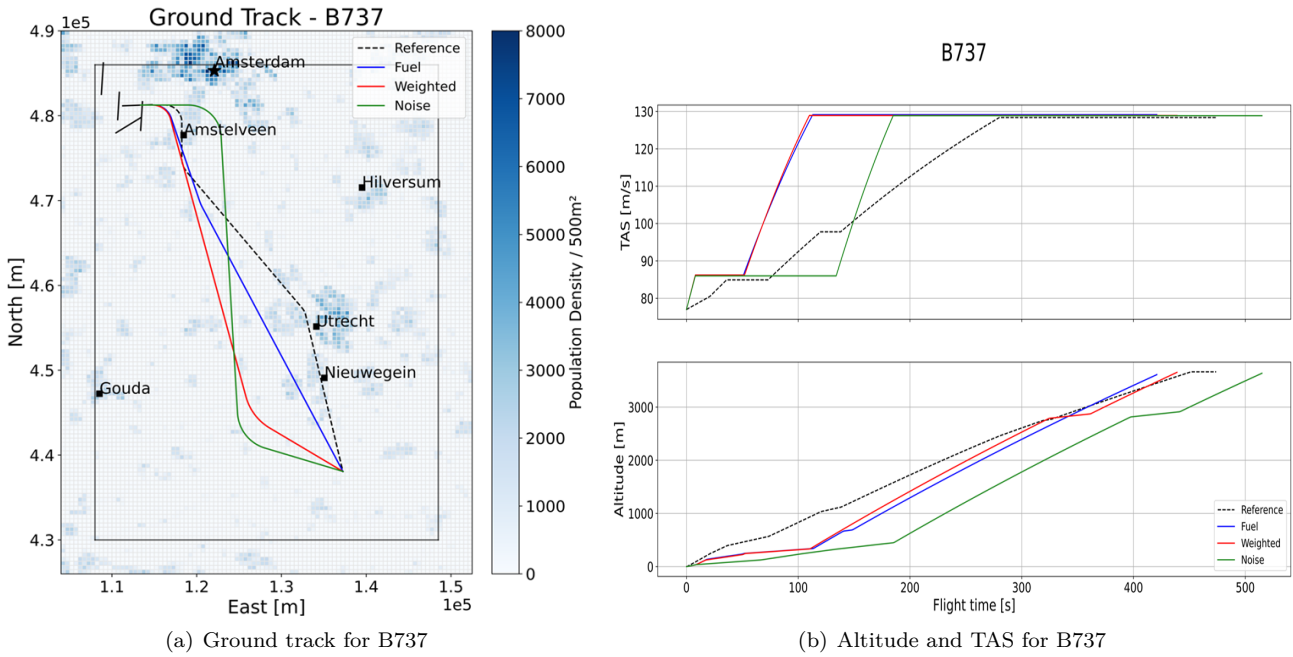


Figure 9: B737 optimal trajectories

A fuel optimal trajectory can save on average 15% fuel while also reducing the amount of awakenings by an average of 39% when compared to the reference SID. For noise optimal trajectories, a 60% decrease in noise was observed while fuel was reduced by an average of 8% compared to the current SID. The percentage change in both objective values for all aircraft types on the fuel, intermediate and noise optimal trajectories compared to the respective reference trajectories are depicted in Figure 10(a). An intermediate trajectory can save 13% fuel and 55% awakenings on average compared to the reference situation.

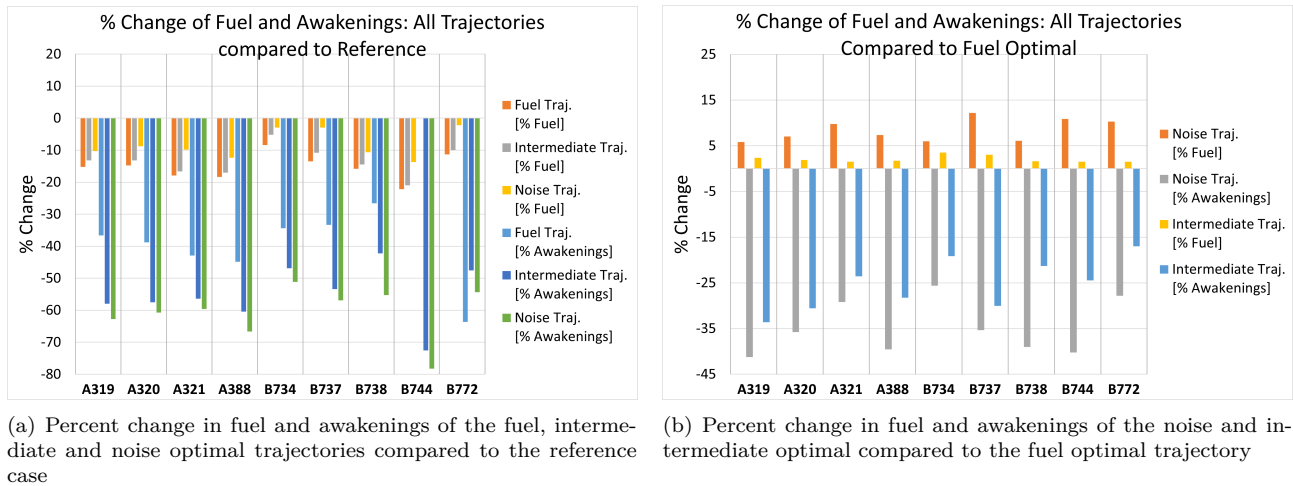


Figure 10: Comparison of the percentile change in objective values for all trajectories

5.2 Fuel Optimal vs Noise Optimal

To judge the trade-off between a noise optimal and a fuel optimal trajectory, the optimized trajectories are compared to each other. The altitude and speed profiles show that mostly the fuel optimal trajectories prefer to climb faster and accelerate earlier than the other optimal trajectories. The fuel optimal trajectories take a direct route to the final departure fix. For all aircraft, the path takes a right turn shortly after take off to change to the heading that brings them to the final LOPIK waypoint. Often no second turn is made, or the final turn has a very small heading change. The fuel trajectory takes less time than other paths, namely up to 7 minutes. The noise optimal routes take two distinct turns at the start and at the end. The turns have a larger heading change and the aircraft fly longer distances. Therefore the trajectory takes longer in general, needing between 8 and 8.5 minutes to reach the departure fix.

A noise optimal trajectory can significantly reduce the amount of awakenings when compared to a fuel optimal route. An average of 35% awakenings can be avoided. While awakenings are reduced, a noise optimal trajectory comes at the cost of higher fuel usage. In the tested scenarios an average of 8.4% extra fuel was consumed compared to fuel optimal trajectories. For the selected intermediate trajectories, fuel consumption is only slightly increased by an average of 2% while noise is reduced by 25% when comparing it to a fuel optimal trajectory. The percentage change in fuel and awakenings is shown in Figure 10(b) for all aircraft types. Here, the optimal noise and intermediate trajectories are compared to the fuel optimal trajectory.

5.3 Flying Other Optimal Trajectories

To reduce the number of separate trajectories all of the aircraft were flown on different optimal trajectories than their own. The goal of this was firstly to determine whether it was possible for aircraft to fly other trajectories and secondly how much the fuel consumption and awakenings would be affected. Many of the lighter aircraft did not manage to fly the trajectory of heavier ones. Therefore, the aircraft were grouped in two weight categories; medium and heavy. The medium aircraft could fly most of the other medium trajectories successfully. All of the A320 trajectories were invalid for other aircraft types except for the A319. The B734 was not able to fly any other trajectories than its own optimal ones. The heavy aircraft had substantially more trouble with the other heavy trajectories. Only the B744 was capable of flying all of the other trajectories in its category.

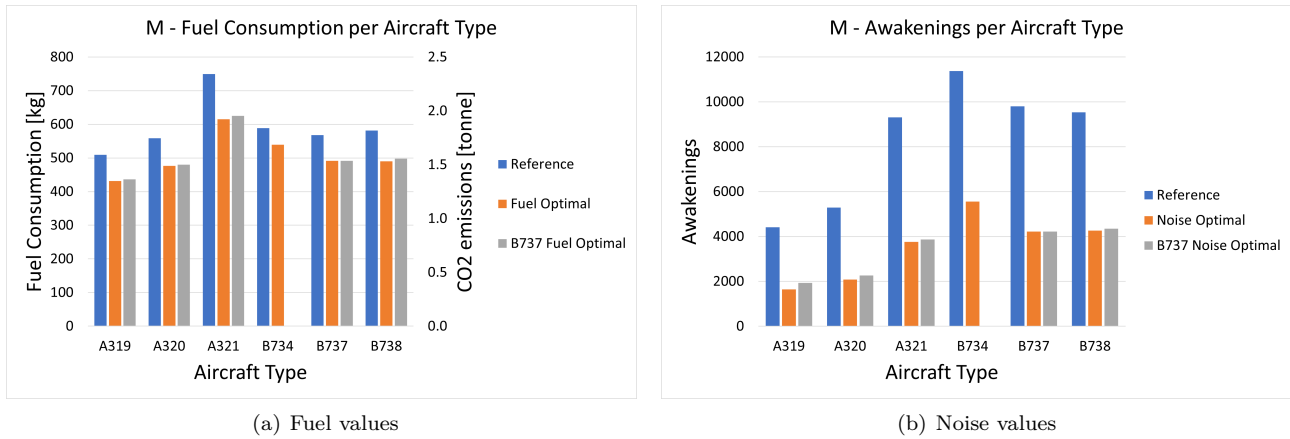


Figure 11: Fuel and noise values for optimal trajectories of medium aircraft

In the medium category, having other aircraft fly the B737 fuel optimal trajectory spends the least amount of extra fuel, namely 6.5 kg on average. The B738 trajectory resulted in a very small decrease in fuel consumption for all other flights. In terms of noise optimal solutions, the B737 trajectory also performs best for all aircraft types in the medium category. Other aircraft flying on this trajectory results in an average of 167 extra awakenings. Figures 11(a) and 11(b) show the amount of fuel and awakenings produced on each aircraft's own fuel and noise optimal trajectories, respectively, compared to the aircraft flying the trajectories of the B737 and the reference SID. The fuel consumption is translated to CO_2 emissions on the secondary axis in Figure 11(a). Heavy aircraft do not perform well on trajectories that are not their own optimized ones. All of the heavy aircraft are capable of flying the B772 fuel, intermediate and noise optimal trajectories, but at a huge cost. An extra 270 kg of fuel is consumed on average when other heavy aircraft fly the B772 fuel optimal trajectory when compared to their own fuel optimal trajectory. Furthermore, 7627 more awakenings will occur on the noise optimal trajectory. The intermediate trajectories cause an average of 168 kg extra fuel and 12,000 extra awakenings.

5.4 Computational Complexity

The optimization was run for 100 generations with a population size of 100. The time to run one iteration was 2.9 seconds on average resulting in a total duration of around 8 hours for the whole optimization. The optimization was performed using the jMetalPy framework in Python [53]. Figure 12 shows how the separate objective values evolve over time for one test case. The fuel objective converges very quickly and does not show improvements after 8 minutes. The awakenings seemingly does the same, however improvements are still found after 4 hours up until the final evaluations. This indicates that the noise objective has still not fully converged after the total 10,000 evaluations. It is clear that the awakenings objective is the limiting factor when it comes to computational complexity. The optimal fuel value is found quickly as the model is able to simply calculate the most direct route from the starting coordinate to the final one. Finding the optimal number of awakenings

is far more time consuming since for every iteration it needs to calculate the SEL value in every single grid-point in the noise evaluation area. There are 9266 grid-points in total.

Run time can be reduced by setting a different stopping criterion. For example, stopping the optimization once no improvements are found after a certain number of iterations. In this case, however, it would likely have resulted in less optimal values for the awakenings objective. Furthermore, to reduce the time it takes to obtain an optimal value for the number of awakenings the noise evaluation area can be made smaller. This will reduce the number of grid points over which the SEL value needs to be calculated, thereby decreasing the computation time. Reducing the noise evaluation area can potentially lower the accuracy of the results since for some aircraft the $>50\text{dB(A)}$ SEL contours already exceed the evaluation area.

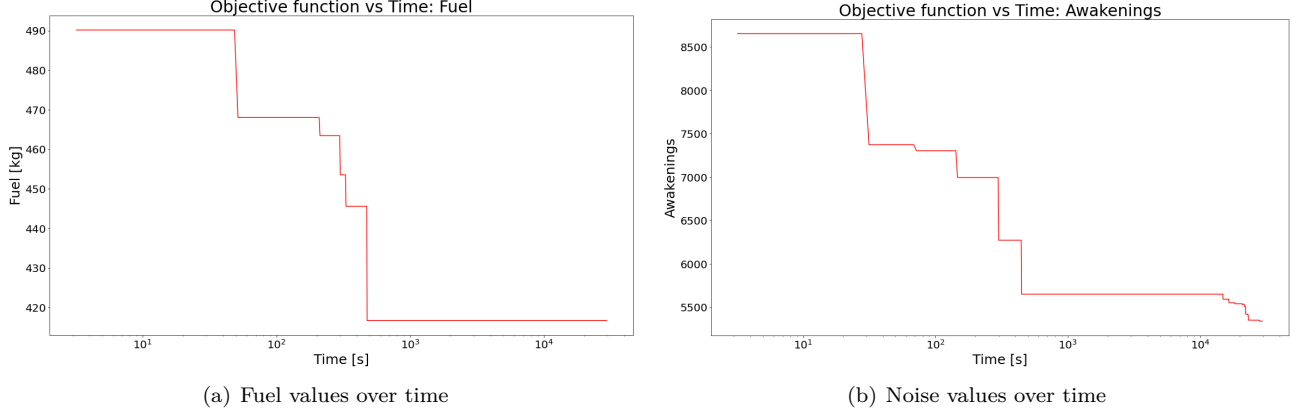


Figure 12: Evolution of objective value over time during optimization

6 Discussion

6.1 Optimal vs Reference

The optimized trajectories are able to significantly reduce fuel consumption and awakenings when compared to the reference case. The aircraft prefer to accelerate rather than climb in the first segments of all optimal trajectories, no matter the objective. Due to earlier and faster flap retraction on the fuel optimal profiles, the aircraft produces less drag and burns less fuel. With a lower thrust setting, the engine noise is reduced and less fuel is consumed as well. The direct route of the fuel optimal trajectory results in the shortest distance flown which minimizes fuel burn. Flying at a low altitude results in a lower spread of noise [18]. While the noise level directly under the aircraft is increased, fewer people are affected by it overall, resulting in fewer awakenings. To prioritize climbing over accelerating, the minimum flight path angle can be defined to be larger in the first two vertical segments to make sure that the aircraft is climbing with at least 3° . This would reduce the noise directly under the trajectory. The model calculates the total number of awakenings from the trajectories by adding the awakenings from each grid point together. For the optimization it is therefore not important where the awakenings occur. A low flying aircraft can cause a high percentage of awakenings in the grid points directly below the trajectory while avoiding the spread of noise towards more grid points around the trajectory. If the population within the grid points directly under the trajectory is lower than in the surrounding ones, which can be achieved by adjusting the ground track, then even though the SEL value is higher right under the trajectory, overall fewer total awakenings will occur. Most of the noise reduction can thus be achieved by flying longer distances to avoid noise sensitive areas and grid points. This is because the model uses the number of awakenings as an optimization objective and not explicitly the SEL value. The SEL value is a time dependent metric. Flying at higher speeds will shorten the noise event which will have a positive impact on the SEL value. For individual departures this will decrease the number of awakened people. However, when considering that a higher acceleration translates to a higher throughput capacity for take-off, more aircraft departing from a runway will ultimately have adverse effects on noise to the population near the airport. An important aspect to note is that atmospheric and environmental factors, such as non-standard ISA conditions and reflection, that could affect the propagation of aircraft noise are not considered in this study.

Further reasons for the large reduction in fuel and noise can be given. Firstly, the reference SID is modeled using the same ground path and vertical profile for all aircraft types, resulting in inefficient departure trajectories. The trajectory optimization model on the other hand finds the best noise and fuel minimal departure path and profile that is tailored to one specific aircraft type. This results in either direct routes for fuel optimization or avoiding cities to reduce noise. Secondly, the new trajectories are optimized based on recent population data while the reference SID has been in use since Schiphol Airport expanded largely in the late 1960s [14]. Through

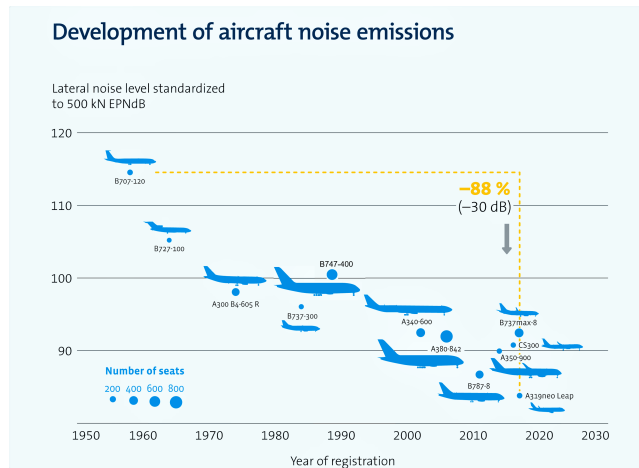


Figure 13: Development of aircraft noise over time [56]

the years limited changes were made to the SID and only at low altitudes close to the airport [54] [19]. The expansion of Utrecht towards the west, where the current LOPIK departure crosses, was not considered. As mentioned, the model tries to optimize the number of awakenings and not explicitly the SEL value. While the SEL can be reduced by optimized vertical profiles, a high reduction in awakenings can already be achieved by simply rerouting along areas with a lower population density.

Finally, the B747-400 is used in the analysis which results in high fuel and noise savings compared to the reference. This aircraft is very heavy, loud and inefficient which means it has a lot to gain from a trajectory that is specifically tailored to its performance. While the optimal trajectories significantly improve fuel consumption and noise exposure, the B744 is still more noisy and inefficient than any other aircraft. In 2019, the flights that caused the most complaints from the local community to the Bewoners Aanspreekpunt Schiphol (BAS) were B744s departing from the same runway as was used in this study, the 'Buitenveldertbaan' [50]. Many older aircraft types such as this one are being phased out by most airlines as they are too loud and inefficient. For example, KLM has already phased out the B747-400 passenger fleet in 2020 and replaced it with the quieter and cleaner B787 Dreamliner. This aircraft is up to 40% quieter and emits 35-40% less CO_2 [50]. A fleet of newer aircraft can cut airport costs for airlines in the long run. In general, aircraft are getting quieter to adhere to noise certification requirements and noise limits. Improvements in aircraft technology have resulted in an 88% decrease in aircraft noise since the 1950s as seen in Figure 13. The B747-400 was registered in 1989 and has a measured lateral noise level of around 100 EPNdB (Effective Perceived Noise Level) [55].

6.2 Fuel Optimal vs Noise Optimal

Fuel and awakenings are two opposing objectives. When one is reduced, the other increases and vice versa. This is made clear from the convex nature of the Pareto curve. A trade-off needs to be made between flying a fuel optimal or a noise optimal trajectory. When analysing the objectives individually, there are significant benefits to choosing either of the two extremes. A fuel optimal trajectory is beneficial for the environment. Reducing fuel burn results in fewer CO_2 emissions. This aids in reaching the environmental goals set by CORSIA and SESAR to mitigate the effect of greenhouse gases on climate change. In turn, the costs of flying can be reduced for airlines. One tonne of fuel emits 3.16 tonnes CO_2 while one tonne of CO_2 currently costs €55 [25]. The cost of CO_2 is increasing steadily and these numbers add up in the long run when considering the amount of aircraft movements per year.

A noise optimal trajectory is valuable for the future growth of air transport at Schiphol Airport due to the current restriction of 500,000 aircraft movements per year. Only by decreasing the number of highly annoyed people living in the vicinity of the airport can the restrictions be loosened. Implementing a noise optimal trajectory would therefore allow a larger number of aircraft movements to take place. It is important to note that the range of awakenings is much larger than that of fuel consumption when looking at the Pareto fronts. This means that when choosing a noise optimal trajectory, the amount of fuel that is added as opposed to a fuel optimal trajectory is a much smaller percentage than the change in number of awakenings when choosing the noise optimal over the fuel optimal path.

An intermediate solution can be a good compromise for realistic operations. With only a very small percentage increase in fuel, still a much larger amount of awakenings can be avoided when comparing to the fuel optimal trajectory. Importantly, the intermediate trajectories for all aircraft types are still much more superior to the current reference situation.

6.3 Flying Other Optimal Trajectories

The results showed that optimizing individual departure procedures per aircraft type can be beneficial to reduce fuel consumption and noise exposure. However, from an Air Traffic Management perspective it is undesirable to have many separate departure routes leading to the same departure fix. This increases airspace complexity and compromises safety and predictability. The Dutch government has fixed arrival and departure routes as one of their goals of the Dutch Airspace Redesign Project [51] as this will help to reduce CO_2 emissions and the spread of noise. Therefore, it is interesting to see if the different aircraft types can fly the optimal trajectories of other aircraft. Subsequently, a set of solutions can be selected that can be applied to several aircraft, thereby reducing the amount of individual trajectories. The criteria for a successful flight on a different trajectory are fixed:

- The aircraft must reach the final altitude of 3650 m (12000 ft) within 50 m (160 ft).
- The aircraft must reach the final V_{clean} speed of 128 m/s (250 kts).
- The aircraft must reach the final lateral coordinates of the trajectory.

All of the aircraft were able to reach the final speed and lateral coordinates when flying on a different aircraft's trajectories. Some aircraft, however, barely didn't reach the final altitude and were considered invalid due to the strict criteria. In reality, the flight might still be considered a success since the altitude is not always so definite. The lighter aircraft were incapable of flying on the trajectories of heavy aircraft. A reason for this may be that the vertical profile is defined in such a way that once V_{clean} is reached, the aircraft remains on a constant flight path angle (a factor of γ_4) until reaching the final altitude. Only when the aircraft makes a turn does the flight path angle factor change to γ_5 . Once out of the turn it returns to a factor of γ_4 . Since heavy aircraft are less steep climbers than lighter ones, this flight path angle may not be sufficient for some other aircraft to reach the final altitude within the same time as the heavy aircraft. In reality the aircraft could still adjust flight path angle and throttle setting to reach the end of the trajectory, or it would simply take longer to reach the altitude. To allow all aircraft types to reach the final altitude when flying on a different aircraft's trajectory, the model could be altered by changing the criteria for the flight path angle in the fourth vertical segment. To recall, in the fourth segment the aircraft climbs with a constant speed (V_{clean}) until the final altitude is reached. A constraint can be put on γ_4 to be set to the minimum value that is necessary to reach the final altitude and be optimized above this value. In this manner every aircraft would be able to fly the trajectories successfully.

When aircraft fly a different trajectory than their own optimal ones, it comes at the cost of the respective objective. The own optimal fuel trajectory should have the least amount of fuel consumption and the own optimal noise trajectory should have the fewest awakenings. This is true for all trajectories except for the B738. When other aircraft fly on these trajectories, a very small decrease in awakenings is observed. This should not be possible and can be explained by the optimization process not having converged as much for this aircraft, or the process got stuck in a local minimum. This means that the solutions for the B738 trajectories are not the absolute optimal solutions and cannot be considered valid.

In the medium weight category, the B737 trajectory proved to be the best compromise. By letting all medium aircraft fly on the B737 trajectory, the number of separate trajectories can be reduced without an excessive increase in fuel and awakenings. Heavy aircraft flying on other trajectories causes a very large increase in fuel and noise, therefore it would not be worth placing them on a different trajectory. Even though this increases the amount of separate trajectories, the excess fuel and noise would not be sustainable in the long run.

7 Conclusions

In this study a trajectory optimization model was developed that uses multi-objective optimization to create fuel and noise minimal departure trajectories for different aircraft types at Schiphol Airport. The overarching goal was to increase sustainability in air transport by reducing noise annoyances and CO_2 emissions to encourage further growth of the industry.

The method showed that tailored trajectories are capable of reducing fuel consumption and awakenings due to noise. A high amount of savings is possible when compared to the current SID because each optimized trajectory is able to adapt the vertical profile and ground track to a specific aircraft and objective. The results for the specific 09 LOPIK departure are of significance because in the near future more flights will be able to fly direct routes towards south-eastern destinations from Schiphol Airport. The implication of fewer noise disturbances and less CO_2 emissions per departure is an increase in aircraft movements that would support growth. This is advantageous for Schiphol since it is currently limited by noise and emission restrictions. Airlines also benefit from reduced costs and can thus offer more flights. Less fuel consumption results in lower CO_2 emissions. With optimal departure trajectories a significant step can be set in reaching the climate goals in aviation by reducing

the effect of greenhouse gases and climate change.

While fuel and noise can be optimized simultaneously, they are opposing objectives meaning they have an inverse relationship. Since both objectives are limiting factors for air transport growth and sustainability, it is not desirable to only implement one of the two extremes. An intermediate trajectory from the middle of the Pareto front offers a compromise for more realistic operations. While fuel and noise are increased as opposed to the optimal trajectories, the solution is still far superior to the current situation. Depending on the time of day, either noise or fuel consumption may be the governing objective. At night for example, an intermediate trajectory can be adapted to favor noise minimization over emissions and fuel consumption.

When each aircraft flies its own optimal trajectory, the amount of separate trajectories would become infeasible when applied to all runways and departure fixes. On the other hand, when limiting separate routes by letting aircraft fly the optimal trajectory of one other aircraft it comes at the cost of both noise and fuel consumption. The extra costs when medium aircraft fly on a common trajectory are manageable while the same does not apply for heavy aircraft.

8 Recommendations

Several recommendations are made for future research into the topic of aircraft type dependent departure trajectories at Schiphol Airport. The outcome of this research is relevant for one case scenario at Schiphol Airport comprised of a specific runway and departure fix combination. This implies that for different runways or departure fixes the optimization results may differ. Additional research should be done for each departure scenario at Schiphol to quantify the benefit of tailored trajectories for the entire airport. This includes an investigation into the operational feasibility and complexity of implementing separate departure trajectories per aircraft type for each runway.

The proper assignment of runways and departure trajectories based on aircraft type, destination, and time of day could serve to further reduce noise and fuel emissions. Such an allocation model could also help in determining the optimal trajectory to choose as a shared trajectory. For example, a weighting scheme based on the aircraft operating at the airport could change how a shared trajectory is determined. Additionally, since airports are placing an increased emphasis on cleaner and quieter aircraft types this would be represented in such a model. Since some of the aircraft types used in this study will be, or have already been, phased out by airlines, implementing newer ones would provide insight into future operations. To do so the required aircraft coefficients and parameters are needed which are not always readily available for new aircraft.

The aircraft are split into two weight categories in this research based on their MTOW. The categories are based on the ICAO wake vortex separation requirements generally describing three weight classes (light, medium, heavy). The Wake Turbulence Re-categorization (RECAT) provides more weight categories that give a more accurate representation and comparison between aircraft types. Future research should be conducted on the effect of re-categorization of the aircraft on the selection of shared trajectories.

The trajectory optimization in this study was performed using purely the MTOW of each aircraft. The take-off weight of an aircraft has a great impact on the performance during the departure procedure and an individual aircraft's take-off weight can vary greatly. Performing a sensitivity analysis using different percentages of the MTOW for each aircraft and implementing it into the trajectory optimization model will give insight into how the optimal trajectories are affected by weight changes. This should be investigated in future research.

The implemented fuel flow model uses engine specific coefficients along with a linear altitude correction. For departure procedures this model is applicable, however when considering cruise conditions the mach number, air density and temperature should be taken into account. Future research on the topic should make use of a more complex fuel flow model that can more accurately represent different phases of flight.

Since fuel burn and noise exposure are two opposing objectives, instead of having separate fuel optimal and noise optimal trajectories, it is worth investigating one general path that takes noise into account at lower altitudes and focuses on emissions and fuel burn at higher altitudes. The "Luchtvaart Nota" provides rules and requirements for the development of safe and sustainable civil aviation in the Netherlands. A guiding principle applies according to this document, namely that above 6000ft altitude emissions are prioritized whereas below 6000 *ft* noise abatement is considered the primary objective [7]. Combining these guidelines with the trajectory optimization technique for aircraft type dependent departure trajectories is an area of interest for future research.

References

- [1] M. Pretto, P. Giannattasio, M. De Gennaro, A. Zanon, and H. Kuehnelt, “Forecasts of future scenarios for airport noise based on collection and processing of web data,” *European Transport Research Review*, vol. 12, no. 1, 2020.
- [2] V. Ho-Huu, S. Hartjes, H. G. Visser, and R. Curran, “Simultaneous design of different aircraft departure routes taking community noise exposure events into account,” *Inter.noise Madrid - 48th International Congress and Exhibition on Noise Control Engineering*, 2019.
- [3] International Air Transport Association, “World Air Transport Statistics 2020,” *Airlines Magazine*, 2020.
- [4] D. S. Lee, D. W. Fahey, A. Skowron, M. R. Allen, U. Burkhardt, Q. Chen, S. J. Doherty, S. Freeman, P. M. Forster, J. Fuglestedt, A. Gettelman, R. R. De León, L. L. Lim, M. T. Lund, R. J. Millar, B. Owen, J. E. Penner, G. Pitari, M. J. Prather, R. Sausen, and L. J. Wilcox, “The contribution of global aviation to anthropogenic climate forcing for 2000 to 2018,” *Atmospheric Environment*, vol. 244, no. 9, 2020.
- [5] P. Peeters and J. Melkert, “Toekomst verduurzaming luchtvaart: een actualisatie,” *Parlement en Wetenschap*, 2021.
- [6] United Nations, “Towards a Climate-Neutral Europe: Curbing the Trend,” in *Paris Agreement*, (Paris), 2015.
- [7] Ministerie van Infrastructuur en Waterstaat, “Verantwoord vliegen naar 2050: Luchtvaartnota 2020-2050,” Tech. Rep. November, Ministerie van Infrastructuur en Waterstaat, Den Haag, 2020.
- [8] Ministerie van Infrastructuur en Milieu, “Geluidsbelastingkaarten luchthaven Schiphol voor het gebruiksjaar 2016,” Tech. Rep. Juni, Ministerie van Infrastructuur en Milieu, Den Haag, 2017.
- [9] E. M. Ganic, F. Netjasov, and O. Babic, “Analysis of noise abatement measures on European airports,” *Applied Acoustics*, vol. 92, pp. 115–123, 2015.
- [10] A. Behere, D. Lim, Y. Li, Y.-C. D. Jin, Z. Gao, M. Kirby, and D. N. Mavris, “Sensitivity Analysis of Airport Level Environmental Impacts to Aircraft Thrust, Weight, and Departure Procedures,” in *AIAA Scitech*, (Orlando, FL), American Institute of Aeronautics and Astronautics, 2020.
- [11] European Commission, “Flightpath 2050: Europe’s Vision for Aviation,” tech. rep., European Commission, Luxembourg, 2011.
- [12] M. Zhang, A. Filippone, and N. Bojdo, “Multi-objective optimisation of aircraft departure trajectories,” *Aerospace Science and Technology*, vol. 79, pp. 37–47, 2018.
- [13] X. Prats, V. Puig, and J. Quevedo, “A multi-objective optimization strategy for designing aircraft noise abatement procedures. Case study at Girona airport,” *Transportation Research Part D: Transport and Environment*, vol. 16, no. 1, pp. 31–41, 2011.
- [14] J. Hardiman, “A Brief History of Amsterdam’s Schiphol Airport,” 2021.
- [15] International Civil Aviation Organization, “Assembly Resolutions in Force (as of 4 October 2013),” in *ICAO Assembly*, (Montreal), pp. 1–58, International Civil Aviation Organization, 2014.
- [16] R. Torres, J. Chaptal, C. Bès, and J. B. Hiriart-Urruty, “Optimal, environmentally friendly departure procedures for civil aircraft,” *Journal of Aircraft*, vol. 48, no. 1, pp. 11–22, 2011.
- [17] International Civil Aviation Organization, “Aircraft Operations,” Tech. Rep. 5, ICAO, Montreal, 2006.
- [18] H. W. Veerbeek and M. A. Brouwer, “Noise measurement analysis during a noise abatement departure procedure trial,” tech. rep., Nationaal Lucht- en Ruimtevaartlaboratorium, Amsterdam, 2012.
- [19] Air Traffic Control the Netherlands, “EHAM AMSTERDAM / Schiphol,” tech. rep., LVNL, Amsterdam, 2021.
- [20] International Civil Aviation Organization, “Carbon Offsetting and Reduction Scheme for International Aviation (CORSA) - Frequently Asked Questions (FAQs),” tech. rep., ICAO, 2020.
- [21] E. Schoeffmann and E. Platteau, “SESAR and the Environment,” tech. rep., SESAR Joint Undertaking, Brussels, 2010.

- [22] O. Inderwildi, C. Carey, G. Santos, X. Yan, H. Behrendt, A. Holdway, L. Maconi, N. Owen, T. Shirvani, and A. Teytelboym, “Future of Mobility Roadmap: Ways to Reduce Emissions While Keeping Mobile,” tech. rep., University of Oxford, Smith School of Enterprise and the Environment, Oxford, 2009.
- [23] International Air Transport Association, “Jet Fuel Price Monitor,” 2021.
- [24] European Union Aviation Safety Agency, “European Aviation Environmental Report 2019,” tech. rep., EASA, 2020.
- [25] ICE (Intercontinental Exchange), “Daily Carbon Prices,” 2021.
- [26] H. G. Visser and R. A. Wijnen, “Optimization of noise abatement departure trajectories,” *Journal of Aircraft*, vol. 38, no. 4, pp. 620–627, 2001.
- [27] S. Hartjes, H. G. Visser, and S. J. Hebly, “Optimisation of RNAV noise and emission abatement standard instrument departures,” *Aeronautical Journal*, vol. 114, no. 1162, pp. 757–767, 2010.
- [28] X. Prats, V. Puig, J. Quevedo, and F. Nejjari, “Multi-objective optimisation for aircraft departure trajectories minimising noise annoyance,” *Transportation Research Part C: Emerging Technologies*, vol. 18, no. 6, pp. 975–989, 2010.
- [29] V. Ho-Huu, S. Hartjes, H. G. Visser, and R. Curran, “An efficient application of the MOEA/D algorithm for designing noise abatement departure trajectories,” *Aerospace*, vol. 4, no. 4, 2017.
- [30] V. Ho-Huu, S. Hartjes, H. G. Visser, and R. Curran, “Integrated design and allocation of optimal aircraft departure routes,” *Transportation Research Part D: Transport and Environment*, vol. 63, pp. 689–705, 2018.
- [31] S. Hartjes and H. G. Visser, “Efficient trajectory parameterization for environmental optimization of departure flight paths using a genetic algorithm,” *Journal of Aerospace Engineering*, pp. 1–9, 2016.
- [32] S. Hartjes and H. Visser, “Parameterization of Noise Abatement Departure Trajectories,” tech. rep., TU Delft, Delft, 2015.
- [33] M. Battel and T. M. Young, “Simplified thrust and fuel consumption models for modern two-shaft turbofan engines,” *Journal of Aircraft*, vol. 45, no. 4, pp. 1450–1456, 2008.
- [34] J. Sun, *Open Aircraft Performance Modeling Based on an Analysis of Aircraft Surveillance Data*. PhD thesis, Delft University of Technology, 2019.
- [35] International Civil Aviation Organization, “ICAO Aircraft Engine Emissions Databank (EEDB),” 2020.
- [36] P. Siegmund, D. Houthuijs, R. Hogenhuis, S. Hebli, J. Devilee, O. Breugelmans, and J. Beintema, “Vliegtuiggeluid : meten, rekenen en beleven,” tech. rep., Rijksinstituut voor Volksgezondheid en Milieu, 2019.
- [37] E. Boeker, E. Dinges, B. He, G. Fleming, C. Roof, P. Gerbi, A. Rapoza, and J. Hemann, “Integrated Noise Model (INM) Version 7.0 Technical Manual,” tech. rep., U.S. Department of Transportation, Cambridge, MA, 2008.
- [38] S. Hartjes, “INMTM v3 Noise Calculation Tool Specification,” Tech. Rep. 3, Clean Sky, 2010.
- [39] Schiphol Amsterdam Airport NOMOS Online, “Over Geluid - Wat is geluid,” 2021.
- [40] Centraal Bureau voor de Statistiek, “Kaart van 500 meter bij 500 meter met statistieken,” 2019.
- [41] Federal Interagency Committee on Aviation Noise, “Effects of Aviation Noise on Awakenings from Sleep,” tech. rep., FICAN, 1997.
- [42] M. T. Emmerich and A. H. Deutz, “A tutorial on multiobjective optimization: fundamentals and evolutionary methods,” *Natural Computing*, vol. 17, pp. 585–609, 2018.
- [43] B. Ceulemans, “Tailored SID and Profile Allocation for Amsterdam Airport Schiphol,” Master’s thesis, Delft University of Technology, 2016.
- [44] Royal Schiphol Group, “Kerngegevens 2019,” tech. rep., Royal Schiphol Group, 2020.
- [45] Royal Schiphol Group, “Facts about Schiphol Airport,” 2021.

- [46] H. H. Hesselink, J. M. Nibourg, L. D’Estampes, and P. Lezaud, “Airport Capacity Forecast: Short-term Forecasting of Runway Capacity,” in *Proceedings of the fourth SESAR Innovation Days*, SESAR WPE, 2014.
- [47] Royal Schiphol Group, “Evaluatie Gebruiksprognose 2019,” tech. rep., Royal Schiphol Group, 2019.
- [48] Nationaal Lucht- en Ruimtevaartlaboratorium, “Managementsamenvatting: Het berekenen van vliegtuiggeluid,” tech. rep., NLR, Amsterdam, 2008.
- [49] Royal Schiphol Group, “Nieuw Normen- en Handhaving-stelsel Schiphol,” tech. rep., Royal Schiphol Group, Schiphol, 2020.
- [50] Minder Hinder Schiphol, “Strenger Ontmoedigingsbeleid Bepaalde Vliegtuigtypes,” 2021.
- [51] Ministerie van Infrastructuur en Waterstaat, “Ontwerp- Voorkeursbeslissing Luchtruimherziening,” tech. rep., Ministerie van Infrastructuur en Waterstaat, Ministerie van Defensie, Luchtverkeersleiding Nederland, Commando Luchtstrijdkrachten, Maastricht Upper Area Control Centre, 2021.
- [52] Luchtverkeersleiding Nederland, “Standard Departure Chart - Instrument Departure RWY 09,” 2018.
- [53] A. Benítez-Hidalgo, A. J. Nebro, J. García-Nieto, I. Oregi, and J. D. Ser, “jmetalpy: A python framework for multi-objective optimization with metaheuristics,” *Swarm and Evolutionary Computation*, p. 100598, 2019.
- [54] SkyVector, “Aeronautical Charts,” 2021.
- [55] M. Nöding and L. Bertsch, “Application of Noise Certification Regulations within Conceptual Aircraft Design,” *Aerospace*, vol. 8, no. 210, 2021.
- [56] German Aviation Association, “Aviation invests billions in active and passive noise control,” 2021.

Appendices

A SID Chart Runway 09

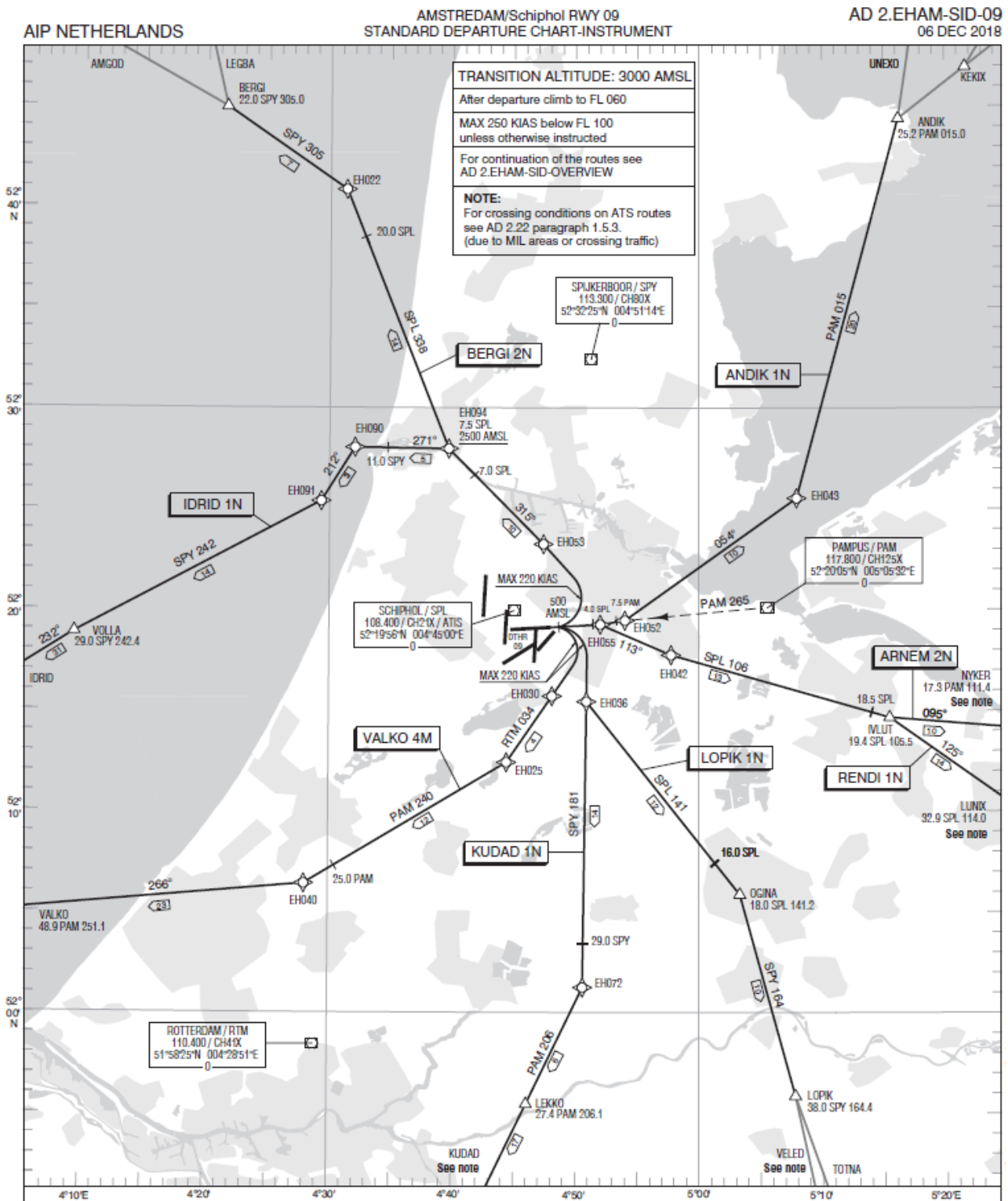
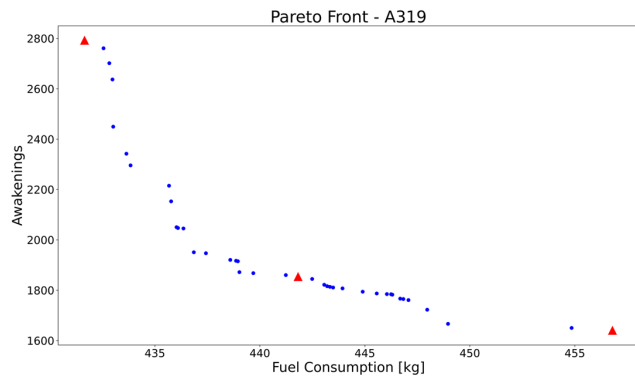
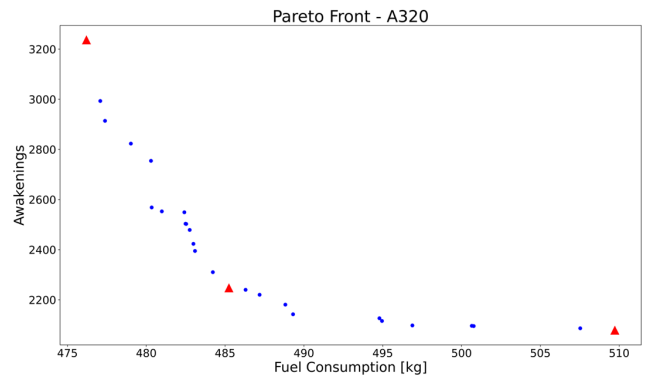


Figure 14: Departure chart for RWY 09

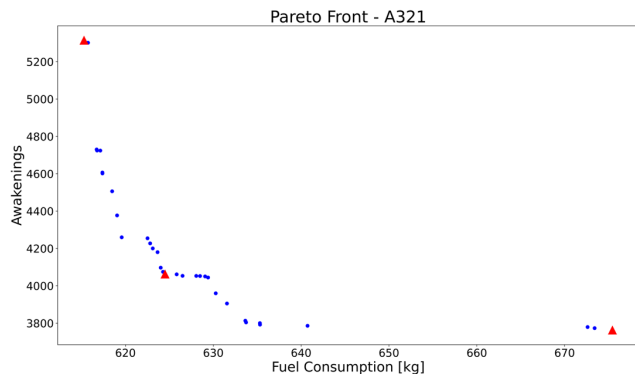
B Pareto Fronts



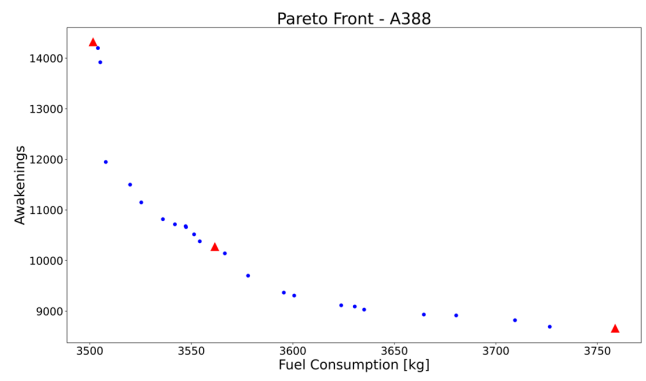
(a) Pareto Front A319



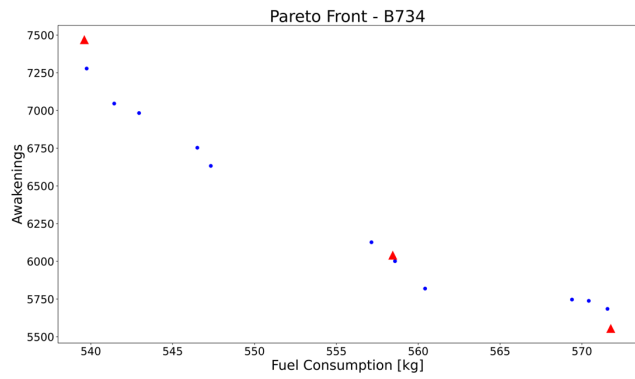
(b) Pareto Front A320



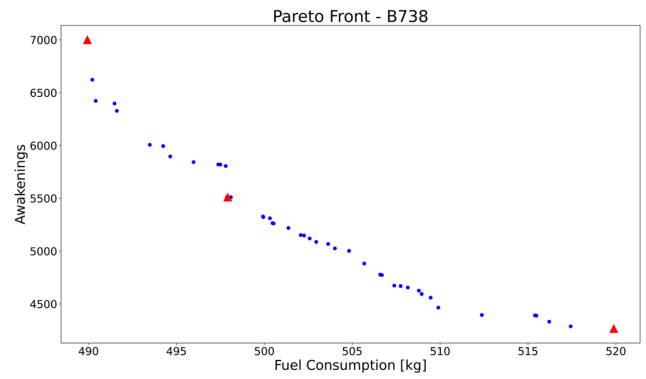
(c) Pareto Front A321



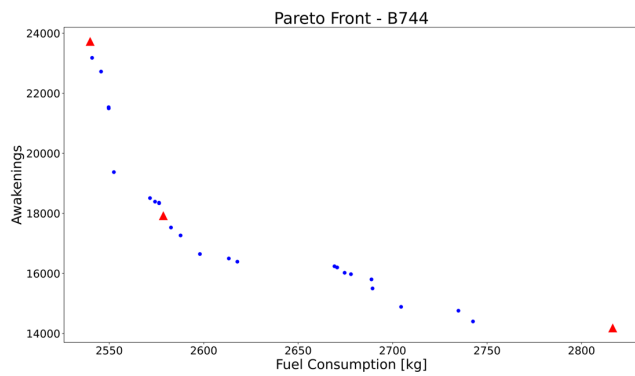
(d) Pareto Front A388



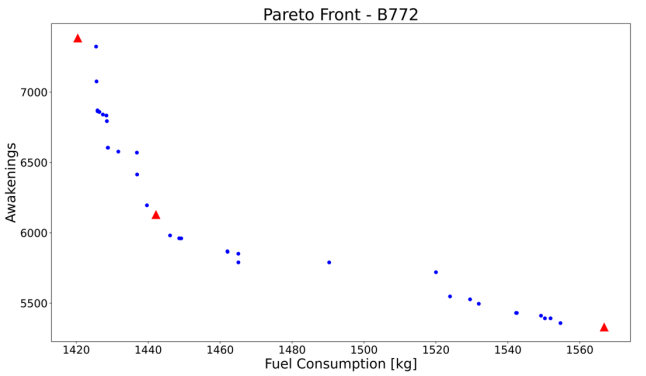
(e) Pareto Front B734



(f) Pareto Front B738



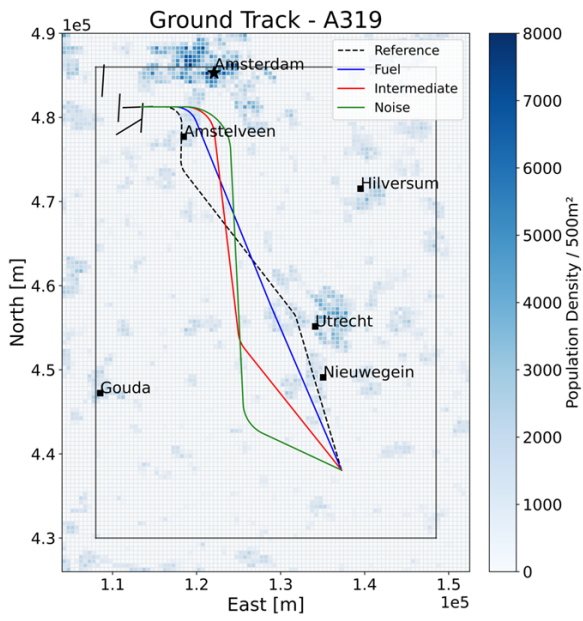
(g) Pareto Front B744



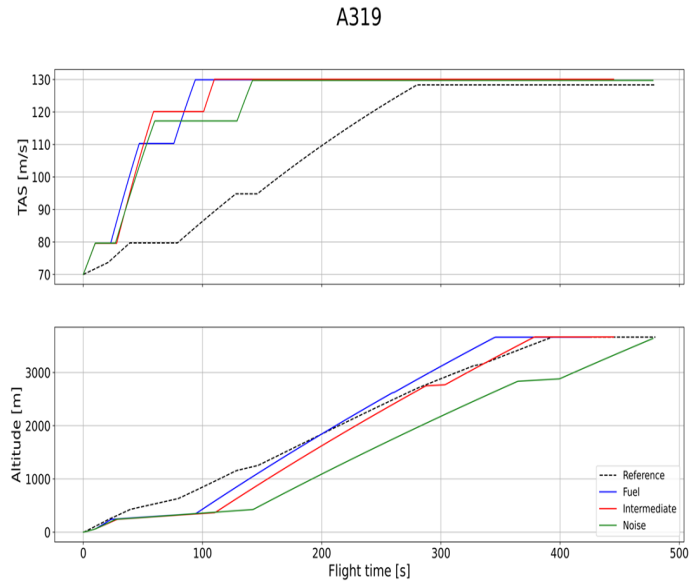
(h) Pareto Front B772

Figure 15: Pareto fronts for each aircraft type

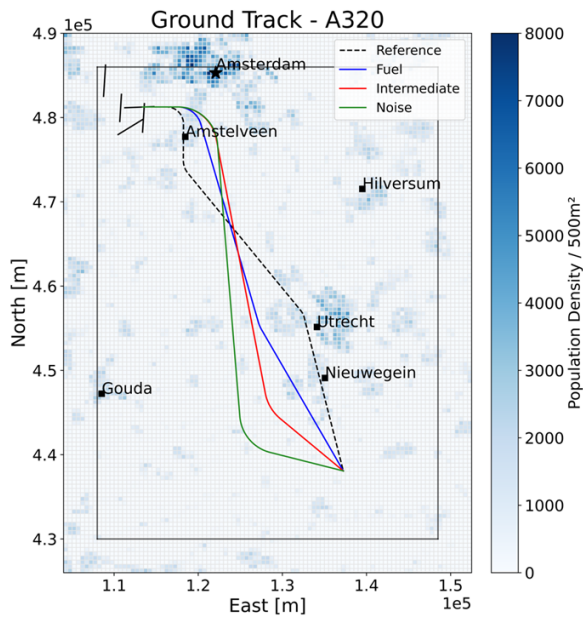
C Optimal Trajectories



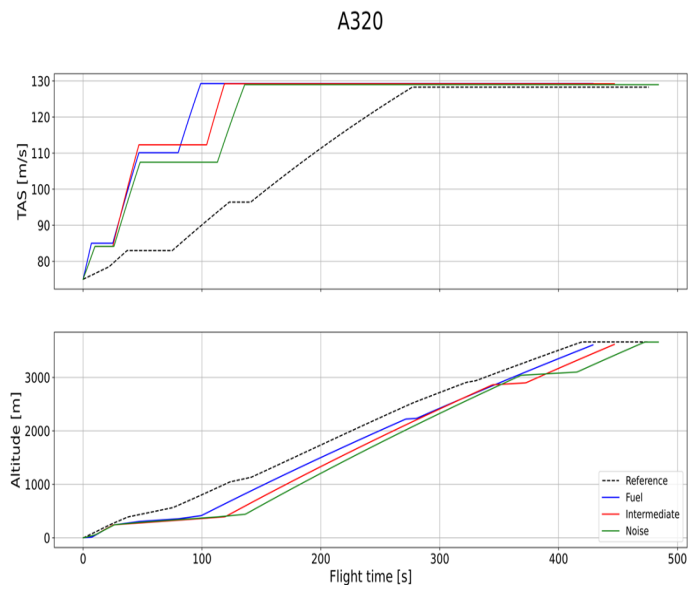
(a) Ground track for A319



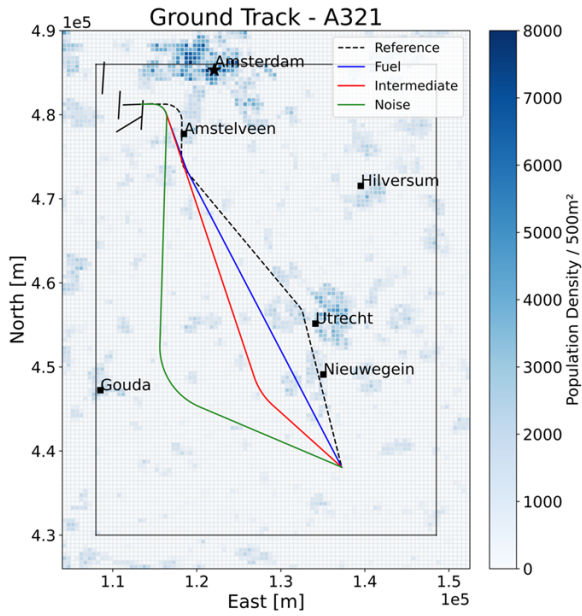
(b) Altitude and TAS for A319



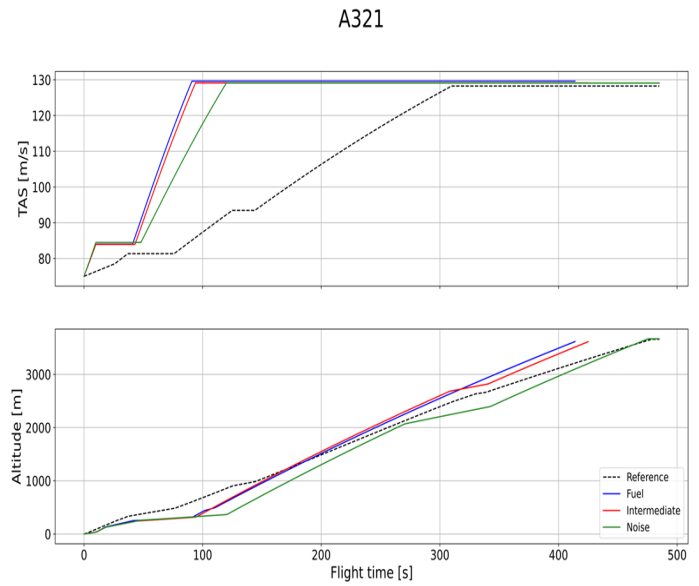
(c) Ground track for A320



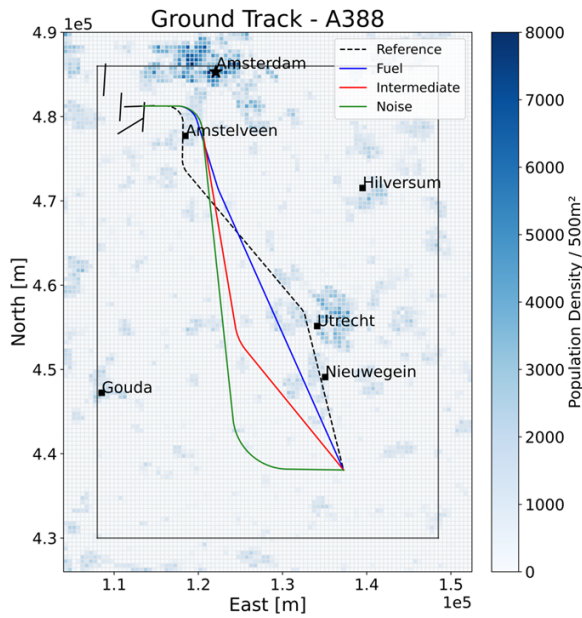
(d) Altitude and TAS for A320



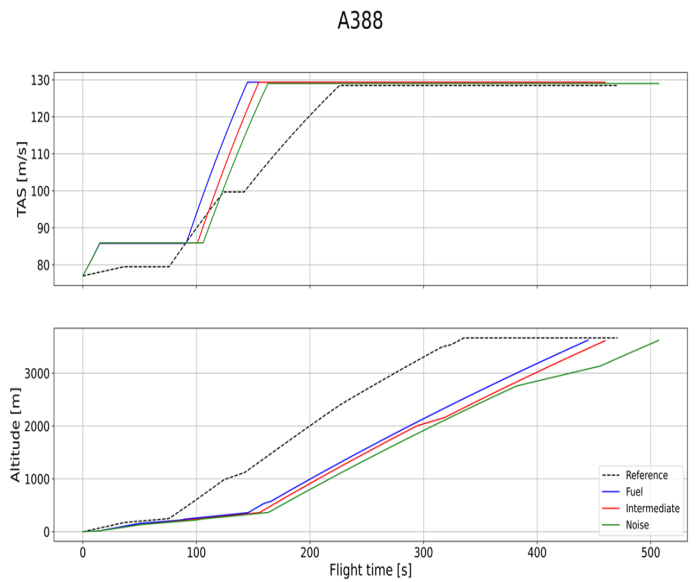
(e) Ground track for A321



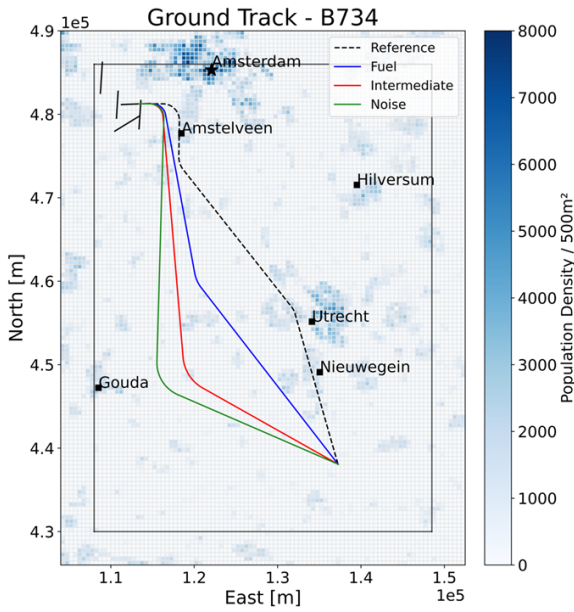
(f) Altitude and TAS for A321



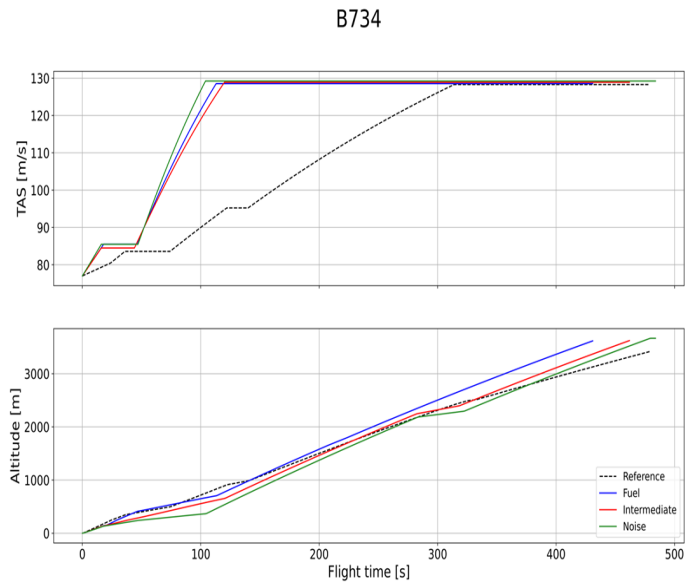
(g) Ground track for A388



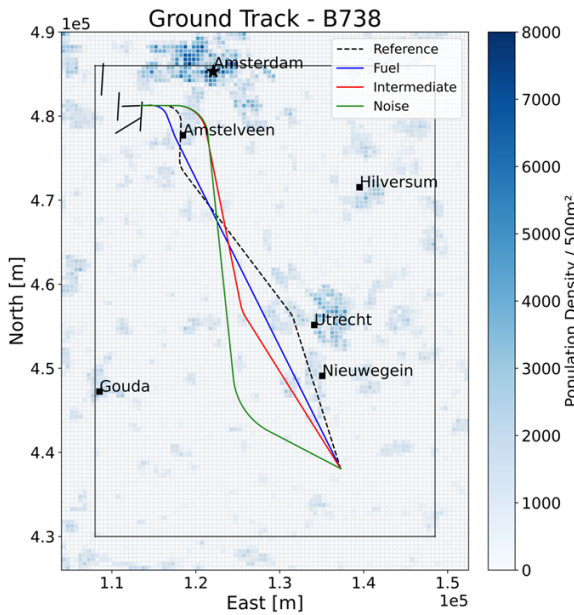
(h) Altitude and TAS for A388



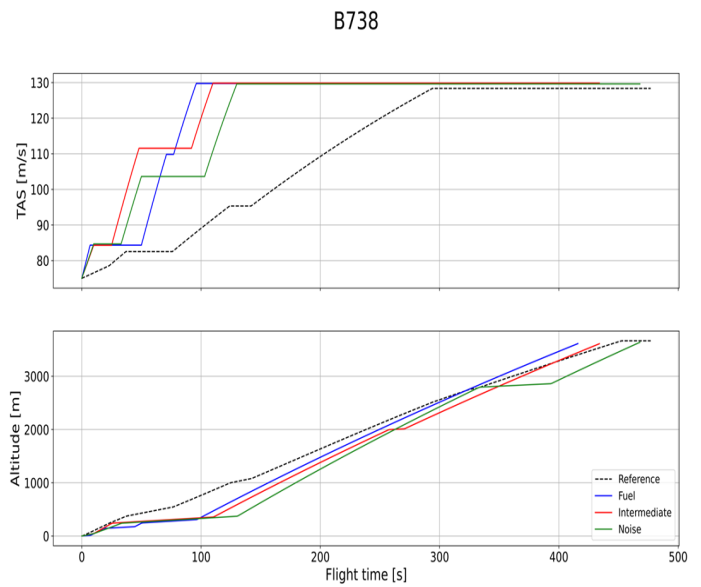
(i) Ground track for B734



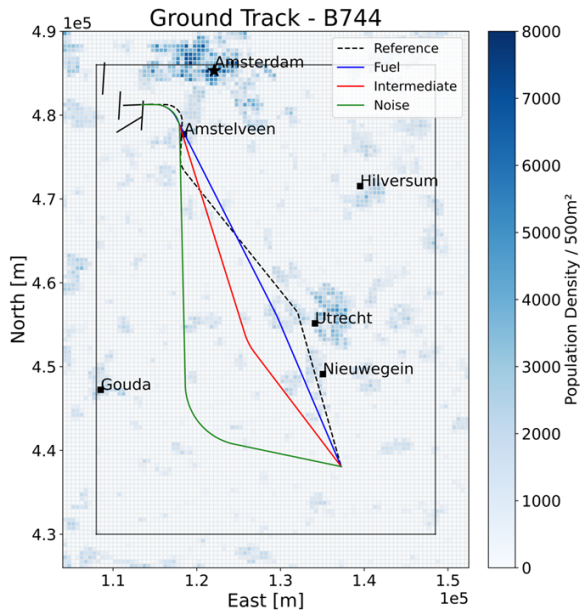
(j) Altitude and TAS for B734



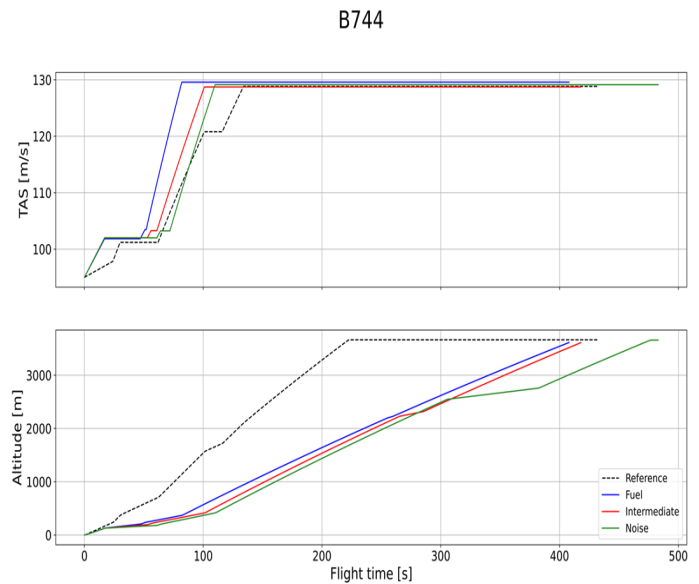
(k) Ground track for B738



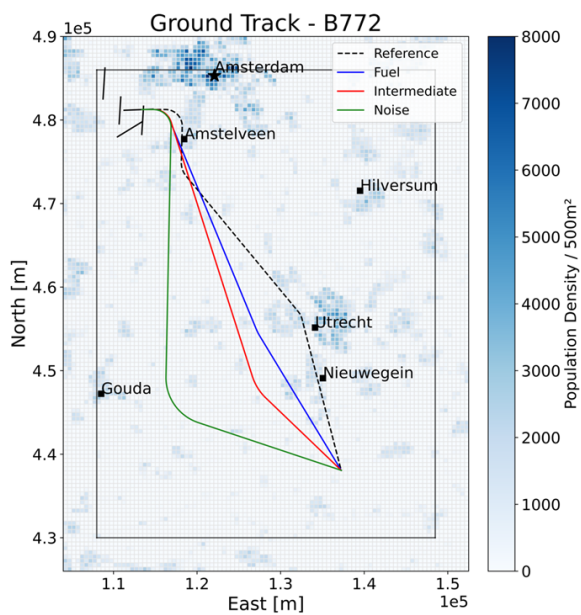
(l) Altitude and TAS for B738



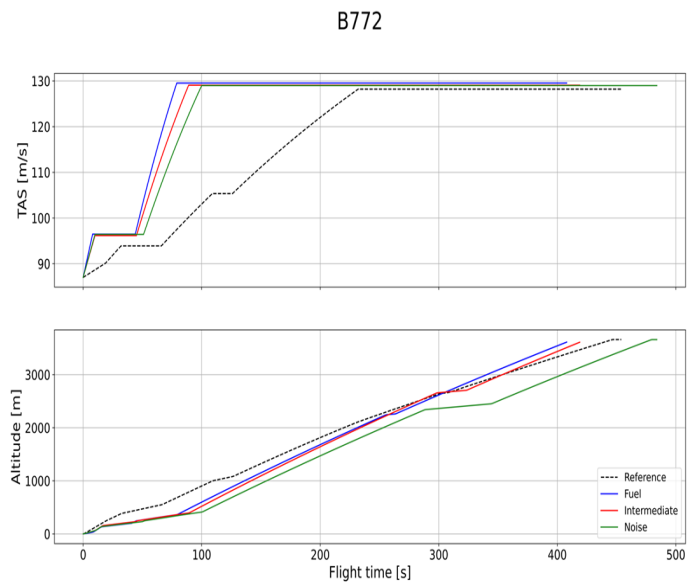
(m) Ground track for B744



(n) Altitude and TAS for B744



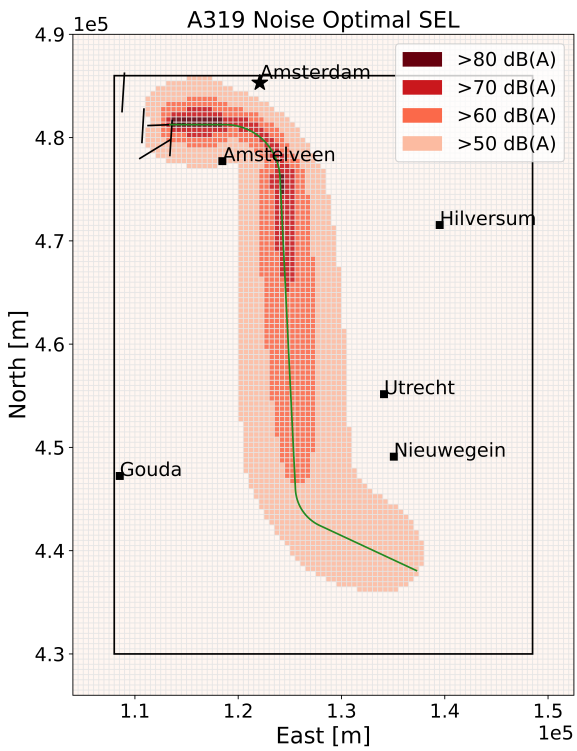
(o) Ground track for B772



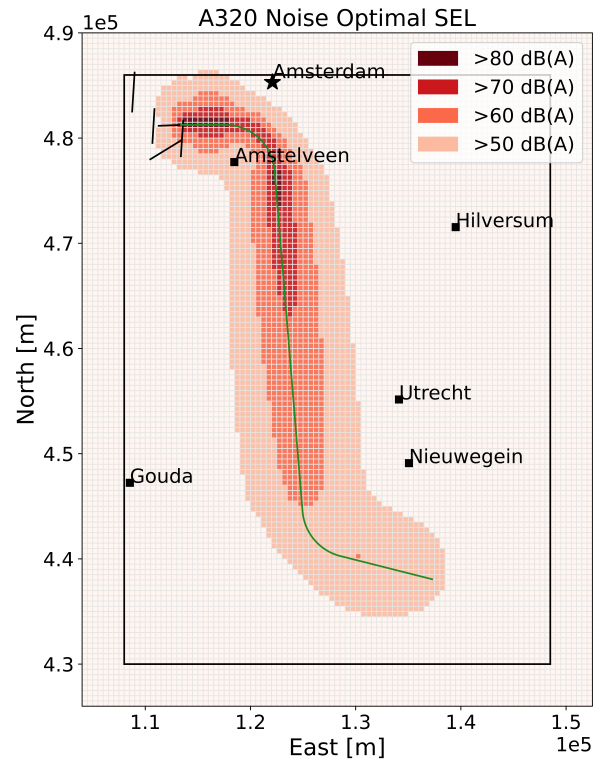
(p) Altitude and TAS for B772

Figure 15: Optimal trajectories for each aircraft type

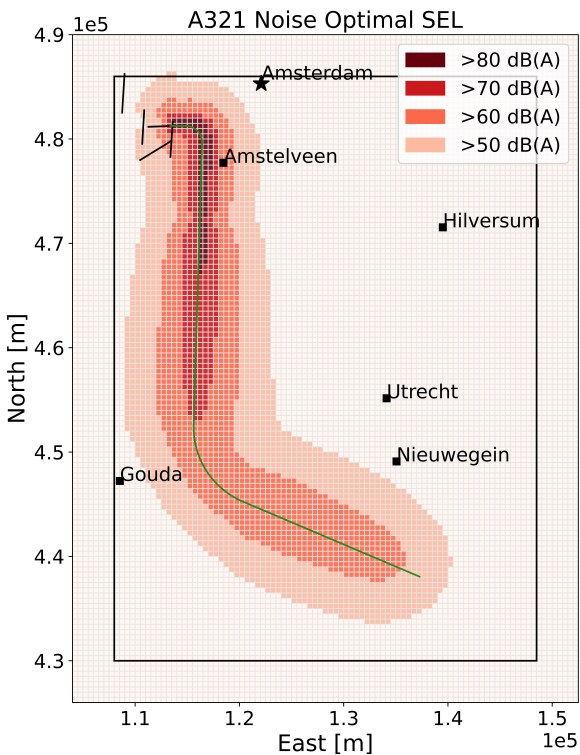
D SEL Contours



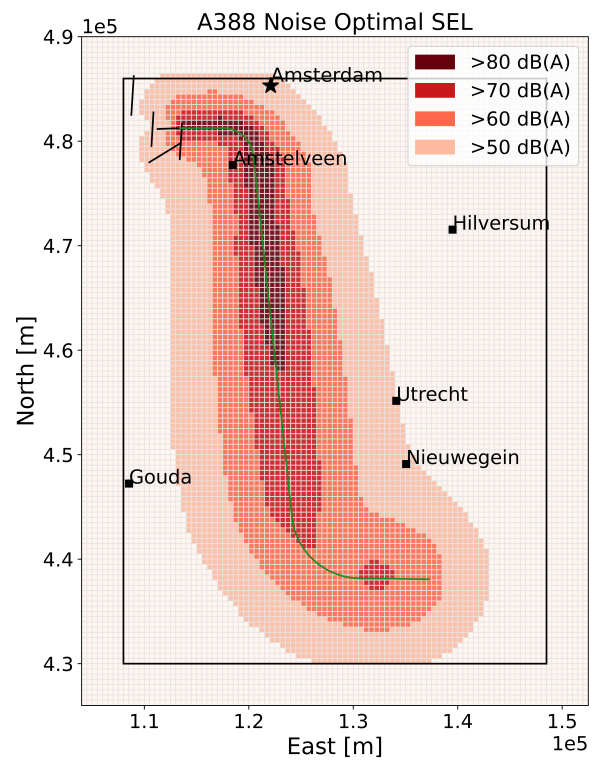
(q) SEL contour for noise optimal trajectory of A319



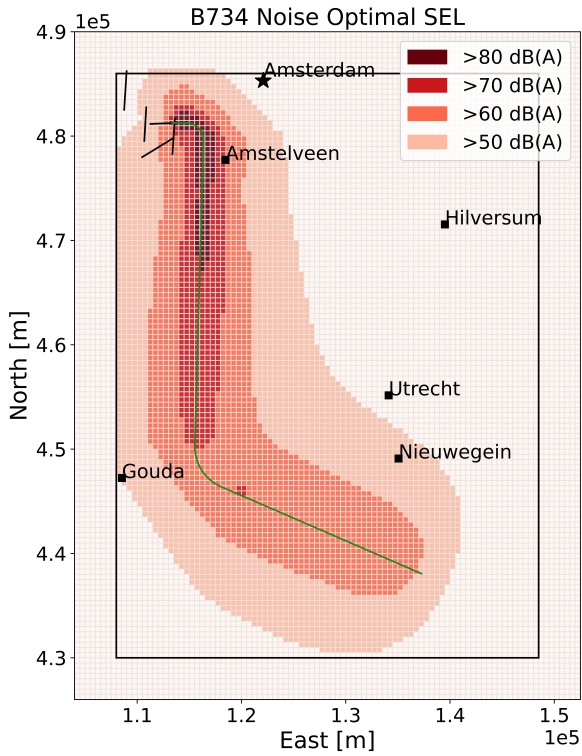
(r) SEL contour for noise optimal trajectory of A320



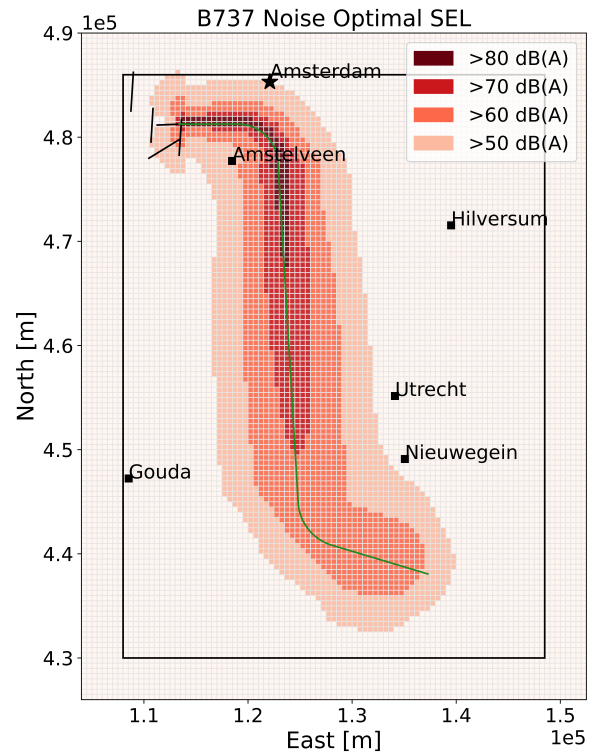
(s) SEL contour for noise optimal trajectory of A321



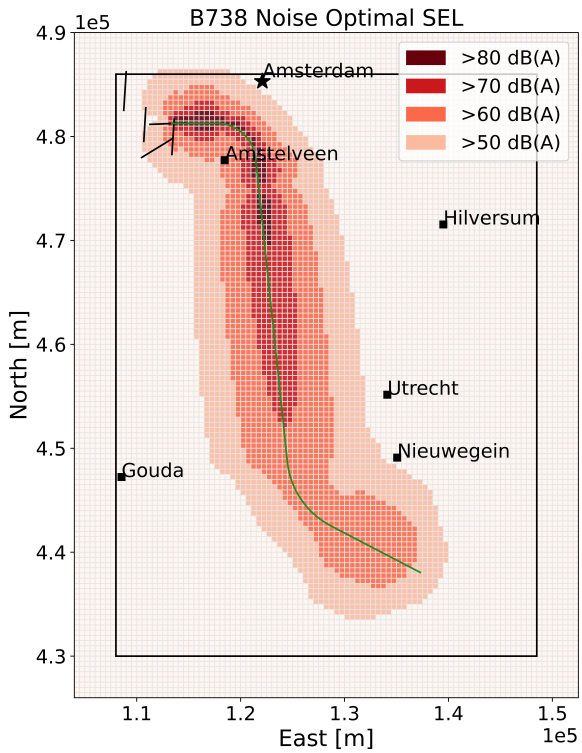
(t) SEL contour for noise optimal trajectory of A388



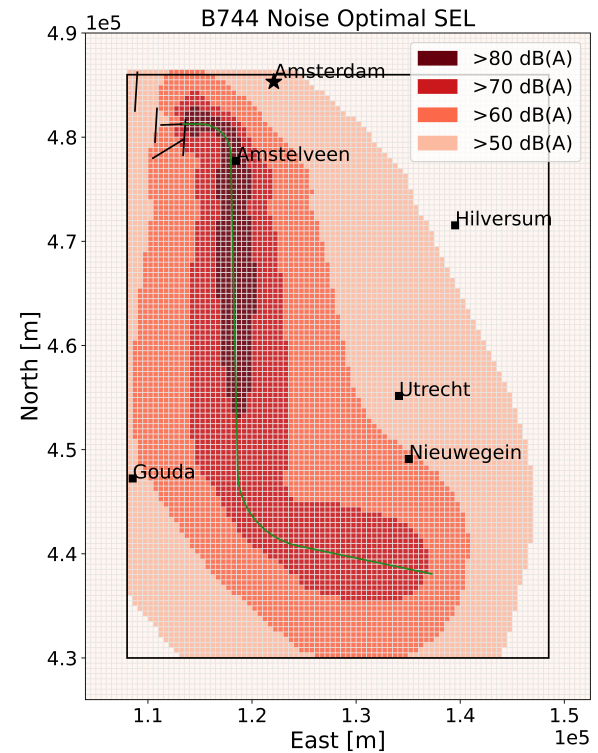
(u) SEL contour for noise optimal trajectory of B734



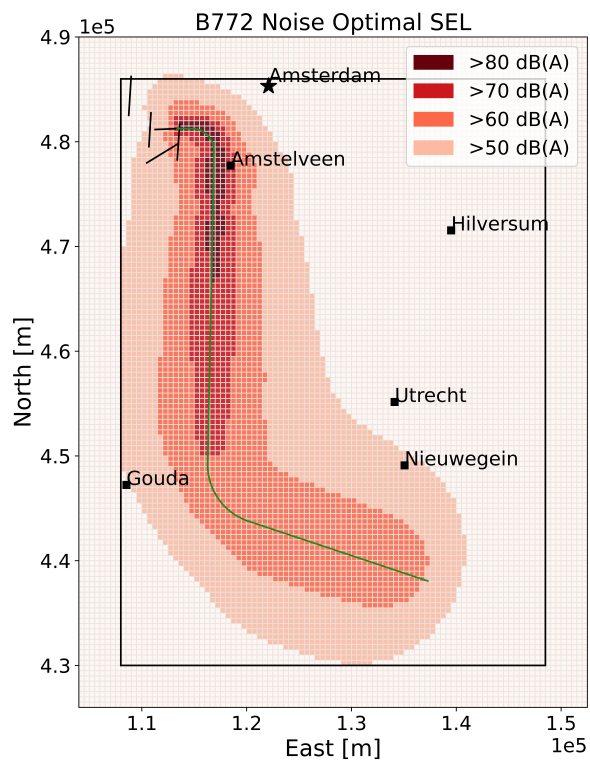
(v) SEL contour for noise optimal trajectory of B737



(w) SEL contour for noise optimal trajectory of B738



(x) SEL contour for noise optimal trajectory of B744



(y) SEL contour for noise optimal trajectory of B772

Figure 16: SEL contours for noise optimal trajectories

II

Literature Study
previously graded under AE4020

1

Introduction

Noise and air pollution are by far the main factors that are inhibiting airport growth [13]. Demand for air travel has been greatly increasing over the past decades, resulting in airports continually expanding to meet demand. However the problem is that the larger an airport becomes, the more aircraft movements can occur, causing more noise nuisance to the surrounding population and degrading the local air quality. Problems relating to this can range from causing minor disturbances to health risks from loss of sleep or harmful emissions [37].

A continuous goal within the air transport industry is thus making flying and airports more sustainable. This is also a necessity for development since oftentimes there are constraints or restrictions set by the government to incite change. Such constraints can take the form of curfews, noise quotas or, most commonly in the Netherlands, aircraft movement restrictions. Amsterdam Airport Schiphol, for example, has a limit of 500,000 daily aircraft movements and 32,000 night time movements [9]. These constraints could be avoided if solutions are found to reduce noise and aircraft emissions around airports.

To this end, a lot of research has been done focusing on fuel and noise mitigation. The bulk of recent research on this topic has focused on two aspects [30]. Firstly, tackling the problem from the source i.e. improving and developing engines to be quieter and more fuel efficient. While this seems to solve the problem, it is only effective in the long-term since research and development takes time. A solution that is applicable in the short-term is implementing noise abatement and fuel efficient operational procedures at airports, especially during arrival and departure.

A considerable amount of research has already been done on advanced arrival techniques, specifically Continuous Descent Approaches/Arrivals (CDA) [46] [44] [25]. This is an idle thrust approach that is dependent on the aircraft's performance. CDA is already being implemented at several airports. Just like arrivals, departures are a significant source of noise. Advanced departure techniques aim to reduce noise by changing departure procedures and profiles to be more fuel and noise efficient, such as with Standard Instrument Departures (SID). However, the use of tailored departure trajectories and procedures that are dependent on aircraft type and weight have not yet fully been scrutinized.

Thus, the topic of this thesis centres around the departure paths, profiles and procedures at an airport and how these can be adapted and customized towards specific aircraft types and weights as well as the time of day. More specifically, it aims to answer the question "What is the benefit of aircraft type dependent departure trajectories and procedures at an airport in terms of aircraft noise and fuel consumption? This leads to the following research objective:

To assess the benefit of aircraft type dependent departure trajectories and procedures at an airport by developing multi-objective optimization models that can create and simulate tailored SIDs and optimize aircraft allocation for noise reduction and fuel consumption.

This literature study report aims to provide a basis for an MSc Thesis at the department of Air Transport

and Operations at Delft University of Technology. The structure of the report is as follows. Chapter 2 provides a problem description including a problem statement and an elaboration of the research objective. Subsequently, in Chapter 3 the environmental impact of aviation is discussed to provide a basis for this topic in terms of what the problem is and what is being done to improve it. Chapter 4 provides insights on what has already been researched in the tailored arrivals and departures field. Then, Chapter 5 discusses runway configurations and how these affect airport operations, specifically how certain runway configurations can cause problems. The methodology of this project is examined in Chapter 6, giving several algorithms and models that could potentially be used to solve the optimization problems. Finally, a preliminary timeline of the project is provided in Chapter 7.

2

Problem Definition

2.1. Problem Statement

Currently, most airports use some form of Standard Instrument Departures that apply to every departing aircraft [24]. This means that regardless of the aircraft type or weight, every flight takes the same departure trajectory and follows the same departure procedure when taking off. To clarify, the departure trajectory refers to the horizontal path taken and the departure procedure prescribes the thrust vs altitude vs speed settings and when an aircraft must accelerate to the desired climb or cruise speed. The problem with this approach, however, is that although the same trajectory and procedure is flown, the departure profile i.e. the vertical component of the departure trajectory will be different for varying aircraft types, weights and atmospheric conditions. Due to this unpredictability factor, it is interesting to investigate the effects of tailoring departure trajectories and procedures per aircraft type and weight to identify possible benefits in terms of fuel consumption and noise.

Noise is an ever-growing concern in the aviation industry, especially near airports. Due to this issue, often times restrictions in aircraft movements are set up by the government to limit the noise to the surrounding population. This greatly reduces capacity and puts a barrier on the demand for growth in aviation. Therefore, the industry must continue to come up with noise abatement measures applicable to airports and aircraft. Several solutions are already being implemented. For example aircraft engines are being developed to become more efficient and less noisy, and aircraft movements and procedures are being adapted as well. There are Noise Abatement Departure Procedures (NADP) already in place at many airports [29]. These are set up by the International Civil Aviation Organization (ICAO) and the Federal Aviation Administration (FAA). NADP-1 aims to reduce noise near the airport, while NADP-2 focuses on areas further away from the airport by defining altitudes where the flap retraction schedule must come into play.

Noise abatement procedures during landing are being applied more and more in the form of Continuous Descent Approaches (CDA), the performance of which are dependent on aircraft type and characteristics due to it being an idle thrust procedure. Some research has been done to apply similar advanced techniques to the departure process, keeping not only noise in mind but also fuel consumption. Minimizing fuel consumption is advantageous on several fronts. For example, to reduce airline costs or, more importantly, reducing fuel also reduces engine emissions that contribute to the negative impact that aviation has on the environment. Reducing emissions can be achieved by developing bio-fuels that are less or not harmful to the environment. However, a more short term approach is performing more efficient aircraft procedures and flying departure trajectories and profiles that reduce fuel consumption.

2.2. Research Objective

The aforementioned problem leads to the following research question:

What is the benefit of aircraft type dependent departure trajectories and procedures at an airport in terms of aircraft noise and fuel consumption?

This question goes hand in hand with the following objective:

To assess the benefit of aircraft type dependent departure trajectories and procedures at an airport by developing multi-objective optimization models that can create and simulate tailored SIDs and optimize aircraft allocation for noise reduction and fuel consumption.

This objective can be split into several sub-objectives to clarify the goal of the project:

- Choose representative aircraft for each aircraft type and weight
- Trajectory optimization model:
 - Define departure trajectories dependent on aircraft type and take-off weight
 - Define departure procedures
 - Calculate noise and fuel consumption of every aircraft type and weight for each SID and profile combination
- Allocation optimization model:
 - Optimize flight allocation for noise and fuel
- Define several noise limits/contours to assess the effectiveness of the tailored trajectories
- Case study
 - Select an appropriate airport to perform a case study
 - Apply the trajectory and allocation models on a typical flight schedule at that airport

The main aim of the research is thus to contribute to making aviation more sustainable. Since air transport cannot grow, develop and keep up with demand without becoming more sustainable, this has been a top priority in the industry for recent years and will be a continuing goal in the future.

3

Environmental Impact of Aviation

Air transport has become a necessity for the economy and is continuously growing due to a rise in demand. However, this comes with setbacks in the form of negative environmental impacts. Noise pollution and emissions from fuel burn are two of the largest contributors deferring airport development. This section introduces these issues and solutions to mitigate their effect.

3.1. Fuel and Emissions

It is no secret that the aviation industry has negative effects on the environment due to greenhouse emissions. According to the Intergovernmental Panel on Climate Change (IPCC), CO_2 is the primary greenhouse gas [10]. CO_2 is also the primary pollutant emitted by aircraft engines, but by far not the only one. Nitrogen oxides, sulphur oxides, unburnt hydrocarbons, carbon monoxide and particulate matter [11] also play a role, however, the main focus usually lies with CO_2 production. It has been found that aviation creates about 3% of the total annual global CO_2 emissions due to human activity, and this is set to increase [10]. Data shows that CO_2 emissions have increased between 1990 and 2016 from 88 to 171 million tonnes, which is a 95% increase. Future CO_2 emissions are expected to rise by another 21% in 2040 and NO_x emissions by 16% [11]. Emissions increase in proportion to fuel use. According to ICAO, 1kg of jet fuel burned equates to 3.16kg of CO_2 emitted [26]. This makes it essential to minimize fuel consumption as much as possible to mitigate adverse climate effects.

Although emissions are the primary concern, airlines have additional motivation to reduce their fuel usage because it contributes a large amount to their operating costs. A total of 23.7% of expenses in the airline industry are due to fuel burn [36].

3.2. Noise

Aircraft noise is one of the largest hindrances to airport development and has become an increasing issue with the growth of air transport. Building or expanding an airport needs to take two opposing aspects into account. It needs to be accessible to large cities and thus should be located close by. On the other hand, an airport should be located further away from densely populated regions to mitigate noise annoyances [37]. Another issue is that since the population in cities keeps growing, the residential areas are encroaching on existing airports. This means a growing number of people are being affected, if not severely annoyed, by aircraft and airport noise [13]. Not only are people annoyed by the persistent noise, but studies show that it can also have adverse health effects. For instance, it can cause cardiovascular and psychological diseases [37].

The severity of aircraft noise is very much dependent on several elements. One aircraft can have a different impact than another of the same type just due to its weight or different atmospheric conditions. Changing aircraft operations also has different effects. For example during take-off the required thrust of the engines mainly determines the amount of aircraft noise [38], whereas during landing it is the friction and turbulence created by the deployment of the landing gear and flaps that generates the most noise [42].

Noise levels around airports throughout the world is measured through the use of several average day-night level (DNL) contours and how many people live within a certain contour to find out how many people are

affected and severely annoyed by the noise [26]. According to ICAO, there are four approaches to managing aircraft noise [22]:

1. Reduction of noise at the source
2. Land-use planning and management
3. Operating restrictions
4. Noise abatement operational procedures

Tackling the noise at the source means improving aircraft engines, making them more efficient and thereby quieter. Although this is a good solution in terms of reducing emissions as well, it is relatively long-term. By introducing land-use zoning around airports, the population affected by airport noise can be minimized. Operating restrictions that reduce noise include phase-out, curfews, night-time restrictions and noise quotas. Finally, noise abatement operational procedures are an effective, relatively short-term solution for reducing noise. There are two Noise Abatement Departure Procedures (NADP) defined by the FAA and ICAO. These are the so called "close-in" NADP (also known as NADP-1 or ICAO-A) and the "distant" NADP (also known as NADP-2 or ICAO-B) [29].

NADP-1

This procedure aims to reduce noise in the vicinity of the airport and is thus dubbed "close-in". By waiting to retract the flaps only when a certain altitude is reached, the aircraft can increase its climb gradient in order to reach a specified altitude at an earlier distance from the airport. As a result, the aircraft will be at a greater distance from the noise receptors on the ground and thus from the population living close to the airport. With the flaps deployed the aircraft remains at a constant climb speed until the altitude is reached. Then, at the end of the procedure when the flaps are retracted at an altitude of 3000ft (900m)[24] above the airport, the aircraft needs to spend thrust so it can accelerate to an en-route climb speed [29]. Figure 3.1 gives an overview of the relevant altitudes and speeds during the "close-in" NADP.

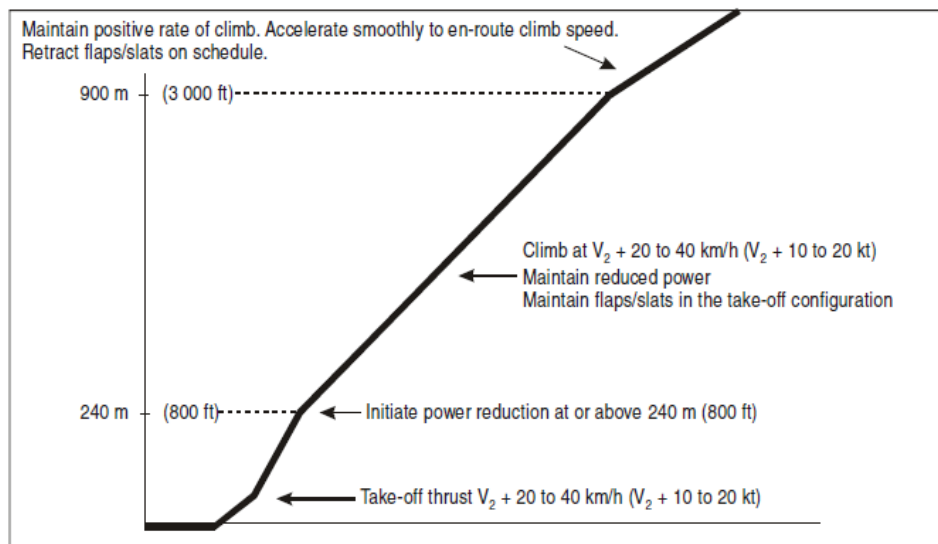


Figure 3.1: Schematic of NADP-1 [24].

NADP-2

The goal of the "distant" NADP is, as the name suggests, to mitigate noise further away from the airport. This procedure is quite similar to a standard procedure, as in the flaps are retracted according to the normal schedule. The differences are usually in the altitude where the aircraft transitions from take-off to climb thrust [29]. Figure 3.2 shows the "distant" NADP along with altitudes and speeds.

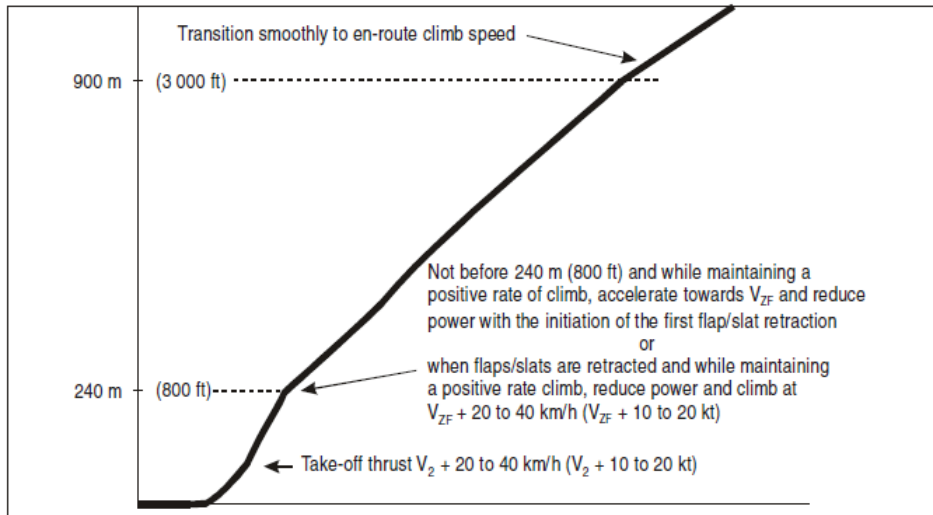


Figure 3.2: Schematic of NADP-2 [24].

These NADPs are one of the ways that airports can reduce noise pollution to satisfy most stakeholders. However, much more research has been done to further advance arrival and departure procedures to become more sustainable in terms of noise as well as fuel. This is discussed in the next section.

4

Tailored Arrival and Departure Procedures

4.1. Tailored Arrivals

When considering advanced arrivals for noise and fuel reduction, Continuous Descent Operations (CDO) come to mind. This type of approach is aircraft type dependent in the sense that the characteristics and capabilities of the aircraft determine the performance of the operation. With low engine thrust settings and a low drag configuration, fuel burn and thus emissions as well as noise can be reduced during landing. The operation gets its name due to the vertical profile being a continuously descending path with minimum level-off segments. The optimal CDO will depend on aircraft type, weight, atmospheric and weather conditions [25]. These factors also make the operation unpredictable at times, making it extremely important to have a safe and efficient management of the airspace as capacity can be negatively influenced.

Continuous Descent Approaches (CDA) are widely researched and already implemented at different airports around the world. Many studies have been performed at Schiphol airport to quantify the benefit of CDA in terms of fuel and noise. Wat et al. [46] performed a trial on 192 aircraft flying their optimum flight profile during arrival, meaning the aircraft flies a continuous descent at flight idle power settings from Top of Descent (TOD) to final approach glideslope intercept. It was indeed found that, as predicted, an optimal CDA lowered fuel consumption. Due to staying at a cruising speed longer, the operation also saved time. Furthermore, results showed that aircraft noise farther away from the airport is significantly reduced due to the elimination of level-off segments, with an improvement of up to 3dBA. Moreover, local air quality also improved greatly because the aircraft no longer flies at a higher power and burning more fuel at lower altitudes. An important conclusion of this study was that the main differences in fuel savings and noise reduction could be attributed to the differences in aircraft performance, i.e. aircraft type.

Another study performed by Takeichi et al. [44] aims to facilitate CDA at busy airports. They found, through arrival time analyses, that tailored arrival paths that are determined by changing the waypoint positions can produce a higher controllability compared with determining paths based on Top of Descent position. Moreover, it is possible to do so without additional fuel consumption. During this so called Tailored Arrival (TA), each aircraft follows its own specifically designed flight path given by ATC to help with separation and the CDA.

It is thus evident that CDAs can be beneficial for airports, however it is crucial to keep in mind that the big difficulty remains the impact on capacity. A similar statement can be made about tailored departures.

4.2. Tailored Departures

4.2.1. Continuous Climb Operations

Similar to CDO, the equivalent for departures, called Continuous Climb Operations (CCO), has gained increasing attention in recent years, however is still not nearly as well studied and implemented as CDA. CCO, as the name suggests, allows aircraft to climb continuously using optimum climb engine thrust and speeds until reaching cruising levels, thereby eliminating intermediate level-offs and thus providing benefits such as reduced fuel burn and emissions, noise and fuel costs. ICAO defines it as "an aircraft operating technique made possible by appropriate airspace and procedure design and appropriate air traffic control clearances enabling the execution of a flight profile optimized to the performance of the aircraft. [27]. Another advantage is that it leads to more consistent flight paths per aircraft type, thus reducing radio communication and

therefore pilot and ATC workload [45].

Diaz et al [45] conducted a study in 2019 on the influence CCO has on runway capacity. They found that CCOs can result in improvement of the trajectory efficiency when individually operated, but has a negative impact on the operational efficiency of the Terminal Manoeuvring Areas (TMA) as a whole. The departure trajectories in this study were multi-objective optimized CCOs based on the optimal control theory and designed using a pseudo spectral direct numerical method. According to Perez-Castan et al [34] the greatest challenge with CCO is indeed the impact on capacity, specifically because separation minima need to be increased to ensure aircraft safety. This is due to uncertainties in performance of different aircraft types. Thus the main area of concern at the moment with CCO is the actual implementation. The new separation minima were estimated in this study using Monte Carlo simulations to obtain a large sample and the uncertainty of the trajectory was modelled by considering aircraft type, mass, speed, positioning error, temperature and wind. It was found that mass adds the most uncertainty while positioning errors barely affected the profile. The conclusion was that the best CCO is performed at a constant speed profile. An important aspect to consider is that arriving aircraft were not taken into account.

Another study by McConnachie et al [31] investigated the benefits of CCO in the USA, specifically at Boston Logan International Airport, Denver International Airport and Los Angeles International Airport. It was found that CCO could save between 6 and 19kg of fuel per departure at these airports, saving between 3380 and 7360 tons of CO_2 per year.

It is evident that CCO come with many benefits, especially environmental in the form of noise and fuel reduction. However, as mentioned, it is the implementation that remains an issue. Perez-Castan et al [35] developed a conflict-risk assessment model for CCO in complex airspace. This takes horizontal and vertical conflict into account with arriving aircraft. Using simulations and real data, the approach is based on altitude distribution at conflict points. The probability of a conflict is thus statistically determined. If the CCO is correctly designed, there should not be any need for ATC intervention.

When purely considering fuel savings, Mori [32] found that by reducing thrust near Top Of Climb (TOC), 40-80lbs of fuel can be saved per flight, depending on aircraft type and Take Off Weight (TOW).

4.2.2. Other Advanced Departure Techniques

CCOs are not the only solutions that have been considered. Heibly et al [15] presents the concept of custom optimized departure profiles for noise abatement purposes, with fixed routes in combination with individually optimized vertical departure profiles. The NOISHHH tool is used to create routes and flight paths for both arrivals and departures that are beneficial in terms of noise while satisfying safety and operational constraints. This is done by combining a noise model, a dose-response relationship, a geographic information system and a dynamic trajectory optimization algorithm. The new trajectories do increase airspace complexity but can significantly reduce the environmental impact by means of trajectory optimization. It was found that the optimized profiles clearly outperformed the standard ICAO-A procedure.

Also using the NOISHHH tool, Ho-Huu et al [19] designed noise abatement departure trajectories using a Multi-Objective Evolutionary Algorithm based on decomposition (MOEA/D). First, a bi-objective optimization problem involving noise and fuel consumption is formulated that optimizes the ground track as well as the vertical departure profile simultaneously. Then, a trajectory parameterization technique is used to make it feasible.

Ho-Huu et al [17] went on to develop a new version of the MOEA/D optimization algorithm which provides solutions that can balance the number of annoyed people, fuel burn and number of people exposed to certain noise levels and amount of aircraft movements. Here, a non-linear, multi-objective optimization problem is formulated with three objectives. With this approach, each SID has a minimum of two different routes, possibly causing operational challenges and increasing workload. Another optimization framework used by Ho-Huu et al [18] reduced the number of people annoyed by aircraft noise by up to 31% and fuel consumption by 7.3% during departure relative to a reference case. This framework consisted of two steps. First, a multi-objective trajectory optimization was used to create a set of paths used as input for the second step, namely the optimal allocation of flights to these trajectories for noise and fuel minimization. Once again, the influence on capacity has not been considered.

4.2.3. Thesis: Tailored SID and Profile Allocation

Ceulemans [7] conducted research on the topic of tailored SIDs and profile allocation at Schiphol Airport in 2016. The objective of this research was to "quantify the potential benefit of tailored SID and profile allocation

for Amsterdam Airport Schiphol by developing a model that is capable of simulating departure trajectories per runway departure fix and optimize the overall allocation of departing aircraft for noise and fuel consumption". This was achieved by developing two models. A trajectory optimization model is used to compute tailored SID and profiles that depend on flight category. This is done by parameterizing the ground track and profile segments, as described by Hartjes and Visser [14]. The trajectory model uses an aircraft performance model and an Integrated Noise Model (INM) to determine fuel and noise. Using a multi-objective genetic algorithm, the solutions are presented on a Pareto optimal front. A selection of these solutions are used as input for the second model. This allocation model optimally allocates aircraft to one of the new trajectories w.r.t noise and fuel consumption. This is achieved using Mixed Integer Linear Programming (MILP).

These models are applied in a case study for Amsterdam Airport Schiphol. To simplify things, only one runway departure fix combination is chosen. Several assumptions are made for feasibility purposes. Two aircraft types are chosen, namely the B733 and B744, to represent narrow and wide-body aircraft respectively along with three different take-off weights (low, medium, heavy), resulting in 6 combinations.

Ceulemans achieved extreme positive results in terms of noise abatement. This was due to several factors. Firstly, the allocation model tries to keep as many noise grid points as possible below the noise limit, meaning many points reach cumulative noise levels that are just below the noise level limits that were defined. Furthermore, a noisy runway departure fix combination was used, as well as a dominant aircraft choice for all wide body aircraft in terms of noise.

4.2.4. Conclusion

The goal of the current thesis is to, initially, replicate the aforementioned research by Ceulemans and apply it to a different airport to judge the benefits it could have in other areas with different factors affecting the outcome. Secondly, the aim is to change and improve the models that have already been developed. This can be achieved in different ways. For example, one could take things into account that were previously not, such as the effect of the tailored SIDs on capacity & delay and the interaction of the departing traffic with arriving traffic, or the application of the model to more than one runway departure fix combination for a more global result. Furthermore, one could review the parameters that have been chosen, such as using more aircraft type and weight combinations or defining more noise limits/contours around the airport that would be used to determine a new trajectory.

Another method of improving the research could be to use a different algorithm in the models. Ceulemans uses a multi-objective genetic algorithm for the trajectory optimization model and MILP for the allocation optimization model, but perhaps there are more efficient or accurate ways to achieve the desired goal. In addition, the method of presenting results for the trajectory model, a Pareto optimal front, may not be the most practical or accurate, and this becomes a problem seeing as those solutions become the input for the second allocation model. These aspects will be discussed in more detail in Chapter 6.

As mentioned, the models will be applied to a specific airport. This airport is yet to be determined, however there are some aspects to keep in mind. For one, the airport must be located in a fairly densely populated area because these are the airports that have the most benefit from reducing noise exposure and improving the air quality by fuel reduction. It is also interesting to look at an airport's runway layout and configuration to determine what issues they are facing and how tailored departures could improve first and foremost the noise and fuel consumption, but also the efficiency and capacity of the given configuration. Thereby, arriving traffic and capacity are also taken into account. Several runway configurations and their benefits and disadvantages are outlined in the next chapter.

5

Runway Configurations

Runway configuration has a large affect on the capacity and efficiency of an airport. The term is best explained as the layout of runways, including the number and orientation of these on an airfield and the operations that occur on said runways (arrivals and departures) [47]. Choosing an appropriate runway configuration is mainly dependent on weather conditions such as crosswinds and poor visibility [4]. There are four general runway configurations that airports can have, these are single, open-V, intersecting and parallel. Some larger airports can have two or more operating simultaneously [47].

5.1. Single

A single runway configuration, as the name suggests, is a one runway airport. This runway accommodates alternating arrivals and departures in a so called "mixed-mode" [47]. This type of configuration is usually for small airports, although having only one runway does not have to mean that the capacity is low. Take London Gatwick Airport for example, it is the most efficient single runway airport in the world [1]. The benefit of a single runway is that aircraft can land and take off within a short amount of time [28]. One runway also means short taxiing distances to and from the terminal.

5.2. Open-V

An open-V layout consists of two runways whose extended centre lines will intersect beyond the thresholds [47], they are thus oriented in different directions but do not intersect. There are two possibilities in terms of aircraft operations on this type of runway system: Converging and diverging. A converging layout means operations move towards the "point" of the V, and diverging means operations start at the "point" and move outward and away from each other. The latter mode is more efficient and thus allows for more movements per hour. When there is little to no wind, both runways can be used simultaneously. If there are strong winds, it becomes a single runway system [28].

5.3. Intersecting

An intersecting runway layout is when two or more runways cross anywhere along their length. This system is used at airports where wind is a big issue because no matter the wind direction, one runway will always be available. When there is low wind, both runways can be used, however there is a higher hazard for collisions due to the intersection. Thus, operations on these runways need to be heavily monitored [28]. There are differences in where the intersection is located, namely an intersection near the end of the runways has less of an impact on capacity and safety than an intersection in the middle of the runways. A downside to this configuration is that there are increased waiting times while queuing for the crossing runway to clear or while waiting to taxi across a runway. This can cause unfavorable delays.

5.4. Parallel

A parallel runway configuration consists of two or more runways whose centre lines are parallel to each other. There are three types of parallel configurations. Close parallel is when the centre lines are less than 2500ft

(762m) apart, intermediate parallel when the centre lines are between 2500 and 4300ft (762-1310m) apart and far parallel when they are more than 4300ft (1310m) apart [47]. Furthermore, there are different modes of operation for a parallel runway configuration. These modes fall under three categories: Simultaneous parallel approaches, simultaneous parallel departures and segregated parallel approaches/departures [23].

5.4.1. Simultaneous parallel approaches

This category encompasses two modes of operation. The first one, Mode 1, is independent parallel approaches. This means that the approaches to the two runways are not affecting each other, i.e. radar separation minima are not required for simultaneous approaches to parallel instrument runways [23]. A depiction of Mode 1 is given in Figure 5.1. Mode 2 then describes the opposite, which are dependent parallel approaches. In this case radar separation minima are prescribed for safety because the runways are closely spaced [23]. A depiction of Mode 2 is provided in Figure 5.2.

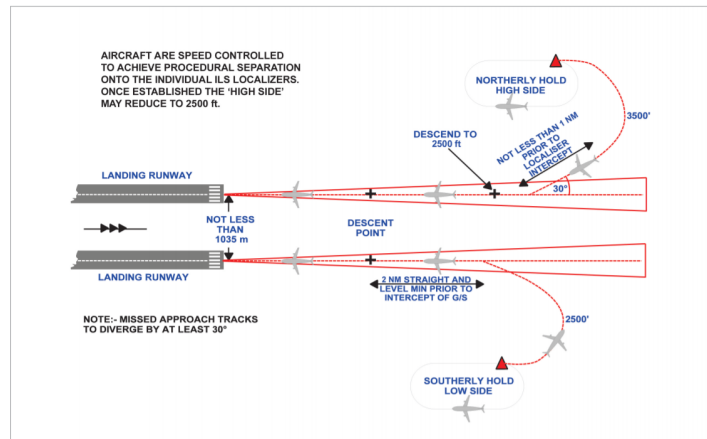


Figure 5.1: Independent parallel approaches [6]

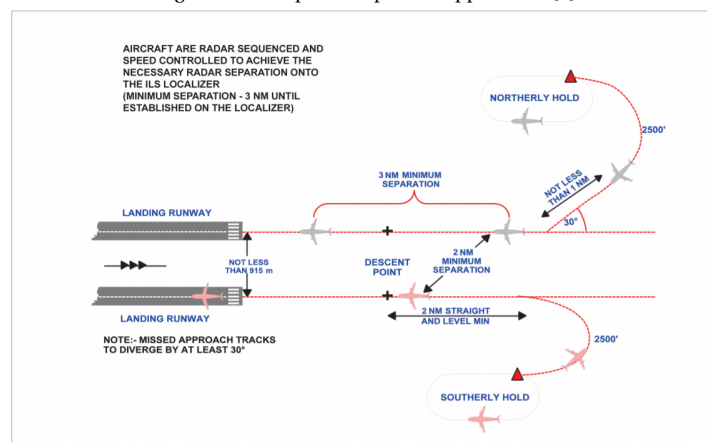


Figure 5.2: Dependent parallel approaches [6]

5.4.2. Simultaneous parallel departures

Mode 3 describes independent instrument departures from parallel runways. In this mode aircraft depart in the same direction simultaneously from parallel runways. This is only possible when the runways are spaced by 760m or more. There are a few configurations that are possible for this mode. First, both runways are used exclusively for departures. Secondly, one runway is used for departures and the other is used for both arrivals and departures. This is called semi-mixed operations. Finally, both runways can be used for arrivals and departures in a mixed mode. A requirement for Mode 3 is that the departure tracks after take off diverge by at least 15 degrees for safety reasons [23]. This and more information can be seen in Figure 5.3.

It is important to note that when two aircraft are departing simultaneously in the same direction from parallel runways, the noise exposure to the surrounding population is much higher since not just one but two aircraft are departing over an area of land very close to each other. This means people experience an increased noise

level and there is a larger area that experiences higher noise levels. Several airports apply this mode of operations, such as San Francisco International Airport [41]. In this case, however, the departure paths are above the San Francisco Bay in northern direction. An airport where these noise concerns for parallel departures are more imminent is Houston George Bush Intercontinental Airport, where the departure paths of the parallel runways lead over populated regions towards the south-east of the airport and towards the north of the city of Houston [20].

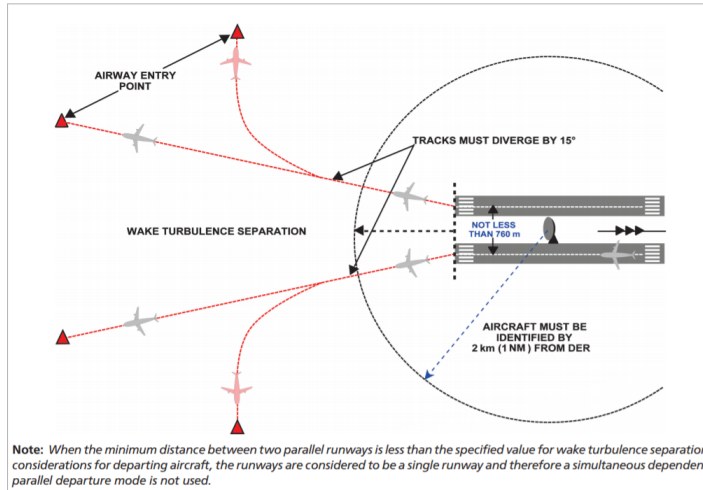


Figure 5.3: Simultaneous parallel departures [6]

Simultaneous departures from closely spaced parallel runways are most problematic when runway thresholds are adjacent because the aircraft will remain at more or less the same altitude at the same distance from the runway, until they diverge due to the 15 degree restriction. When runway thresholds are staggered there is also some vertical separation introduced, allowing runway spacing to be smaller. A rule of 30m reduction for every 150m of overlap applies [6].

5.4.3. Segregated parallel approaches/departures

Finally, Mode 4 regards segregated parallel operations. In this case one runway is exclusively used for arrivals and the other is used only for departures. A safety requirement is that the departure track diverges by at least 30 degrees from the missed approach track of the other aircraft right after take-off [23]. Figure 5.4 describes Mode 4 in more detail.

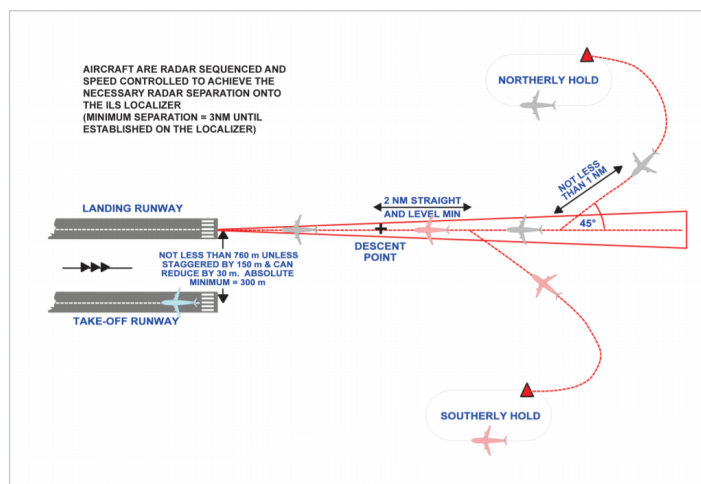


Figure 5.4: Segregated parallel approaches/departures [6]

6

Methodology

To answer the proposed research question two models will be developed. One to simulate the optimized tailored trajectories and the other to optimally allocate aircraft to these trajectories for noise and fuel reduction. In order to do so, one must take a look at the concepts of trajectory optimization, allocation optimization and multi-objective optimization. Furthermore, there are diverse algorithms and programs that can be applied and used to solve these problems. Some of these will be discussed in this section.

6.1. Trajectory Model

Trajectory optimization is "the process of designing a trajectory that minimizes (or maximizes) some measure of performance while satisfying a set of constraints" [39]. In this case we are trying to minimize two objectives, noise and fuel, making it a multi-objective optimization problem. Constraints include elements such as operational requirements during departures.

There are several applicable metaheuristic methods. This section will discuss Tabu Search, Simulated Annealing and Genetic Algorithm. The following information is from "Introduction to Operations Research" by Hillier and Lieberman [16].

6.1.1. Tabu Search

Tabu search includes a local search procedure that allows not only improvements in solutions but also slight degradations. A so-called "steepest ascent/mildest descent" approach is applied. This means that at each iteration the move that "climbs up the hill" fastest is chosen, or when there is no upward move available, the move that goes downward the least is selected. An issue with this is that once the process moves away from a local optimum, it will circle back to the same local optimum. To prevent this, the moves that go back to already visited solutions are temporarily forbidden, thus the name "Tabu". These "Tabu moves" are recorded on a "Tabu list". An exception to this rule is when a Tabu move is actually an improvement to the best feasible solution found so far. This form of memory is distinctive to the Tabu Search method. To summarize this method, a short outline is presented:

1. Initialization: Starting with a feasible initial trial solution
2. Iteration: using a local search procedure, feasible moves into the local neighborhood of the current trial solution are defined. Any Tabu moves are removed. The remaining moves are examined to find the best solution, which is then adopted as the new trial solution no matter if it is better or worse than the current one. The Tabu list must be updated to prevent circling back to the current trial solution.
3. Stopping rule: A stopping criterion is defined. This can be a set number of iterations, a set CPU time or a set number of iterations that do not show an improvement over the previous solution. The search is also stopped when there are no feasible solutions in the local neighborhood of the trial solution. The best solution on any iteration is then chosen as final solution.

The downside of Tabu search is that it checks every single local maximum/minimum instead of searching directly for a global optimal solution. This can become very time consuming.

6.1.2. Simulated Annealing

Simulated annealing focuses on searching for the global optimum. To achieve this, the first steps are to move in random directions while rejecting some moves that go "downwards". In this way, a large chunk of the feasible region is explored and since most moves are an improvement, the search will drift towards the part that contains the global optimum. Over time, the process finds this "tallest hill". In simulated annealing, as well as Tabu search, each iteration moves to an immediate neighbor of the current trial solution, the difference is in how the neighbor is chosen. At first, a random neighbor is chosen that is always accepted if it is better than the current trial solution. If it is not, it is only accepted with a certain probability that is dependent on how much worse it is. The probability of acceptance is defined in the following expressions:

$$Prob\{acceptance\} = e^x \quad (6.1)$$

$$x = \frac{Z_n - Z_c}{T} \quad (6.2)$$

Here Z_n is the objective function value of the current trial solution and Z_c is the objective function value of the candidate for the next trial solution. T is a parameter that determines the likelihood of a candidate that is worse than the current trial solution being accepted. In simulated annealing, T starts with a large value, meaning the probability of acceptance is quite big and the search can move in close to random directions. As the process continues, T is gradually decreased and the focus is more put on candidates that are better than the previous solution as the probability of acceptance of worse solutions decreases. This aspect of randomness that is not present in the Tabu search allows for more flexibility for moving towards a different part of the feasible region to look for the "higher peak". Due to the decreasing T parameter, the process is called simulated annealing. This is an analogy to the physical annealing process in which metal is melted at very high temperatures and then slowly cooled until it reaches a low energy stable state with desirable properties. The decreasing parameter T can thus be compared to the cooling temperature. An outline of the simulated annealing process goes as follows:

1. Initialization: a feasible initial trial solution is chosen.
2. Check T schedule: once a set number of iterations at the current T value have been performed, decrease T to the next value in the schedule and continue performing iterations.
3. Stopping rule: stop when a set number of iterations have been completed at the smallest value of T , or when none of the immediate neighbors are accepted. The best trial solutions from any iterations (from all T values) is the final most optimal solution.

6.1.3. Genetic Algorithm

The final metaheuristic method is the genetic algorithm. This algorithm works differently from the previous two. It is based on the theory of evolution formulated by Charles Darwin that introduced the concept of "survival of the fittest". Each species has different characteristics, it is those that adapt to the environment, creating superior qualities, that survive to the next generation. With this method, the solutions gradually evolve to become the most optimal one [16]. An outline for a genetic algorithm is given:

1. Initialization: start with a population of feasible trial solutions that can be generated at random. Evaluate the value of the objective function, i.e. the "fitness" of each individual.
2. Iteration: a random, even number of superior members of the population are chosen to become parents. The parents are paired up, also at random, and each pair has two children, translating to feasible trial solutions. The children have features from both parents, or have mutated features. If a solution is infeasible, this is referred to as a "miscarriage". When this happens, the process of having children is repeated until a child is a feasible solution. For the next iteration, an equally sized population is selected from the superior children and sometimes from the better members of the current "parent" population. Once again the characteristics and "fitness" of each individual of the new population is evaluated.
3. Stopping rule: The process stops when the stopping criterion has been satisfied. This can be a set number of iterations, CPU time or a set number of iterations that did not show an improvement in the previous trial solutions. Once the process has stopped the best trial solution so far is chosen as the final solution.

6.1.4. Multiobjective Optimization

In multiobjective optimization, a vector of objectives must be minimized (or maximized), meaning there can not be one optimal solution. This is due to the fact that they are noninferior solutions. This means that when one objective improves, the other will degrade [8]. One must thus find a solution that is optimal enough for both objectives. This can be done using the Pareto Optimality method. The outcome of a multi-objective optimization problem can be a large set of solutions whose values can be presented on a Pareto Frontier (or Front). An example of such a front is given in Figure 6.1

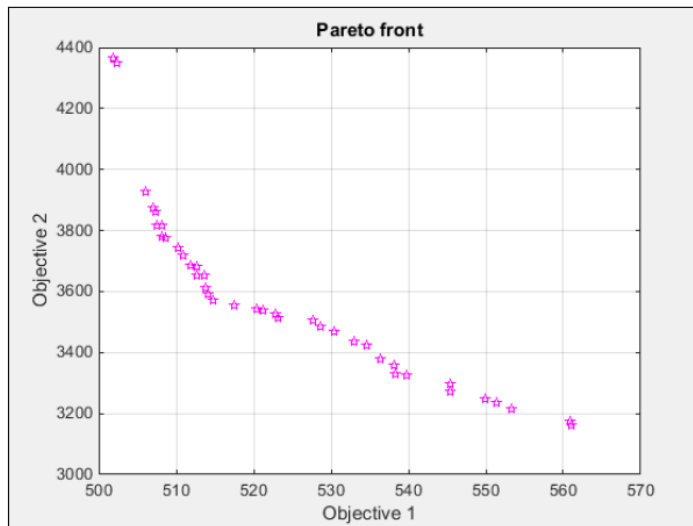


Figure 6.1: An example of a Pareto Front [7]

Although a Pareto front can present all the solutions, it can become close to impossible to select the preferred solution or solutions. This is due to the large size of the solution set overcrowding the representative Pareto front. For this reason, support tools have been developed to help the decision maker make a choice. There are two broad methods that can be applied; an "a priori" method i.e. before even optimizing the problem, or "a posteriori" i.e. afterwards [2].

A priori method

In this type of method, a so called Guided Multi-objective Genetic Algorithm (G-MOGA) allows decision makers to implement their preferences into the algorithm to bias the search for the optimal solutions. The outcome of this method is a Pareto frontier that is already focused on the preferred region of the objective function space. A downside to this is that, even though there are fewer solutions provided, now the decision maker needs to choose between very similar preferred solutions. Furthermore, this method calls for the decision maker to make preference trade-offs between objectives which can be quite complex when he/she has no experience with the matter. Thus, a posteriori methods can be applied with satisfactory results as well.

A posteriori method

This method eases the decision making process after all the solutions have already been found. It either looks for the solution that optimizes all the objectives simultaneously, or it applies the preference of the decision maker on the solutions to identify the best one. There are two ways of accomplishing this. First, subtractive clustering can be used to group the solutions on the Pareto front into homogeneous "families" according to their relative distances. Using Level Diagrams or fuzzy preference assignment, depending on whether the decision maker has a preference, the most representative solution in each cluster is determined. The decision maker only has to pick the optimal cluster radius, define the preference matrix and use the Level Diagrams to assess the solutions according to their proximity to the ideal solution which is optimal with respect to all objectives. A second approach is a two step procedure using a Self Organizing Map (SOM) that clusters the solutions and then Data Envelopment Analysis (DEA) to eliminate the least efficient ones and identify representative efficient solutions. The DEA also evaluates the solution performance based on a relative efficiency criterion. The decision maker is thus left with a smaller amount of solutions to choose

from. However, when keeping the decision makers preference in mind, the method becomes less effective. This is because the solution selection is based on the relative efficiency and thus the solutions that the decision maker prefers may not be the most efficient ones.

It is possible to combine a priori and a posteriori methods. For instance, after applying the a priori method, the solutions reduction procedure by clustering can be applied to the reduced Pareto front, making it simpler to decide between solutions. However, it is still difficult to define the amount one objective should be preferred over the other, i.e. how much of one objective the decision maker is willing to let go of for a particular increase in another objective, since there are no reference values to base it on. It goes without saying that, the more objectives there are, the more complicated this will get.

6.1.5. Integrated Noise Model

To incorporate a noise model into the optimization simulation, the Integrated Noise Model (INM) has been used by the FAA as a standard method for noise assessment since 1978 [5]. This is a computer program that assesses noise impact with several different metrics for several different scenarios. INM computes noise-level or time-based metrics near an airport which are presented on a grid of "observer points" or contour levels. There are three groups of metrics computed in INM:

- A-weighted sound levels (L_A): provides a good approximation of the response of the human ear and thus compares to a person's judgment of how loud something is. It diminishes the low and high frequencies of the spectrum.
- C-weighted sound levels (L_C): simulates human perception of how loud a sound above 90 decibels is. It relates more to low frequencies than A-weighting.
- Tone-corrected perceived noise levels (L_{PNT}): estimates perceived noise from broadband sources like aircraft.

INM then computes three types of metrics from these levels:

- Exposure based: total sound exposure over a time period at an observer location
- maximum noise level: maximum noise level (of a set of aircraft operations) at an observer location
- time-based metric: time or percentage of time that the noise level exceeds a certain threshold (for aircraft operations over a given time period).

INM can be integrated into the optimization model to calculate noise in order to optimize the trajectories for this objective.

6.2. Allocation Model

The allocation model allots departing aircraft to an optimal trajectory. This type of problem is most commonly solved using Mixed Integer Linear Programming (MILP). The most common type of linear programming is allocating resources to activities, which is a comparable task. MILP is different to linear programming only in the way that the variables can, but don't have to, have integer values. In MILP there is a function to be maximized (or minimized) that is subject to a set of restrictions or constraints. The linear programming standard form is given in the following expressions [16].

$$\text{Maximize } Z = c_1x_1 + c_2x_2 + \dots + c_nx_n$$

subject to the restrictions

$$a_{11}x_1 + a_{12}x_2 + \dots + a_{1n}x_n \leq b_1$$

$$a_{21}x_1 + a_{22}x_2 + \dots + a_{2n}x_n \leq b_2$$

$$\vdots$$

$$a_{m1}x_1 + a_{m2}x_2 + \dots + a_{mn}x_n \leq b_m$$

and

$$x_1 \geq 0, \quad x_2 \geq 0, \quad \dots, \quad x_n \geq 0$$

A program for solving MILP problems is the IBM ILOG CPLEX Optimization Studio. This program "uses decision optimization technology to optimize decisions, develop and deploy optimization models quickly and create real-world applications" [21].

7

Project Timeline

In this section I will give a concise overview of the project and its timeline. This project will last a total of 7 months, from the beginning of September 2020 until the beginning of April 2021. There are three milestone meetings with the exam committee during this time. First of all the Kick-off meeting where the research goal and plan are presented. This will take place in the first week of September. Secondly, the mid-term takes place half-way through, in the first week of December, to discuss progress and make sure the project is ready to enter the final phase. Finally, the Green-light meeting determines whether the project has been completed successfully. This will take place at the beginning of March. It is possible that more progress meetings will be planned in between these three to monitor the process better. Towards the end of March the final thesis will be delivered and the defence is planned at the beginning of April.

After the initial kick-off, the initial phase of the project begins. In this phase the two models are created and verified based on [7] research. Furthermore, an appropriate airport to conduct a case study is chosen and researched. After the mid-term meeting, the models will be improved and augmented and the case study will be performed. After each task is completed, the research needs to be verified and validated and the thesis report needs to be updated continuously.

Appendix A provides a Gantt chart with the current plan including tasks, meetings, deadlines and holidays.

8

Conclusion

This literature study discussed various aspects of the contents and process for completing this MSc thesis. It is important to understand that noise and fuel consumption are the two critical aspects in hindering airport expansion and growth in the industry. Current procedures take these aspects into account, however there is room for improvement, especially during departures. Standard departures do not take the performance characteristics of individual aircraft types and weights into account and are therefore not optimized. Research has been done on tailored departures in the form of Continuous Climb Operations or custom optimized departure profiles. Several algorithms and models are used such as a Multi-Objective Evolutionary Algorithm, NOISHHH along with an Integrated Noise Model and aircraft performance models. The current thesis aims to make flying more sustainable by answering what is the benefit of aircraft type dependent departure trajectories and procedures in terms of aircraft noise and fuel consumption. This will be done by creating two models based on [7] research. First, a trajectory optimization model that creates tailored departure profiles and procedures per aircraft group. This model will use an optimization algorithm such as a tabu search, simulated annealing or a genetic algorithm. The second allocation model uses MILP to allocate flights to the tailored departure routes. The models are created using MATLAB and will be applied to an airport in a case study. This airport is chosen based on characteristics such as population density surrounding the airport as well as current runway configuration. Simultaneous parallel departures from closely spaced runways for example can become critical, so new departure profiles and procedures would need to be carefully designed to avoid conflict. The outcome of this project will be optimized noise and fuel values.

Finally a preliminary project timeline was created for organizational purposes. The project will run for seven months from September until beginning of April. The provided Gantt chart gives an overview of the important tasks and when they should be completed.

III

Supporting work

Trajectory Optimization Model

In this section additional information on theory and calculations are given for various sub-models of the trajectory optimization model. This serves as supporting work to substantiate claims made in the scientific paper.

1.1. Maximum Thrust Calculation

The maximum thrust is modelled separately for take-off and climb conditions. The maximum take-off thrust is calculated using a second degree polynomial function of speed with engine specific coefficients. The take-off thrust also depends on a variable G_0 , which is called the gas generator function. This variable represents the usable power of the engine and can be derived from the relationship between specific enthalpy and specific entropy [3]. The relationship used for G_0 in Eq. 1.1 comes from Fig. 5 in [3].

$$G_0 = 0.0606\lambda + 0.6337 \quad (1.1)$$

The equation for maximum take-off thrust is then given by Eq. 1.2. Here, T is the maximum take-off thrust, T_0 is the maximum static thrust at sea level, λ is the bypass ratio and M is the Mach number. This equation calculates the thrust for a single engine. It is assumed here that the runway is at sea level. For altitude adjustments, Eq. 1.3 can be considered.

$$\frac{T}{T_0} = 1 - \frac{0.377(1 + \lambda)}{\sqrt{(1 + 0.82\lambda)}G_0}M + (0.23 + 0.19\sqrt{\lambda})M^2 \quad (1.2)$$

$$\frac{T}{T_0} = A - \frac{0.377(1 + \lambda)}{\sqrt{(1 + 0.82\lambda)}G_0}ZM + (0.23 + 0.19\sqrt{\lambda})XM^2 \quad (1.3)$$

where

$$\begin{aligned} A &= -0.4327 \left(\frac{p_{amb}}{p_{amb0}} \right)^2 + 1.3855 \frac{p_{amb}}{p_{amb0}} + 0.0472 \\ Z &= 0.9106 \left(\frac{p_{amb}}{p_{amb0}} \right)^3 - 1.7736 \left(\frac{p_{amb}}{p_{amb0}} \right)^2 + 1.8697 \frac{p_{amb}}{p_{amb0}} \\ X &= 0.1377 \left(\frac{p_{amb}}{p_{amb0}} \right)^3 - 0.4374 \left(\frac{p_{amb}}{p_{amb0}} \right)^2 + 1.3003 \frac{p_{amb}}{p_{amb0}} \end{aligned} \quad (1.4)$$

The maximum thrust during climb is split into three segments in [3]. The departure trajectory in this research ends at 12000ft. Since it is still considered the initial departure, climb segment 1 is used. This results in the linear function in Eq. 1.5 to define the maximum climb thrust.

$$\frac{T}{T_{30}} = m \frac{p_{amb}}{p_{amb30}} + \left\{ \left[\frac{T_{10}}{T_{30}} \right] - m \left(\frac{p_{amb10}}{p_{amb30}} \right) \right\} \quad (1.5)$$

Here, m is a factor that incorporates the influence of flight speed and climb rate setting and it is given in Table 4 of [3]. The model in Eq. 1.5 first requires the thrust at 10,000ft, T_{10} , to be calculated using Eq. 1.6. T_{30} is a

cruise thrust that is given in [43] per aircraft type and p_{amb} is the ambient pressure at the respective altitudes. V_{cas} and V_{casref} are the calibrated airspeed and the calibrated airspeed at cruise (30,000ft) respectively.

$$\frac{T}{T_{30}} = a \left[\frac{p_{amb}}{p_{amb30}} \right]^{-0.355 \left(\frac{V_{cas}}{V_{casref}} \right) + n} \quad (1.6)$$

where

$$a = \left[\frac{V_{cas}}{V_{casref}} \right]^{-0.1} \quad (1.7)$$

and n is a factor that takes into account the different TET settings that result in different climb rates. These values are given in Table 3 of [3]. In this model a reference thrust, T_{30} , is defined at 30,000ft (cruising altitude) instead of the usual sea level. This is because the engine performance and thus the climb requirements are generally specified at the top of climb by aircraft manufacturers.

1.2. Trajectory Parameterization

By parameterizing the trajectory, the amount of decision variables for the optimization is minimized. The final two decision variables, namely the heading change of the last turn and the length of the last straight segment, can be calculated and do not need to be optimized, given that the final coordinate of the trajectory is known. Figure 1.1 depicts a scenario where the initial coordinates, L_1 , R_2 , and the final coordinates are known. From this, $\Delta\chi_2$ as well as L_3 can be calculated using the equations 1.8 - 1.11.

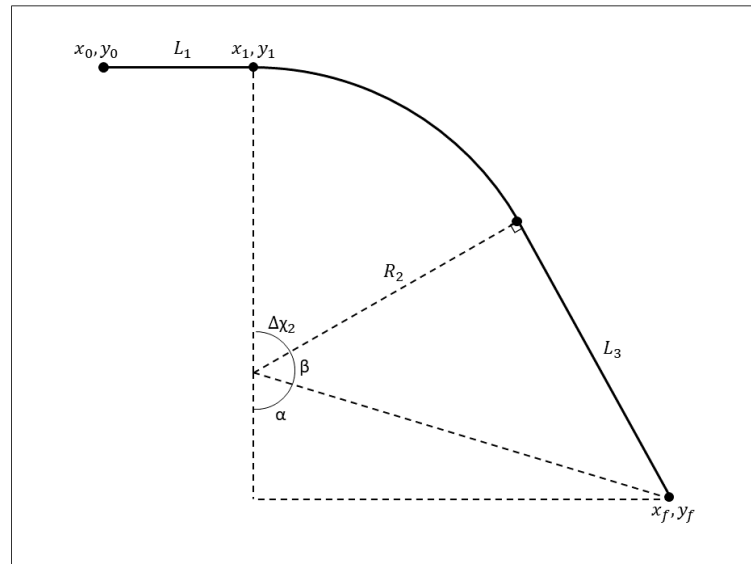


Figure 1.1: Ground track parameterization calculation

$$\Delta\chi_2 = 180 - \alpha - \beta \quad (1.8)$$

$$\alpha = \tan^{-1} \left(\frac{|x_f - x_1|}{|y_f - y_1| - R_2} \right) \quad (1.9)$$

$$\beta = \cos^{-1} \left(\frac{R_2}{\sqrt{(|x_f - x_1|)^2 + (|y_f - y_1| - R_2)^2}} \right) \quad (1.10)$$

$$L_3 = R_2 \tan \beta \quad (1.11)$$

1.3. Optimization

The working of the NSGA-2 algorithm was briefly described in the paper. The details of the optimization settings that were applied in the model are given below.

- Maximum evaluations: 10,000 (100 generations)
- Population size: 100
- Offspring size: 100
- Mutation probability: $\frac{1}{\#of\ variables}$
 - Distribution index: 20
- Crossover probability: 0.8
 - Distribution index: 10

The termination criterion of the optimization is a maximum number of evaluations. The population size determines the amount of solutions generated per iteration. The initial population is random. The mutation probability determines the probability of parent solutions being changed to create a new solution, unlike the crossover probability where parent solutions are recombined to generate offspring. The distribution indices determine the amount of deviation in the decision variables. A lower value improves the resilience to early convergence. The NSGA-2 pseudo-code is presented below in Algorithm 1 [12].

Algorithm 1 NSGA-II Algorithm

```

1: initialize population  $P_0 \subset \chi^\mu$ 
2: while not terminate do
3:   {Begin variate}
4:    $Q_t \leftarrow \phi$ 
5:   for all  $i \in \{1, \dots, \mu\}$  do
6:      $(\mathbf{x}^{(1)}, \mathbf{x}^{(2)}) \leftarrow \text{select\_mates}(P_t)$  { select two parent individuals  $\mathbf{x}^{(1)} \in P_t$  and  $\mathbf{x}^{(2)} \in P_t$  }
7:      $\mathbf{r}_t^{(i)} \leftarrow \text{recombine}(\mathbf{x}^{(1)}, \mathbf{x}^{(2)})$ 
8:      $\mathbf{q}_t^{(i)} \leftarrow \text{mutate}(\mathbf{r})$ 
9:      $Q_t \leftarrow Q_t \cup \{\mathbf{q}_t^{(i)}\}$ 
10:  end for
11:  { End variate }
12:  {Selection step, select  $\mu$  - "best" out of  $(P_t \cup Q_t)$  by a two step procedure;}
13:   $(R_1, \dots, R_l) \leftarrow \text{non-dom\_sort}(\mathbf{f}, P_t \cup Q_t)$ 
14:  Find the element of the partition,  $R_{i_\mu}$ , for which the sum of the cardinalities  $|R_1| + \dots + |R_{i_\mu}|$  is for
  the first time  $\geq \mu$ . If  $|R_1| + \dots + |R_{i_\mu}| = \mu$ ,  $P_{t+1} \leftarrow \cup_{i=1}^{i_\mu} R_i$ , otherwise determine set  $H$  containing
   $\mu - (|R_1| + \dots + |R_{i_\mu-1}|)$  elements from  $R_{i_\mu}$  with the highest crowding distance and  $P_{t+1} \leftarrow (\cup_{i=1}^{i_\mu-1} R_i) \cup H$ 
15:  { End of selection step.}
16:   $t \leftarrow t + 1$ 
17: end while
18: return  $P_t$ 

```

1.4. Optimal Solutions

After the trajectory model outputs a Pareto front of optimal solutions, three optimal departure trajectories are chosen per aircraft type to proceed with the analysis. The outermost points of the Pareto front are easily selected. These are the fuel optimal and noise optimal solutions. The third optimal solution needs to be extracted mathematically. This is done after the optimization process is complete and is therefore an "a posteriori" method.

The goal is to choose a point that can save a sufficient amount of one objective without largely increasing the other. An example of the method is shown in Figure 1.2 [7]. D_1 and D_2 are the respective derivatives between the points.

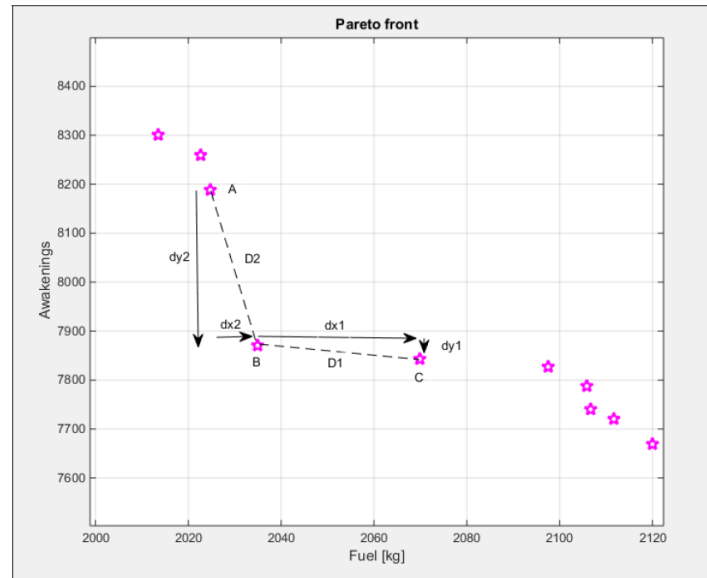


Figure 1.2: Selecting a third point from the middle of the Pareto front

Here, D_1 will be a small negative number and D_2 will be a large negative number. Subtracting them from each other will result in a large positive number, which indicates the preferred solution is point B. The plot makes clear that choosing B above C results in substantial fuel savings while only marginally increasing the awakenings. When compared to point A, point B achieves significant noise savings while little fuel is added. The intermediate solution is selected from the middle of the Pareto fronts.

2

Case Study

2.1. Sensitivity Analysis

In order to potentially improve the flexibility of the ground track, more lateral segments can be added to the trajectory. This allows the path to avoid highly noise sensitive areas better by giving it the chance to take more turns. A sensitivity analysis was performed to decide with how many segments the optimization should take place.

With each case two extra segments (one turn and one straight leg) were added to the trajectory. This resulted in an optimization for 5, 7 and 9 ground segments, or 2,3 or 4 turns in the trajectory respectively. The analysis was performed for two aircraft types in different weight categories, namely the B737 (medium) and the B772 (heavy).

The initial version of the trajectory optimization model uses five ground segments. While improving flexibility to the route, adding extra segments also increases the computation time significantly. Adding a turn and a straight segment brings more complexity to the model since three extra decision variables (L , R and $\Delta\chi$) need to be optimized. Therefore, adding four extra segments to reach 9 total ground segments will be even more computationally complex and the computation time will increase considerably.

2.1.1. Results

The sensitivity analysis was performed on the same runway and departure fix combination at Schiphol as the case study, namely the 09 LOPIK departure. The optimization bounds were kept identical for all cases. The results for both aircraft are presented in Figures 2.1 and 2.2. The results show that the 5 segment optimization has the better results when looking at both aircraft types. The blue Pareto fronts are more noise optimal for both aircraft, especially for the B772. The 7 segment solutions are far worse with both Pareto fronts being higher and further right on the plot. A reason for this deterioration is that it wasn't able to converge as far within the given maximum evaluations. Furthermore, while the 9 segment run does provide good optimal solutions, the optimization took hours longer making it less manageable for the amount of runs that are needed in this study. Previous work that was performed on this topic chose 5 ground segments due to the decent flexibility as well as manageable run times [7]. The decision variables of the trajectories also show that often the aircraft did not make use of the third and fourth turn, or only a small heading change was observed indicating that the turns were not always necessary.

In conclusion, although the results of the sensitivity analysis are viewed critically, 5 ground segments are chosen for this research. With the amount of aircraft types considered, the already high computation time plays a big role and cannot be compromised further. The model has already been adapted for 7 and 9 ground segments and this can be explored further in future research.

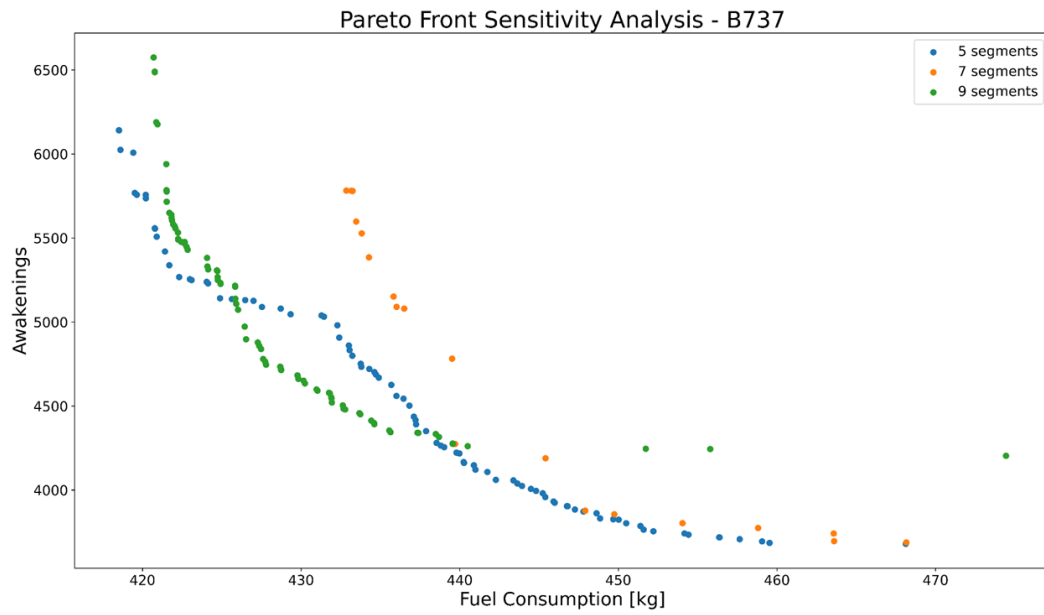


Figure 2.1: Sensitivity analysis results for the B737

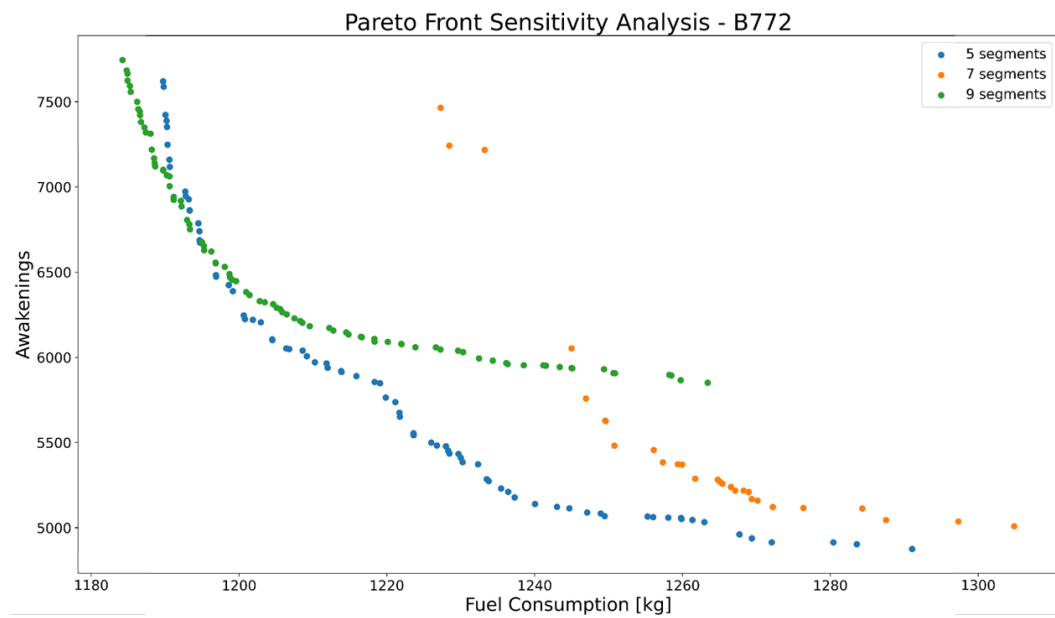


Figure 2.2: Sensitivity analysis results for the B772

Bibliography

- [1] The most efficient single- runway airport in the world relies on effective data management. *The Economist*, 2018.
- [2] Umut Asan, Ayberk Soyer, and Seyda Serdarasan. A comparison of methods for selecting preferred solutions in multiobjective decision making. *Computational Intelligence Systems in Industrial Engineering*, 6(January):469–479, 2013. doi: 10.2991/978-94-91216-77-0. URL <http://www.springerlink.com/index/10.2991/978-94-91216-77-0>.
- [3] Matthias Battel and Trevor M. Young. Simplified thrust and fuel consumption models for modern two-shaft turbofan engines. *Journal of Aircraft*, 45(4):1450–1456, 2008. ISSN 15333868. doi: 10.2514/1.35589.
- [4] Dimitris Bertsimas, Michael Frankovich, and Amedeo Odoni. Optimal selection of airport runway configurations. *Operations Research*, 59(6):1407–1419, 2011. ISSN 0030364X. doi: 10.1287/opre.1110.0956.
- [5] Eric R Boeker, Eric Dinges, Bill He, and Gregg Fleming. INM v7.0 Technical Manual. page 211, 2008.
- [6] CAE Oxford Aviation Academy. *Air Law: ATPL Ground Training Series*. KHL Printing CO. Pte Ltd, Singapore, 2014.
- [7] B Ceulemans. Tailored SID and Profile Allocation for Amsterdam Airport Schiphol. Master’s thesis, Delft University of Technology, 2016.
- [8] Thomas Coleman, Mary Ann Branch, and Andrew Grace. Optimization Toolbox Matlab 7.8.0. 2009.
- [9] W.H Dalmeijer. Gebruiksprognose 2020. Technical report, Royal Schiphol Group, 2019.
- [10] EASA. Aviation Environmental Impacts. URL <https://www.easa.europa.eu/eaer/climate-change/aviation-environmental-impacts>.
- [11] EASA. Emissions, 2020. URL [easa.europa.eu/eaer/topics/overview-aviation-sector/emissions](https://www.easa.europa.eu/eaer/topics/overview-aviation-sector/emissions).
- [12] Michael T.M. Emmerich and André H. Deutz. A tutorial on multiobjective optimization: fundamentals and evolutionary methods. *Natural Computing*, 17(3):585–609, 2018. ISSN 15729796. doi: 10.1007/s11047-018-9685-y.
- [13] Emir M. Ganic, Fedja Netjasov, and Obrad Babic. Analysis of noise abatement measures on European airports. *Applied Acoustics*, 92:115–123, 2015. ISSN 1872910X. doi: 10.1016/j.apacoust.2015.01.010. URL <http://dx.doi.org/10.1016/j.apacoust.2015.01.010>.
- [14] S. Hartjes and H. G. Visser. Efficient trajectory parameterization for environmental optimization of departure flight paths using a genetic algorithm. *Proceedings of the Institution of Mechanical Engineers, Part G: Journal of Aerospace Engineering*, 231(6):1115–1123, 2017. ISSN 20413025. doi: 10.1177/0954410016648980.
- [15] S. J. Hebly and H. G. Visser. Advanced noise abatement departure procedures: Custom-optimised departure profiles. *Aeronautical Journal*, 119(1215):647–661, 2015. ISSN 00019240. doi: 10.1017/S0001924000010733.
- [16] Frederick S. Hillier and Gerald J. Lieberman. *Introduction to Operations Research*. McGraw Hill Education, New York, 10 edition, 2015.
- [17] V. Ho-Huu, S. Hartjes, H. G. Visser, and R. Curran. Integrated design and allocation of optimal aircraft departure routes. *Transportation Research Part D: Transport and Environment*, 63(July):689–705, 2018. ISSN 13619209. doi: 10.1016/j.trd.2018.07.006. URL <https://doi.org/10.1016/j.trd.2018.07.006>.

- [18] V. Ho-Huu, S. Hartjes, H. G. Visser, and R. Curran. An optimization framework for route design and allocation of aircraft to multiple departure routes. *Transportation Research Part D: Transport and Environment*, 76(October):273–288, 2019. ISSN 13619209. doi: 10.1016/j.trd.2019.10.003. URL <https://doi.org/10.1016/j.trd.2019.10.003>.
- [19] Vinh Ho-Huu, Sander Hartjes, Hendrikus G. Visser, and Richard Curran. An efficient application of the MOEA/D algorithm for designing noise abatement departure trajectories. *Aerospace*, 4(4), 2017. ISSN 22264310. doi: 10.3390/aerospace4040054.
- [20] IAH. Master Plan 2035: Assessment of Existing Conditions. Technical report, George Bush Intercontinental Airport/Houston, Houston, 2015.
- [21] IBM. IBM ILOG CPLEX Optimization Studio. URL <https://www.ibm.com/products/ilog-cplex-optimization-studio>.
- [22] ICAO. ICAO Environment: Aircraft Noise. URL <https://www.icao.int/environmental-protection/Pages/noise.aspx>.
- [23] ICAO. Manual on Simultaneous Operations on Paralell or Near-Paralell Instrument Runways. Technical report, 2004.
- [24] ICAO. Procedures for Air Navigation Services: Aircraft Operations. Technical Report 5, ICAO, 2006.
- [25] ICAO. *Continuous Descent Operations (CDO) Manual*. ICAO, 1 edition, 2010. ISBN 9789292316402.
- [26] ICAO. ICAO 2019 Environment Report. *2019 Aviation and the Environment Report*, 43(3):21–22, 2019. ISSN 0033524X.
- [27] ICAO International Civil Aviation Organization. Doc 9993-AN/495, Continuous Climb Operations (CCO) Manual. 2012.
- [28] Rachel Jayne Kennedy. Four runway configuration types and their relation to arrival delays. *Open Access Theses*, 2015.
- [29] Brian Kim, Ben Manning, Ben Sharp, John-Paul Clarke, Isaac Robeson, Jim Brooks, and David Senzig. *Environmental Optimization of Aircraft Departures: Fuel Burn, Emissions, and Noise*. The National Academies Press, Washington, DC, 2013. ISBN 9780309259033. doi: 10.17226/22565.
- [30] Dajung Kim, Yuan Lyu, and Rhea P. Liem. Flight Profile Optimization for Noise Abatement and Fuel Efficiency during Departure and Arrival of an Aircraft. *AIAA Aviation*, (June):1–18, 2019. doi: 10.2514/6.2019-3622.
- [31] Dominic McConnachie, Philippe Bonnefoy, and Akshay Belle. Investigating benefits from continuous climb operating concepts in the national airspace system. In *11th USA/Europe Air Traffic Management Research and Development Seminar*, pages 1–11, Boston, MA, 2015. ISBN 9781617825132. doi: 10.1109/DASC.2011.6096003. URL http://www.atmseminar.org/seminarContent/seminar11/papers/501-McConnachie_0126150628-Final-Paper-5-7-15.pdf<https://www.scopus.com/inward/record.uri?eid=2-s2.0-77958469451&partnerID=40&md5=7c0774c650d86b2964b324093d5f376c%5Cnhttps://www.scopus.com/inwar>.
- [32] R. Mori. Fuel-Saving Climb Procedure by Reduced Thrust near Top of Climb. *Journal of Aircraft*, pages 1–7, 2020. doi: 10.2514/1.c035200.
- [33] P Peeters and J Melkert. Toekomst verduurzaming luchtvaart: een actualisatie. *Parlement en Wetenschap*, pages 1–22, 2021.
- [34] Javier A. Pérez-Castán, Fernando Gómez Comendador, Álvaro Rodríguez-Sanz, and Rosa M. Arnaldo Valdés. Separation minima for continuous climb operations. *Journal of Aircraft*, 56(1):262–272, 2019. ISSN 00218669. doi: 10.2514/1.C034667.

- [35] Javier A. Pérez-Castán, Fernando Gómez Comendador, Álvaro Rodríguez-Sanz, Rocío Barragán, and Rosa M. Arnaldo-Valdés. Design of a conflict-detection air traffic control tool for the implementation of continuous climb operations: A case study at Palma TMA. *Proceedings of the Institution of Mechanical Engineers, Part G: Journal of Aerospace Engineering*, 233(13):4839–4852, 2019. ISSN 20413025. doi: 10.1177/0954410019831198.
- [36] Key Points. IATA - Economic Performance of the Airline Industry Key Points. 2020. URL www.iata.org/economics.
- [37] Maria Nadia Postorino and Luca Mantecchini. A systematic approach to assess the effectiveness of airport noise mitigation strategies. *Journal of Air Transport Management*, 50:71–82, 2016. ISSN 09696997. doi: 10.1016/j.jairtraman.2015.10.004. URL <http://dx.doi.org/10.1016/j.jairtraman.2015.10.004>.
- [38] A. Rodríguez-Díaz, B. Adenso-Díaz, and P. L. González-Torre. Improving aircraft approach operations taking into account noise and fuel consumption. *Journal of Air Transport Management*, 77(March):46–56, 2019. ISSN 09696997. doi: 10.1016/j.jairtraman.2019.03.004. URL <https://doi.org/10.1016/j.jairtraman.2019.03.004>.
- [39] I.M. Ross. *A Primer on Pontryagin's Principle in Optimal Control*. Collegiate Publishers, San Francisco, 2009.
- [40] Royal Schiphol Group. Evaluatie Gebruiksprognose 2019. Technical Report november 2018, Royal Schiphol Group, 2019.
- [41] SFO. Airfield San Francisco International Airport. URL <https://www.flysfo.com/about-sfo/sfo-tomorrow/airfield>.
- [42] Dick G. Simons, Mirjam Snellen, Roberto Merino-Martinez, and Anwar M.N. Malgoezar. Noise breakdown of landing aircraft using a microphone array and an airframe noise model. *INTER-NOISE 2017 - 46th International Congress and Exposition on Noise Control Engineering: Taming Noise and Moving Quiet*, 2017-Janua, 2017.
- [43] Junzi Sun. *Open Aircraft Performance Modeling Based on an Analysis of Aircraft Surveillance Data*. 2019. ISBN 9789055841745. doi: 10.4233/uuid.
- [44] Noboru Takeichi and Daigo Inami. Arrival-time controllability of tailored arrival subjected to flight-path constraints. *Journal of Aircraft*, 47(6):2020–2029, 2010. ISSN 00218669. doi: 10.2514/1.C000272.
- [45] Manuel Villegas Díaz, Fernando Gómez Comendador, Javier García-Heras Carretero, and Rosa María Arnaldo Valdés. Analyzing the Departure Runway Capacity Effects of Integrating Optimized Continuous Climb Operations. *International Journal of Aerospace Engineering*, 2019, 2019. ISSN 16875974. doi: 10.1155/2019/3729480.
- [46] Joseph Wat, Jesse Follet, Rob Mead, John Brown, Robert Kok, Ferdinand Dijkstra, and Jeroen Vermeij. In service demonstration of advanced arrival techniques at Schiphol airport. *Collection of Technical Papers - 6th AIAA Aviation Technology, Integration, and Operations Conference*, 1(September):482–501, 2006. doi: 10.2514/6.2006-7753.
- [47] Alexander T Wells and Seth Young. *Airport Planning & Management*. McGraw Hill, New York, 5 edition, 2004. ISBN 0071436065.